Laboratory of Synthesis and Analysis
Department of Chemistry
Faculty of Science
University of Helsinki
Finland

IONIC LIQUIDS FOR VALORISATION OF LIGNOCELLULOSIC BIOMASS

Uula Hyväkkö

ACADEMIC DISSERTATION

To be presented, with the permission of the Faculty of Science of the University of Helsinki, for public examination in lecture room A110, Chemicum, on 24th of January 2020, at 12 noon.

Helsinki 2020

Supervisors

Docent Jussi Sipilä
Department of Chemistry, Laboratory of Synthesis and Analysis
University of Helsinki, Finland

Dr. Paula Nousiainen
Department of Chemistry, Laboratory of Synthesis and Analysis
University of Helsinki, Finland

Professor Timo Repo
Department of Chemistry, Laboratory of Synthesis and Analysis
University of Helsinki, Finland

Reviewers

Associate Professor Henrikki Liimatainen
Faculty of Technology, Fibre and Particle Engineering
University of Oulu, Finland

Professor Marco Orlandi
Department of Earth and Environmental Sciences
University of Milano-Bicocca, Italy

Opponent

Professor Raimo Alén
Department of Chemistry, Renewable Natural Resources and Chemistry of Living Environment
University of Jyväskylä, Finland

ISBN 978-951-51-5773-7 (pbk.)
ISBN 978-951-51-5774-4 (PDF)
Unigrafia
Helsinki 2020

ABSTRACT

This thesis explores novel applications that utilize ionic liquids and electrolyte solutions in the treatment of biomass to obtain high-quality, value-added products, such as cellulose, hemicelluloses, and lignin, as relatively pure fractions that can be further processed into useful materials and chemicals. Although ionic liquids have been described as highly chemically and thermally stable solvents, the potential drawbacks of ionic liquids and electrolyte solutions regarding their possible degradation in common processing temperatures are discussed in detail in this thesis.

This thesis is a summary of the author's contribution to four published papers, two posters and unpublished results that were obtained during the work. The objective was to synthesize ionic liquids for the valorisation of biomass and assess their chemical stabilities in the process conditions.

The work commenced with the synthesis of a highly hydrophobic phosphonium ionic liquid trioctylmethylphosphonium triflate [P_{8881}][OTf]. This ionic liquid was studied with other similar commercial ionic liquids as a fractionation medium for wheat straw. The initial results suggested that [P_{8881}][OTf] could not to fractionate wheat straw, and thus the potential of a highly hydrophilic aqueous organic electrolyte solution tetra-*n*-butylphosphonium hydroxide [P_{4444}][OH] was studied in fractionation of wheat straw. The aqueous [P_{4444}][OH] solutions were effective for this purpose. Lignin from the biomass was extracted with varying concentrations of [P_{4444}][OH] in water. The carbohydrate-rich fractions were isolated; and finally, all collected fractions were analyzed. The results showed that 40 w/w% aqueous solutions of [P_{4444}][OH] were stable. Irreversible decomposition kinetics were assessed for a 60 w/w% solution; it was not possible to obtain 70 w/w% or higher concentrations due to the decomposition during evaporation at 25 °C.

The next project assessed the hydrolytic stability of 1,5-diazabicyclo[4.3.0]non-5-enium acetate [DBNH][OAc] that was under intensive investigation in the research group at that time. In this work the

hydrolysis kinetics of [DBNH][OAc] were measured using high performance liquid chromatography (HPLC) analysis. At the time, only a few studies in the literature analyzed ionic liquids with HPLC. [DBNH][OAc] can rapidly dissolve large quantities of cellulose and can be utilized in the IONCELL-F process to convert cellulose pulp into strong cellulosic man-made fibers. The recyclability and sustainability of the IONCELL-F process were addressed. In addition, synthesis routes were studied for the superbase precursors 9-methyl-1,5-diazabicyclo(4.3.0)non-5-ene (9-mDBN), which was assumed to lead to increased hydrolytic stabilities of the final ionic liquid.

In the last research project, an aqueous solution of triethylammonium hydrogen sulfate [TEAH][HSO_4] was studied for fractionation of wheat straw and aspen in comparison with non-sulfated NaOH pulping and various recently discovered pulping methods. All procedures utilized a microwave reactor. Aqueous solutions of [TEAH][HSO_4] are extremely affordable in comparison to most of the other ionic liquids known in the literature. Therefore, there is an increased potential to develop a genuinely economical process. The fractionation procedures with an ionic liquid produced a comparatively low molecular weight distribution for both carbohydrate- and lignin-rich fractions in contrast to other studied systems. All fractions were analyzed with gel permeation chromatography and spectroscopic methods in order to evaluate their potential for further refining.

ACKNOWLEDGEMENTS

This study was performed in the Department of Chemistry at the University of Helsinki during 2012–2019. During this time, I have met many exceptional people to whom I'd like to express my gratitude for.

I would like thank Professor Ilkka Kilpeläinen and Docent Alistair King for introducing me to the world of ionic liquids and biomass processing and giving me the chance to work in their research group–full of enthusiast and talented people. I am very grateful to Docent Jussi Sipilä, Dr. Paula Nousiainen and Professor Timo Repo for providing me the opportunity to continue and ultimately finish my thesis in their group.

I thank the Academy of Finland for funding the 'Valorisation of Wheat Residues to Polymeric Xylan and Cellulose' (VALOWHEAT) project. I also want to thank project partners Professor Maija Tenkanen and Dr. Susanna Heikkinen for their input and cooperation. Docent Pierre-Yves Pontalier, Dr. Leslie Jacquemin, and Dr. Luc Saulnier are thanked for their cooperation and insight on industrial processes and chemical engineering.

I thank Professor Herbert Sixta and Professor Susanne Wiedmer and their groups for their cooperation and fruitful discussions.

Dr. Sami Heikkinen and Dr. Petri Heinonen are thanked for their friendship and help with solving analytical issues.

Thanks to Professor Kristiina Hildén and her group for productive meetings and cooperation.

I would like to thank Dr. Eric Enqvist and Dr. Panu Tikka for interesting discussions and inspiring enthusiasm in processing of biomaterials.

I would like to thank all members of BIOREGS doctoral school–I miss you all and I hope our roads will cross later in life. I would like to thank all members of the CHEMS doctoral school. It has been a pleasure meeting so many enthusiastic scientists and sharing thoughts with you.

My thanks go to my colleagues and friends–Arno, Ashley, Joona, Jussi H., Jussi K., Lauri, Pirkko, Riku, Sara, Tia, Tom, Tuomas, Valtteri and others–for

their support and many, many delightful discussions of science and life. You are great!

I am sincerely grateful to Merja for her support and advice. Also, my thanks to Hanna, Nette, and Sofia for their friendship and support.

I'd like to say thanks to my brother Samuli, his partner Marisanna and their daughter Emma for cheering me up and believing in me and in my efforts in the career I have chosen.

I would like to thank Paula J. and Piko for their companionship and support throughout these years.

Lastly, I would like to thank Laura for her love and support.

† In memory of my parents, whom I lost during my doctoral studies. Rest in peace, my loved ones. †

CONTENTS

LIST OF ORIGINAL PUBLICATIONS

The majority of this thesis is based on the following publications:

I **U. Hyväkkö**, A. W. T. King and I. Kilpeläinen. Extraction of Wheat Straw with Aqueous Tetra-*n*-butylphosphonium Hydroxide. *BioRes*. **2014**, 9, 1565–1577.

II **U. Hyväkkö**, R. Maltari, T. Kakko, J. Kontro, J. Mikkilä, P. Kilpeläinen, E. Enqvist, P. Tikka, K. Hildén, P. Nousiainen and J. Sipilä. On the Effect of Hot-Water Pretreatment in Sulfur-Free Pulping of Aspen and Wheat Straw. *Published online in ACS Omega* **2019**. https://doi.org/10.1021/acsomega.9b02619

III A. Parviainen, R. Wahlström, U. Liimatainen, T. Liitiä, S. Rovio, J. K. J. Helminen, **U. Hyväkkö**, A. W. T. King, A. Suurnäkki and I. Kilpeläinen. Sustainability of Cellulose Dissolution and Regeneration in 1,5-diazabicyclo[4.3.0]non-5-enium Acetate: A Batch Simulation of the IONCELL-F Process. *RSC Adv*. **2015**, *5*, 69728-69737.

IV W. Ahmad, A. Ostonen, K. Jakobsson, P. Uusi-Kyyny, V. Alopaeus, **U. Hyväkkö** and A.W.T. King. Feasibility of Thermal Separation in Recycling of the Distillable Ionic Liquid [DBNH][OAc] in Cellulose Fiber Production. *Chem. Eng. Res. Des*. **2016**, *114*, 287–298.

For publication **I**, the author designed and performed all experimental work and wrote the manuscript.

For **II**, the author co-designed and co-performed the majority of the experimental work, wrote the majority of the first draft of the manuscript and co-wrote the final manuscript.

For **III**, the author determined the number of accumulated inorganics in the spent ionic liquid.

For **IV**, the author analyzed the spent ionic liquid solutions using the methodology developed in **V** and **VI** (see below).

LIST OF OTHER SCIENTIFIC REPORTS

V **U. Hyväkkö**, J. Helminen, A. Parviainen A. W. T. King and I. Kilpeläinen. "Hydrolytic stability of novel distillable ionic liquids: A kinetic and computational study". Poster presented at the FIBIC annual seminar, Helsinki, **2013**.

VI J. Helminen, **U. Hyväkkö**, V. Mäkelä, A. Parviainen, K. Vyavaharkar, A. W. T. King and I. Kilpeläinen. "Stability of recyclable ionic liquids". Poster presented at the ACel Symposium, Helsinki, **2015**.

For **V**, the author synthesized all studied ionic liquids (excluding the hydrolysis reference compounds), performed all hydrolysis experiments and high-performance liquid chromatography (HPLC) analyses and co-interpreted the results. The author wrote the first draft of a manuscript based on this work, which is still unpublished.

For **VI**, the author co-performed the experimental work.

The work presented in **V** and **VI** will be published in a scientific journal later because computer simulations are still on-going.

ABBREVIATIONS

[amim]	1-allyl-3-methylimidazolium
APPA	1-(N-acetyl-3-aminopropane)-pyrrolidin-2-one
[APPH][OAc]	1-(3-ammoniopropane)-pyrrolidin-2-one acetate
AsF_6	hexafluoroarsenate
BF_4	tetrafluoroborate
[bmim] / [C_4mim]	1—*n*-butyl-3-methyl-imidazolium
[bmim]Cl	1—*n*-butyl-3-methyl-imidazolium chloride
BPy	1-butylpyridinium
$(C_2F_5SO_2)_2N^-$	bis(perfluoroethane sulfonyl)imide
[C_4mpyrrol]	1-butyl-1-methyl-pyrrolidinium
DAP	diamino propane
[DBNH][OAc]	1,5-diazabicyclo[4.3.0]non-5-enium acetate
DBN	1,5-diazabicyclo(4.3.0)non-5-ene
DBS	dodecyl benzene sulfonate
DBU	1,8-diazabicyclo[5.4.0]undec-7-ene
DCA	dichloroacetic acid / dichloroacetate
DES(s)	deep eutectic solvent(s)
DIPA	diisopropylamine
DMAP	4-dimethylaminopyridine
DMP	1,2-dimethyl-1,4,5,6-tetrahydropyrimidine
DMSO	dimethyl sulfoxide
DP_W	degree of polymerization
EIM	1-ethylimidazole
[emim] / [C_2mim]	1-ethyl-3-methylimidazolium
[emim][OAc]	1-ethyl-3-methyl-imidazolium acetate
[emim][OTf]	1-ethyl-3-methylimidazolium triflate
[emim][TCM]	1-ethyl-3-methylimidazolium tricyanomethanide
[emim][TMP]	1-ethyl-3-methylimidazolium dimethyl phosphate
EPy	1-ethylpyridinium
$EtCO_2^-$	propionate

GVL	gammavalerolactone
[hmim] / [C_6mim]	1—*n*-hexyl-3-methyl-imidazolium
HSO_4^-	hydrogen sulfate
Hünigs	Hünigs base, *N*,*N*-diisopropylethylamine
HWE	hot water extraction
IL(s)	ionic liquid(s)
LA	levulinic acid
mAPP	1-(3-aminopropyl)-5-methylpyrrolidin-2-one
mDBN/9-mDBN	9-methyl-1,5-diazabicyclo(4.3.0)non-5-ene
$N(CN)_2$	dicyanamide
NMMO	*N*-methylmorpholine-*N*-oxide
NO_3^-	nitrate
OAc^-	acetate
OES	organic electrolyte solution
OP_{888}	trioctylphosphonium oxide
OTs	tosylate
$[P_{4441}][OTs]$	triisobutylmethylphosphonium tosylate
$[P_{4444}]^+$	tetra-*n*-butylphosphonium
$[P_{4444}][OH]$	tetra-*n*-butylphosphonium hydroxide
P_{888}	trioctylphosphine
$[P_{8881}][OTf]$	trioctylmethylphosphonium triflate
$[P_{14666}]^+$	tris(*n*-hexyl)tetradecylphosphonium
$[P_{14666}]Cl$	trihexyl(tetradecyl)phosphonium chloride
$[P_{14666}][DCM]$	trihexyl(tetradecyl)phosphonium dicyanamide
PF_6	hexafluorophosphate
Pyr	pyridinium
RaNi	Raney nickel
$[TEAH][HSO_4]$	triethylammonium hydrogensulfate
Tf_2N^- / $(CF_3SO_2)_2N^-$	bis(trifluoromethylsulfonyl)imide
TGA	thermogravimetric analysis
TMG	1,1,3,3-tetramethylguanidine
VOC	volatile organic compound

1 LITERATURE REVIEW

In the coming decades, the world population is expected to grow from 7.7 billion (in 2019), to 8.5 billion (in 2030), to approximately 9.7 billion in 2050.[1] By the year 2030, there must be over 40 % more food production than in 2010. In this time span, the demand for textiles will increase tremendously (approximately 84 %).[2] Cotton production is expected to stagnate or even slightly decline in the following decades due to the need of arable land for food cultivation.[3] The massive population and income growth will have major impacts on increasing the consumption of textile fibers. Cotton production cannot keep up with the growing demand, and thus it very quickly becomes obvious that production of 'man-made' cellulosic fiber must be increased tremendously to fill the so-called cellulose gap (**Figure 1**).[2]

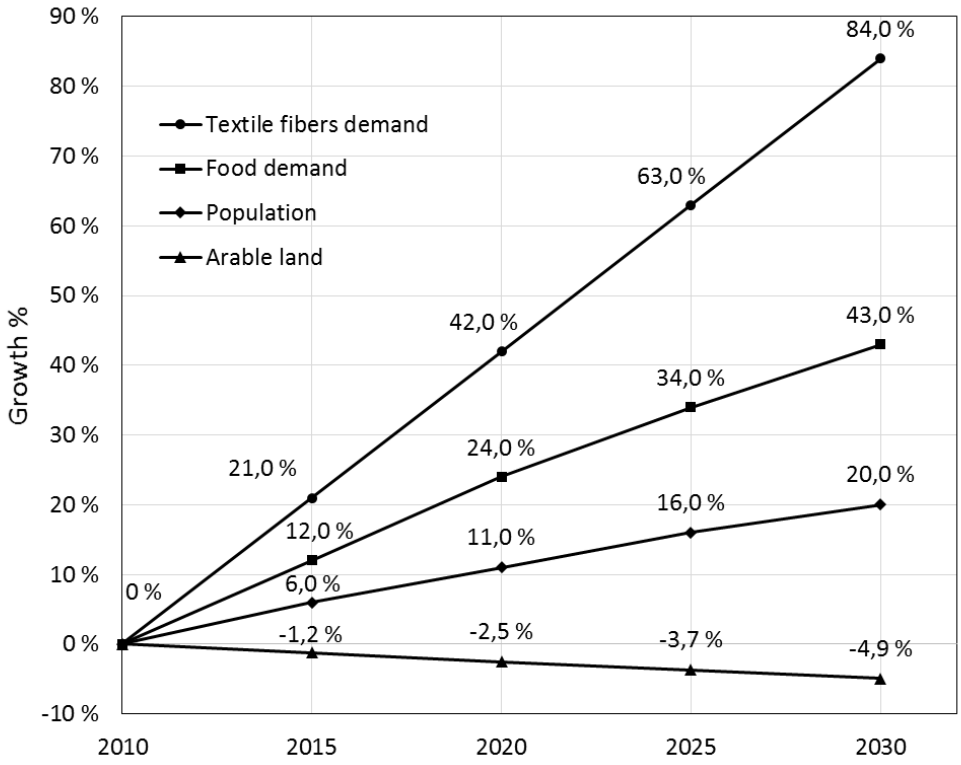

Figure 1 Population growth versus the demand for food and textile fibers and the available arable land. Adopted from ref. 2, with permission from the Lenzinger Berichte editor.

In addition to cellulosic raw materials for textiles, new types of transportation fuels and renewable materials are urgently needed to reduce the dependency on fossil fuels to prevent global warming.[4] In fact, so far the only inexpensive non-food resources for sustainable production of liquid fuels are cellulosic biomasses.[5] The highly desired property in biofuels is that they could be used in current transportation vehicles without any modifications.[6] Unfortunately, with the current market prices, biofuel production directly from pulp is not economically sound because the price of the biofuels is lower than the price of cellulosic pulp. However, Borregaard has announced that they produce bioethanol as a pulping side stream.[7] The Inbicon technology (owned by Ørsted) is a process where straw can be directly converted into a form in which bioethanol can be produced *via* saccharification and fermentation with good yields and reasonable economics.[8]

Ultimately, to prevent climate change and approach a sustainable economy, the world market must grow toward using bio-based resources.[5] Cellulosic biomass is one of the most potential raw materials to manufacture sustainable and renewable materials and products.[9] One of the reasons why cellulosic raw materials should be utilized instead of starch (for example) is because starch originates from direct food sources (first generation of biofuels).[10] Cellulose, on the other hand, can be separated and collected from the waste side stream created by food cultivation, for example, the non-edible part of a plant (such as wheat straw). These components are referred as the second-generation biofuels.

Cellulose is a potential material for various applications because it possesses reactive hydroxyl groups for further modification. Cellulose can be converted into hydrophobic derivatives such as decanoic or palmitic acid esters of cellulose, which have reported potential as biodegradable coating materials.[11] This type of material can be cast into clear films that can serve myriad uses including for packaging purposes.[12] Furthermore, synthetic polyelectrolytes that contain a high charge density can be potentially replaced with cationic cellulose derivatives.[13] Those materials are useful as flocculation agents in several applications, such as papermaking and water purification.

1.1 LIGNOCELLULOSIC BIOMASS

Lignocellulosic biomasses, including hardwoods, softwoods and agricultural residues (e.g., wheat straw) are the most important sources for renewable carbon in the form of biopolymers such as cellulose, hemicelluloses, and lignin (**Figure 2**).

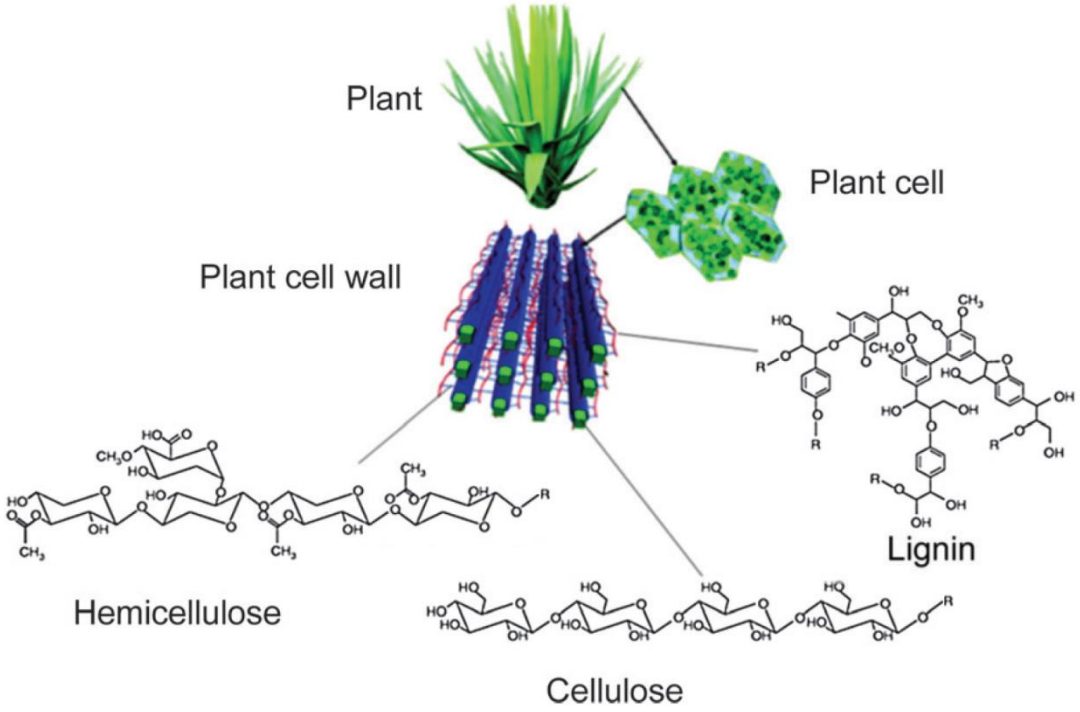

Figure 2 Plant structure and its main constituents. Adopted from ref 14, with permission from the Royal Society of Chemistry.

Cellulose and hemicelluloses represent most of the carbohydrates in plants. Cellulose is a partially crystalline, fibrous, linear 1,4-β-glycoside linked homopolymer of glucose in which every repeating unit is corkscrewed 180° in relation to its neighboring unit.[15] Hemicelluloses are typically branched, amorphous copolymers formed from glucose, galactose, mannose, xylose, arabinose, and glucuronic acid.[16] Lignin is an amorphous, complex three-dimensional polymer that comprises phenylpropanoid units.[17] These three components–together with other minor components–form the rigid, recalcitrant and complex structure of the plant cell wall, which protects plants from their surroundings and weather. For this reason, the thermochemical processing of biomasses often required harsh conditions that may lead to

difficult and expensive processes. The separation of these components from the plant cell wall matrix requires a treatment that allows for the carbohydrate fraction to be collected and further processed into products such as pulp and paper or bioenergy and fuels (**Figure 3**).[6,18]

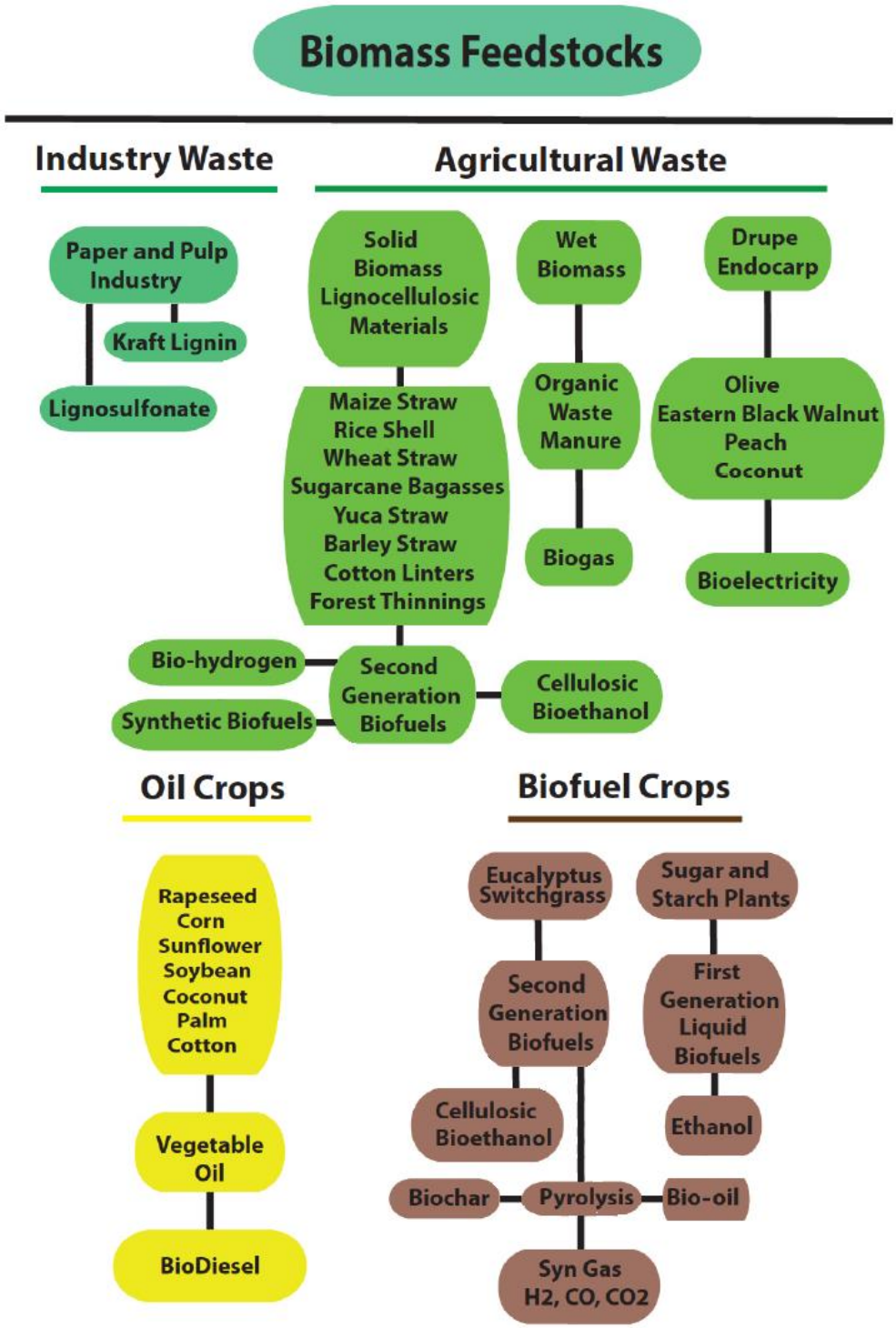

Figure 3 Different approaches that use various biomass for production of fuels and energy. Adopted from ref. 18, with permission from MDPI.

1.1.1 DETERMINATION OF LIGNIN CONTENT IN BIOMASS

In most cases, lignin is considered to be a low-value fraction that is typically combusted to produce heat energy. Lignin can potentially be used as binder, dispersant, emulsifier and sequestrant.[19,20] It is possible to use lignin as a source of high-value aromatic molecules; however, there are not many industrial-scale products besides vanillin.[21,22] The aim in biorefinery is to utilize the raw materials in a closed cycle with minimal environmental impact without waste streams.[23]

It is typically difficult to remove all the lignin when processing biomasses. Therefore, several analytical procedures have been developed for determining the lignin content in lignocellulosic biomasses. However, these methods can provide very different estimates of lignin content for the same sample.[24] These methods are based on either removing the other cell wall constituents than lignin (e.g., Klason lignin [KL] [25] and acid detergent lignin [ADL][26]) or oxidizing lignin as a polymer out of the cell wall matrix (e.g. the potassium permanganate method[27]). In KL and ADL analyses, the cell wall can be removed with sulfuric acid solubilization and/or hydrolysis of cell wall polysaccharides. However, the results can be erroneous if lignin in the sample is soluble in the acid detergent solution.[28,29] In unfortunate instances, the loss of lignin can be as high as 50 % e.g., tropical grasses using the ADL method.[30] The KL method is not applicable for straws and grasses because sulfuric acid reacts with plant proteins and provides overestimates for lignin content.[31,32]

The advantage in the permanganate method over ADL and KL is that it avoids the use of corrosive reagent (i.e. sulfuric acid) and the need for standardization. However, there are drawbacks, including the fact that permanganate can oxidize non-lignin phenolics and unsaturated compounds, such as tannins, pigments or proteins, a phenomenon that can lead to incorrect estimation of lignin content if they are not entirely removed from the sample in pre-analysis preparation.[27]

As an alternative, a spectrophotometric method can be used to quantify the lignin content in biomass. The method is based on dissolution of lignin using a 25 % solution of acetyl bromide in acetic acid. The lignin content in the

sample can be measured and calculated from the absorption at 280 nm. This method is straightforward and requires very small sample sizes (i.e., 4-6 mg). The drawback is that–as any spectrophotometric method–it requires standards in order to have reliable calibration curves.[33]

In the experimental portion of this thesis, the acetyl bromide method was chosen for quantification of lignin content.

1.2 WHEAT STRAW AND ASPEN AS RAW MATERIALS

Bio-based products and fuels can be produced using wheat straw as a raw material. Wheat straw is available in many countries as an abundant agricultural side stream. Manufacturing wheat straw–based products might reduce the carbon footprint in products and avoids the use of resources such as oil or other fossil-based chemicals. Wheat straw consists of mostly cellulose (35–45 %), hemicelluloses (20–30 %), and lignin (15–20 %). However, it also contains a relatively high amount of minerals (e.g., silicates, 5–10 %) and extractives that might bring additional challenges in processing and pulping.[34,35,36]

Wheat straw has a high quantity of potentially valuable carbohydrates that can be used as a low-cost raw material for various applications including biodegradable packaging, fuels, or other renewable chemicals and materials.[37,38] However, the fiber properties of cellulose in wheat straw are poor and therefore the traditional pulp and paper products made from wheat straw have reduced value. Moreover, the amount of non-fibrous cells in wheat straw can also lead to problems in processing the pulp.[39] Low-quality fiber can be used for many applications where fibers are degenerated or they do not play a crucial role, such as saccharification for biofuel production.[40] To overcome the biomass recalcitrance, it is necessary to process the material in a manner that allows for the separation of the valuable components without damaging them. This method enables their valorisation further to materials with desired properties such as a high molar mass or intact chemical structure.

The low density of wheat straw presents a logistical problem. With grinding, the density can be greatly improved (**Figure 4**); however, this

process may affect the cost-effectiveness in straw-based biorefinery because milling can be rather energy intensive.[41]

Figure 4 Change in density before and after grinding wheat straw. Adopted from ref. 41, with permission from John Wiley & Sons.

Aspen does not have similar density issue (**Figure 4**) because it can be transferred as logs. Nevertheless, aspen presents some additional challenges besides the common problems in wood logging. One of the challenges is the increased cost in logging due to the large variance in log diameter, which depends on where the wood was grown. Another issue that increases costs is defects. Aspen can have superficial defects including fungus growth, rough bark of the stem, and crooked branch development. Aspen also can have heart rot, which is caused by a fungus and decreases the profitability of logging.[42]

1.3 ORGANIC SALTS WITH A LOW MELTING POINT

Ionic liquids (ILs) and deep eutectic solvents (DESs) have been studied intensively in recent years. DESs are based on the eutectic phenomenon, where the melting point of a mixture of two compounds is lower than the pure compounds alone. In DESs, there is typically a narrow window in which this phenomenon is extreme, and the mixture can have a surprisingly low melting point. ILs are organic salts that have a low melting point because the cation is typically bulky and asymmetric, and the anion is relatively small (organic or inorganic). These features result in poor crystal structure and packing. The

charge delocalization on several atoms leads to weak Coulombic interactions and low crystal lattice energies; therefore the melting point is significantly lower than most of the common salts.[43,44] Examples of the most common cations and anions that have been used to form ILs are shown in **Figure 5**.

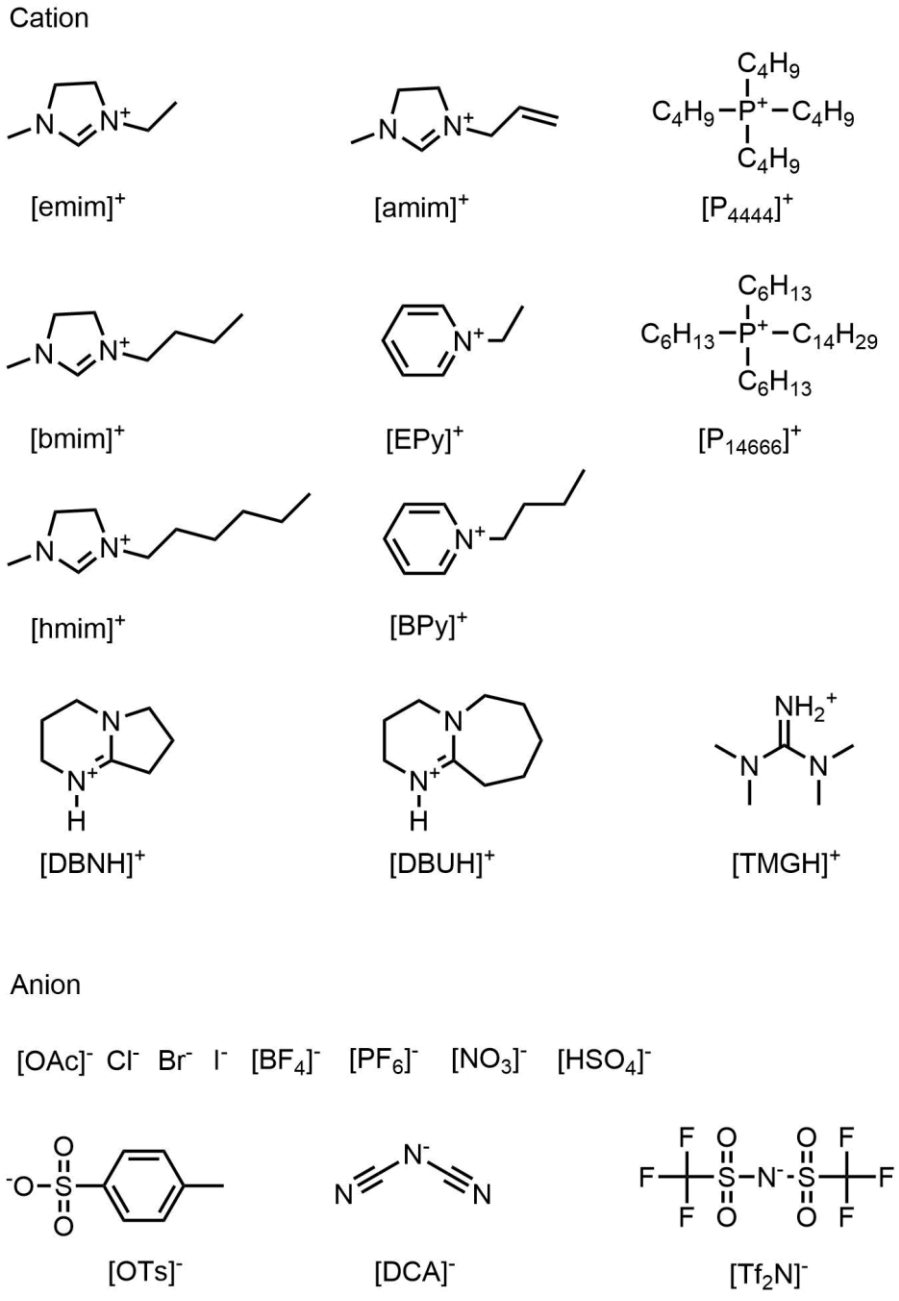

Figure 5 Chemical structures of some of the most common cations and anions in ILs.

ILs are defined to have melting point below 100 °C. Low melting ILs (room-temperature ionic liquids [RTILs]) have been known for more than 100 years.

For instance, $[EtNH_3][NO_3]$ was reported in 1914 to have a melting point of 12 °C.[45] Typically, ILs are not distillable without irreversible chemical decomposition. In 2011, the first cellulose dissolving distillable ILs were discovered. Distillable ILs are typically salts between organic superbases and organic acids. King *et al.*[46] reported the distillation of 1,1,3,3-tetramethylguanidine (TMG) combined with organic acids. The suggested distillation mechanism is the temporary disassociation of ions. Free uncharged compounds are volatile, a feature that allows for them to be distilled. After condensation, the neutral compounds meet at the recovery flask and form the IL again (**Figure 6**). Indeed, this approach is very interesting because distilling may solve the typical recovery and recyclability issues of ILs. However, this method requires a high amount of energy; therefore, a question remains whether the distillation is economical enough for processing on the industrial scale.

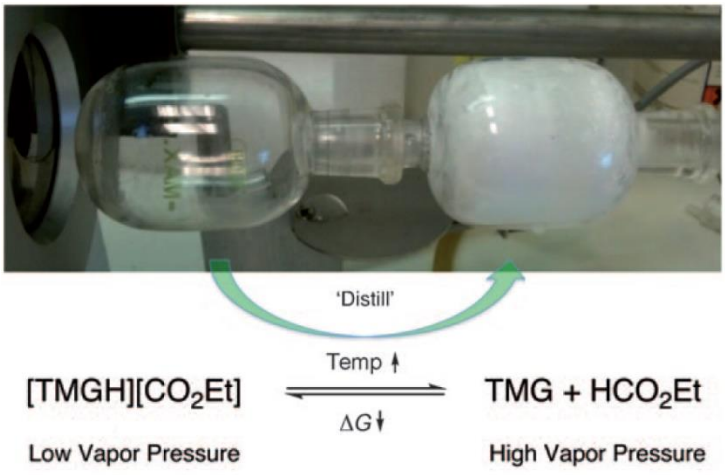

Figure 6 Distillation of [TMGH][OAc] and its vapor pressures at low and high temperatures. Adopted from ref. 46, with permission from John Wiley & Sons.

Due to the ionic nature of ILs, they have unique physical and solvation properties. Their vapor pressures are typically immeasurably low even when heated to common processing temperatures. They are also non-flammable at those temperatures and relatively stable. ILs have many applications such as electrolytes,[47] engineering fluids,[48] media for biomass treatment,[49] and in general as solvents and catalyst for synthetic purposes.[50] Interestingly, ILs can

dissolve materials that are insoluble in common laboratory solvents, e.g., cellulose, lignin, and even wood.[51,52,53] ILs have potential in processing media for various biomass such as wood, wheat straw, and rice hulks.[54] Some of the IL properties can be advantageously affected by carefully choosing the cation and anion. For example, the IL hydrophobicity and charged and polar interactions can be influenced.[44] These properties can have significant impacts on biopolymer dissolution capabilities of the ILs, among other factors.[55] **Table 1.** presents the properties of ILs compared with common organic laboratory solvents.[56]

Table 1. *Comparison between ILs and common organic solvents.*[56]

Property	Organic solvents	Ionic liquids
Number of solvents	>1000	>1 000 000
Applicability	Single function	Multifunction
Catalytic ability	Rare	Common, tunable
Chirality	Rare	Common, tunable
Vapor pressure	Obeys the Clausius-Clapeyron Equation	Typically negligible
Flammability	Usually flammable	Usually non-flammable
Tunability	Limited	Designer solvents
Cost	Inexpensive	2–100 times higher than organic solvents
Viscosity (cP)	0.2-100	22–40 000
Density (kg/l)	0.6-1.7	0.8-3.3

1.4 AMPHIPHILICITY OF CELLULOSE

Dissolution of cellulose is certainly not an easy task. In fact, cellulose is very insoluble polymer to common laboratory solvents. The insolubility is partly due to its ability to form a strong hydrogen bonding network (**Figure 7**).

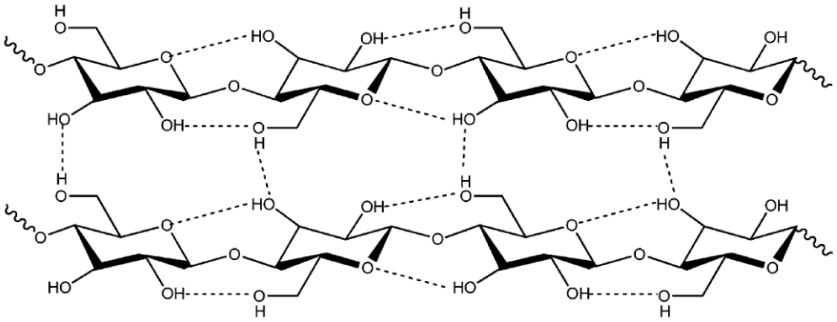

Figure 7 Hydrogen bonding network in cellulose. Reproduced from ref. 57, with permission from Royal Society of Chemistry

Solubilization typically requires derivatizing cellulose to facilitate its dissolution into common laboratory solvents. Cellulose derivatization hinders the inter- and intramolecular hydrogen bonding capabilities *via* substitution of the hydroxyl groups of cellulose: the fewer free hydroxyl groups, the fewer possible inherently strong hydrogen bonding interactions (**Figure 8**).

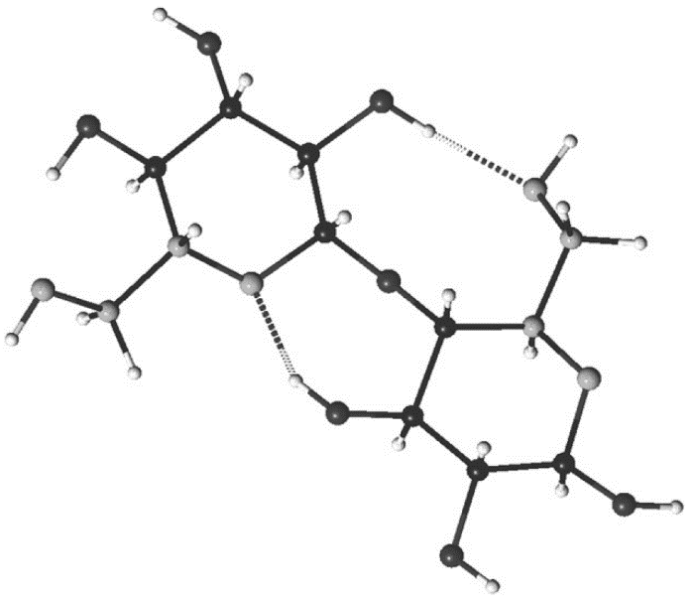

Figure 8 A short segment of a cellulose that highlights the intra-molecular hydrogen bonding interactions. Adopted from ref. 58, with permission from Elsevier.

Cellulose is not soluble in water; however, cellulose derivatized with hydrophobic groups can have increased solubility in water. This phenomenon is counterintuitive because cellulose is a highly hydrophilic polymer due to its hydroxyl groups. Cellulose derivatives such as hydroxyethyl cellulose are soluble in water even though they can form intermolecular hydrogen bonding.

In fact, glucose (i.e., a monomer of cellulose) should not dissolve in water if intermolecular hydrogen bonding would be the most important factor in the dissolution. Moreover, cellulose dissolution may be favored by decreasing the temperature.[58] For example, there is a narrow temperature window where cellulose can be dissolved in a NaOH solution, but it precipitates when heated above 0 °C. In addition, with NaOH treatment (i.e., mercerization) or dissolution followed by precipitation, cellulose undergoes an irreversible structural change from cellulose I to cellulose II. Cellulose II has a different hydrogen bond pattern and increased chemical reactivity compared to cellulose I; it does not appear in the nature.

In the dissolution of cellulose, different intermolecular interactions between cellulose chains must be carefully considered. Interactions, such as hydrogen bonding, van der Waals interactions and hydrophobic interactions, make the dissolution process complicated to explain and understand. Dextran (**Figure 9**) should have a similar capacity for hydrogen bonding interactions as cellulose, but dextran is soluble in water.

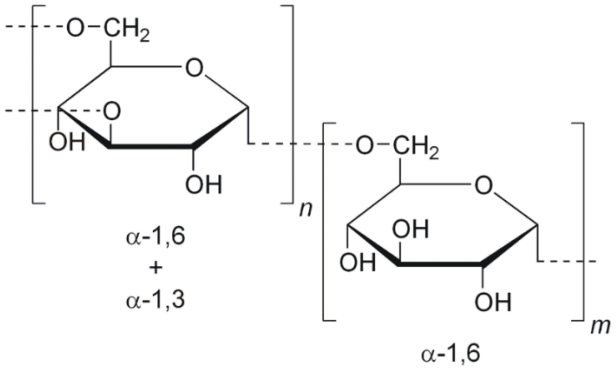

Figure 9 Dextran is a polyglucan that consists of α-1,6 glycosidic bonds between glucose units. The branches in dextran begin from α-1,3 linkages. Reprinted with permission from the author.

Lindman *et al.* discussed the amphiphilicity (i.e., a material possessing both hydrophobic and hydrophilic properties simultaneously) of cellulose, a phenomenon that might explain some of its unexpected behavior. Amphiphilic polymers can self-assemble which is a well-known phenomenon in surfactant and lipid chemistry. However, this behavior is often neglected for homopolymers such as cellulose. Cellulose is also a high molecular weight

polymer, and even slight amphiphilicity can affect its solubility. Solvents that can dissolve cellulose, such as ILs and *N*-methylmorpholine-*N*-oxide (NMMO), clearly belong to the group of amphiphilic solvents. At the top of **Figure 10** a cellulose chain is shown from the side of the polymer. The hydrophobic areas are highlighted above and below the ring. At the bottom of **Figure 10** the hydrophilic hydroxyl groups in the cellulose chain are highlighted. To allow for the dissolution of cellulose, a solvent should have the ability to simultaneously and advantageously satisfy the need of both hydrophobic and hydrophilic interactions. This factor explains why cellulose is not soluble in the most common organic solvents and water. [58,59]

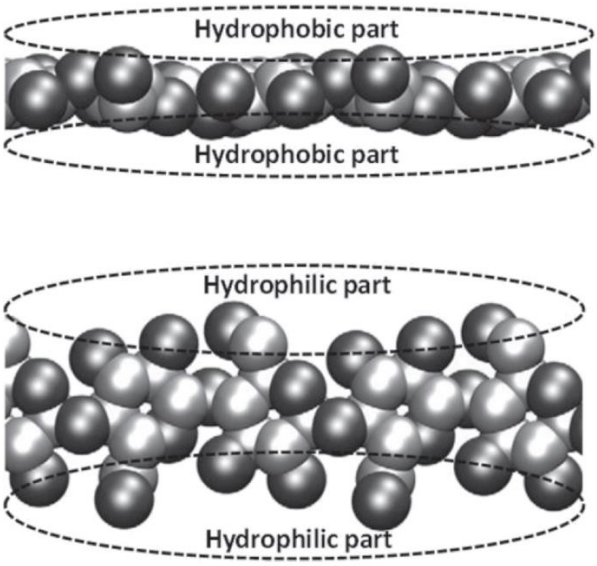

Figure 10 Hydrophilic and hydrophobic areas in cellulose. Reprinted from ref. 59, with permission from Elsevier.

Cellulose contains crystalline and amorphous regions. In the case where cellulose is not dissolved but swollen, a peculiar phenomenon called ballooning can be observed with a microscope. The amorphous regions of cellulose are more easily accessible and thus become swollen, while the crystalline areas remain in relatively unchanged rod-like fiber shape. The ballooning of cellulose mixed in aqueous 8 % NaOH solution is demonstrated in **Figure 11**.

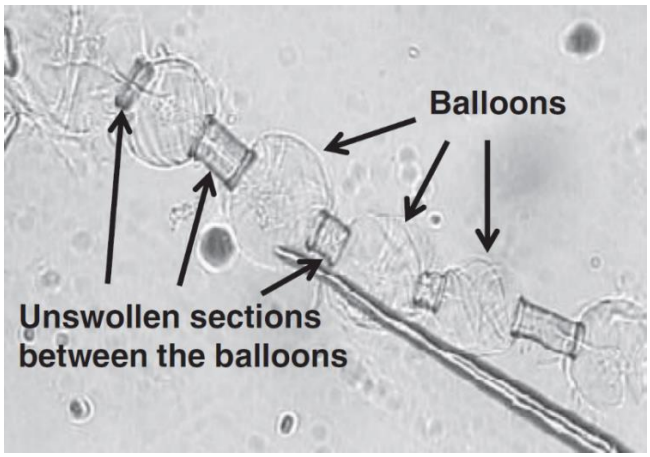

Figure 11 Ballooning phenomenon of cellulose in alkali. Reprinted from ref. 59, with permission from Elsevier.

1.5 SOLUBILITY OF CELLULOSE IN IONIC LIQUIDS

In 1934, Graenacher discovered that cellulose can be dissolved in mixtures of molten *N*-ethylpyridinium chloride and nitrogen-containing bases.[60] However, the method is not practical because the melting point of the system is 118 °C. Several decades later, in 2002, Swatloski *et al.*[61] found that 10 wt% of cellulose can be dissolved in the molten salt [bmim]Cl at 100 °C. In addition, the dissolution can be assisted with microwaves or sonication. They also showed that even small quantities of water reduce the solubility of cellulose, and cellulose could be precipitated from solution by an anti-solvent such as water. This finding launched a massive interest in studying these solvent systems.

In their critical review, Wang *et al.*[57] discussed the fundamentals of interactions with IL cations and anions with cellulose. ILs based on imidazolium, pyridinium, ammonium, and phosphonium cation seem to have capabilities in dissolving cellulose when they are paired with different anions. They concluded that the capabilities of the anions to dissolve cellulose appear to decrease in the order: $[AcO]^-$ > Cl^- > $[HCOO]^-$ > $[DCA]^-$ or $[NTf_2]^-$. They also stated that the aromatic imidazolium and pyridinium cations seem to work best; however, those were the first cations found to be capable of dissolving cellulose and are therefore the most studied cations. When the alkyl chain length in imidazolium-based ILs is increased to a certain length, the ability to dissolve cellulose seems to decrease, i.e., $[C_4mim]Cl$ > $[C_6mim]Cl$ >

[C_8mim]Cl. There is also some evidence of an odd-even effect in favor of dissolution capabilities for with imidazolium-based ILs with fewer than six carbon units.[62]

In their studies, Parviainen *et al.*[63] found that the cellulose dissolution capabilities of certain acid-base conjugate ILs (i.e., protic ILs, IL synthesized from an acid and a base, not *via* alkylation like [C_4mim]Cl) can be predicted by determining their computational gas phase proton affinities ($-\Delta H_{PA}$, energy required to remove a proton). There seems to be a basicity threshold between TMG and DMAP (4-dimethylaminopyridine) that must be exceeded for these ILs with the propionate ($EtCO_2^-$) anion to dissolve cellulose (**Table 2**).

Table 2. *Cellulose dissolving capabilities of different ILs with the propionate ($EtCO_2^-$) anion.*[63]

Base	Acid	Base ($-\Delta H_{PA}$)	Dissolves cellulose
DBU	$EtCO_2H$	**248.88**	Yes
DBN	$EtCO_2H$	**246.44**	Yes
DMP	$EtCO_2H$	**246.14**	Yes
TMG	$EtCO_2H$	**244.88**	Yes
DMAP	$EtCO_2H$	*238.01*	No
Hünigs	$EtCO_2H$	*235.93*	No
DIPA	$EtCO_2H$	*232.16*	No
EIM	$EtCO_2H$	*230.31*	No
Pyr	$EtCO_2H$	*220.68*	No

1.6 IONIC LIQUIDS FOR BIOMASS PROCESSING

There are several approaches to treat biomass with ILs. In one of the most common procedures, an IL is mixed with biomass and dissolution or extraction occurs. Non-dissolved materials are simply filtered off before the addition of the anti-solvent. In the optimal case, this procedure allows for selective precipitation of cellulose which is typically the least soluble material in the IL. Another precipitation step is usually used for collection of the lignin fraction. The advantage of this type of process is that it is potentially extremely

simple, and it only contains simple separation processes and straightforward reuse of the solvent. However, the drawback is that the solvent is never genuinely recycled; rather it is reused without further purification (**Figure 12**). This factor may lead to continuously decreasing performance of the solvent.[64]

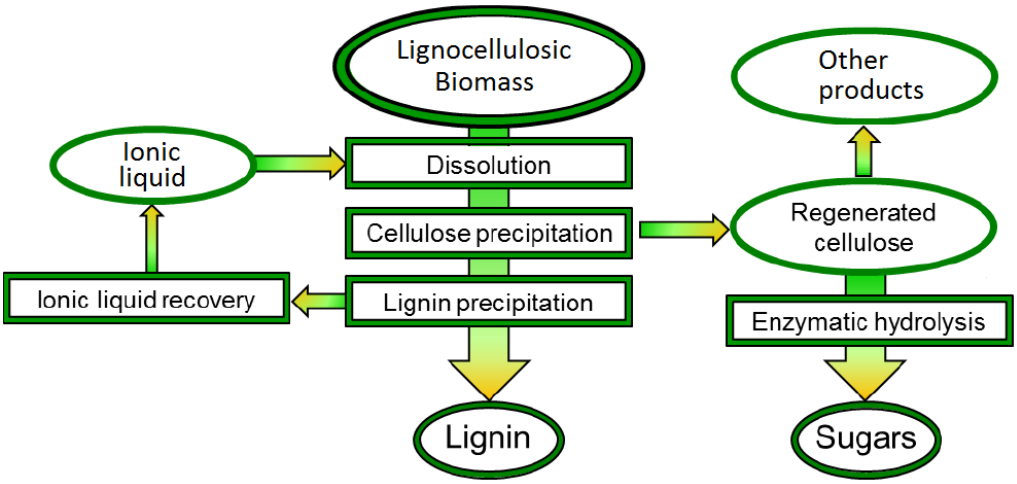

Figure 12 Generic process scheme for complete dissolution of lignocellulosic biomass with ILs. Adopted from ref. 64, with permission from the authors.

Kyllönen *et al.* reported that the dissolution of wood can be enhanced when using non-derivatizing ILs by extensively milling wood. This suggestion is based on the finding that the milling drastically increases the number of OH-groups on the surface that become available for hydrogen bonding with the IL and thus allow for increased solubility. [65]

ILs are typically highly viscous solvents, and this property might lead to mass transfer issues in processing. By using molecular solvents with ILs, the viscosities of the solutions are drastically reduced.[66] Rinaldi showed that it is possible to advantageously affect cellulose dissolution by the addition of a molecular solvent to the IL before obtaining a homogeneous cellulose solution. Surprisingly, only a small molar fraction of IL is sufficient for rapid dissolution. In fact, he described 'instantaneous' dissolution of cellulose in [emim][OAc] electrolyte solution containing 1,3-dimethyl-2-imidazolidinone (DMI) as the molecular solvent.[67]

There have been many other examples of cellulose dissolution and derivatization.[68,69] Kilpeläinen *et al.*[53] showed that certain imidazolium-based

ILs can dissolve powdered wood, sawdust, and even wood chips to some degree (**Table 3**).

Table 3. *Dissolution results of attempts to dissolve wood of different particle sizes in [bmim]Cl and [amim]Cl.* [53]

IL	Sample	Conditions	Solubility
[bmim]Cl	Wood chips	130 °C, 15 h	Partially soluble
[amim]Cl	Pine powder	80 °C, 8 h	8 %
[amim]Cl	Spruce sawdust	110 °C, 8 h	8 %
[amim]Cl	Spruce sawdust	80 °C, 24 h	5 %
[bmim]Cl	Spruce sawdust	110 °C, 8 h	8 %

Subsequently, [emim][OAc] was compared with [bmim]Cl for the ability to dissolve wood particles of different sizes.[70] Lan *et al.* fractionated bagasse into cellulose, hemicelluloses and lignin using [bmim]Cl. They were collected polysaccharide fraction with a significantly reduced lignin content. There were notable color changes after reusing the solution (**Figure 13**). [71]

Figure 13 Discoloration after reusing [bmim]Cl. Fresh IL on the left followed by cycles 1, 2 and 3. Adopted from ref. 71, with permission from American Chemical Society.

Pretreatment with ILs can drastically enhance the enzymatic digestibility of biomass.[72] For example, Fu *et al.* showed that the lignin content of wheat straw is reduced from 15.0 to 8.2 % when using [emim][OAc], and enzymatic digestibility is increased up to 97.6 wt%.[73]

Abe *et al.* showed that cellulose can be rapidly dissolved in large quantities in a solution of tetra-*n*-butylphosphonium hydroxide ($[P_{4444}][OH]$) that contains 40 % water. [74] They were also successful in dissolving wood disks in aqueous $[P_{4444}][OH]$; however, the dissolution took up to several months.[75]

The potential of $[P_{4444}][OH]$ was further studied by gentle heating and using hydrogen peroxide (H_2O_2) as an additive that could advantageously affect the dissolution of woody biomass.[76] Pretreatment of rice husks with aqueous $[P_{4444}][OH]$ was studied by Lau *et al.*[77] They reported enhanced yields for enzymatic and acid hydrolysis. They also found that the lignin and silica contents are greatly reduced by their process.

Switchable ionic liquids (SILs) are obtained by mixing an alcohol with a strong organic base, such as 1,8-diazabicyclo[5.4.0]undec-7-ene (DBU). The SIL becomes active when an acidic gas (e.g. CO_2) is introduced into the mixture. The IL properties are lost by bubbling an inert gas, such as N_2, which causes release of the acidic gas, and the solution again behaves like a common mixture of solvents. This finding indicates that the system is reversible (**Figure 14**). Moreover, the solvent properties of the amine-alcohol solution compared to the active SIL are very different. [78,79]

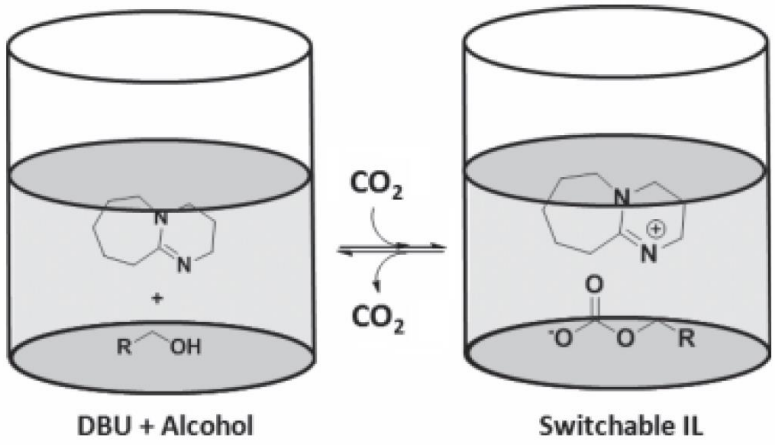

Figure 14 The general principle of the reversibility of switchable ionic liquids (SILs). Adopted from ref. 80, with permission from John Wiley & Sons.

In the case of cellulose dissolution, the alcohol can potentially be cellulose. Furthermore, a homogenous solution can be obtained if DBU, cellulose, CO_2 and a co-solvent (i.e., dimethyl sulfoxide [DMSO]) are mixed.[81] Anugwom *et al.*[82] studied the SIL systems and their potential for selective fractionation of woody biomass.[83,84] They examined a SIL system of monoethanol amine (MEA) and 1,8-diazabicyclo-[5.4.0]-undec-7-ene (DBU) with acid gases such

as CO_2 or SO_2. They produced cellulose-rich fractions with reduced lignin contents. [85,86]

Liu *et al.*[87] introduced a family of ILs that can be synthesized from renewable biomaterials. They introduced a series of choline-based ILs paired with amino acids. These ILs were not very efficient as cellulose solvents; however, those are most likely a small fraction of the possible ILs of this kind.

Holding *et al.*[88] reported the dissolution of cellulose in tetraalkyl phosphonium–based ILs combined with DMSO as a co-solvent. They found that those mixtures were non-derivatizing and could dissolve large quantities of cellulose. Interestingly, those ILs did not dissolve cellulose but the addition of co-solvent allowed for the dissolution (**Figure 15**). The maximum cellulose dissolution capability was reached at approximately 40 w/w% of DMSO as a co-solvent. They also stated that these organic electrolyte solutions (OES) have the potential to be recycled *via* phase separation. The recovery of those ILs can be significantly improved by using certain kosmotropic salts.

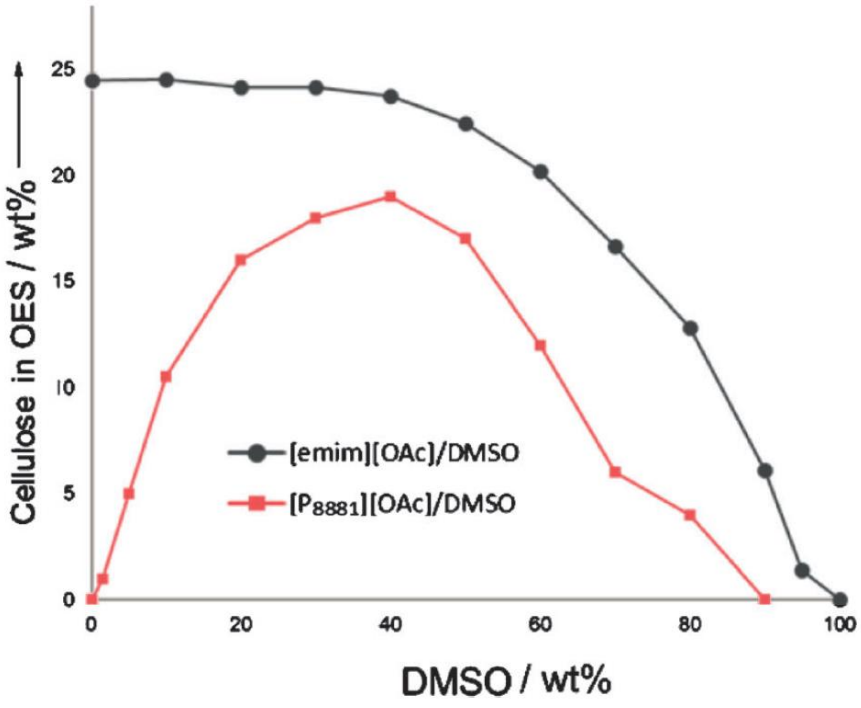

Figure 15 Cellulose dissolving capabilities of [emim][OAc] and [P_{8881}][OAc] in relation to the amount of dimethyl sulfoxide (DMSO) in the solvent system. Adopted from ref. 88, with permission from John Wiley & Sons.

Notably, [DBNH][OAc] can dissolve large quantities of cellulose and be used to advantageously shape regenerated cellulose fibers to produce 'man-made' cellulose fibers as an alternative for viscose and lyocell processes. This so-called IONCELL-F process can produce highly oriented cellulosic fibers that can have comparable and even higher tenacities than the commercial viscose and NMMO-based Lyocell fibers.[89] The sustainability of the IONCELL-F process has been studied in the experimental portion of this thesis.

1.7 THE COST OF IONIC LIQUIDS

One of issues with ILs is that they are often rather expensive; however, not all of them are costly. Chen *et al.* demonstrated that ILs can be synthesized from very affordable components. For example, triethylammonium hydrogen sulfate (**Figure 16**) and 1-methylimidazolium hydrogen sulfate were estimated to cost $1.24 and $2.96–5.88 per kg, respectively.[90] These prices are comparable to common solvents such as acetone or ethyl acetate, which cost $1.30–1.40 per kg. Later, they designed protic ILs based on [HSO_4] anion for pretreatment of lignocellulosics. They concluded that the cost any protic [HSO_4] IL will be determined by the choice of the amine (**Figure 16**) due the extreme affordability of sulfuric acid and the simplicity of the IL synthesis.[91]

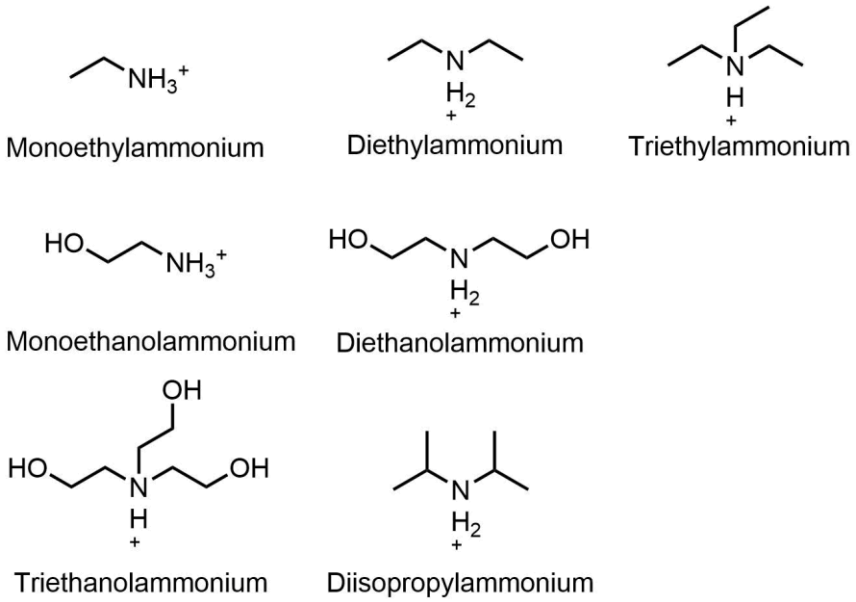

Figure 16 Some inexpensive cations for lignocellulose processing. Adopted from ref. 91, with permission from Royal Society of Chemistry

Fractionation of wheat straw and aspen with an extremely affordable aqueous IL, namely triethylammonium hydrogen sulfate ([TEAH][HSO_4]), was studied in the experimental portion of this thesis and compared to other recently developed organosolv methods and to a non-sulfated NaOH extraction.

1.8 THERMAL STABILITY OF IONIC LIQUIDS

In the past ILs have been generally described in the literature as thermally and chemically stable solvents.[92] This phenomenon is due to their typically very high decomposition temperature. It is slightly inaccurate to assume their stability because some ILs can undergo very slow decomposition at elevated temperatures. Shockingly, some of the most unstable ILs can decompose over time even when stored in the refrigerator under nitrogen.[93]

Thermal stability is a very important property for processes that operate above 100 °C. Short-term thermal stability can be assessed using thermogravimetric analysis (TGA). The stability of some common imidazolium ILs is shown in **Figure 17**.

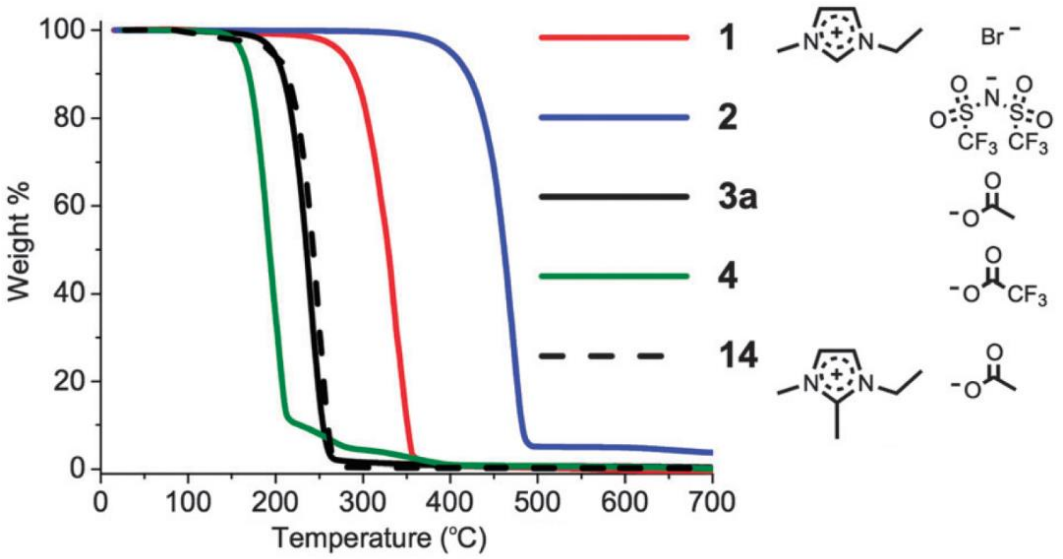

Figure 17 Decomposition results for some common ILs using thermogravimetric analysis (TGA). Adopted from ref. 93, with permission from the PCCP Owner Societies.

Phosphonium salts are typically more thermally stable than the corresponding ammonium salts, and even more stable than imidazolium salts. Phosphonium-based ILs typically yield only volatile decomposition products. ILs can polymerize upon decomposition if they consist of cyano anions and cyclic quaternary ammonium cation. [94]

There have been reports of using high temperatures to break down the recalcitrant plant cell wall structure. Li *et al.* studied the dissolution of bagasse and southern yellow pine in [emim][OAc] at 175–195 °C,[95] and Fu and Mazza treated wheat straw with [emim][OAc] at temperature range 130-170 °C.[96] Later, Clough *et al.* showed that at those temperatures [emim][OAc] is already highly unstable (**Figure 18**). [93]

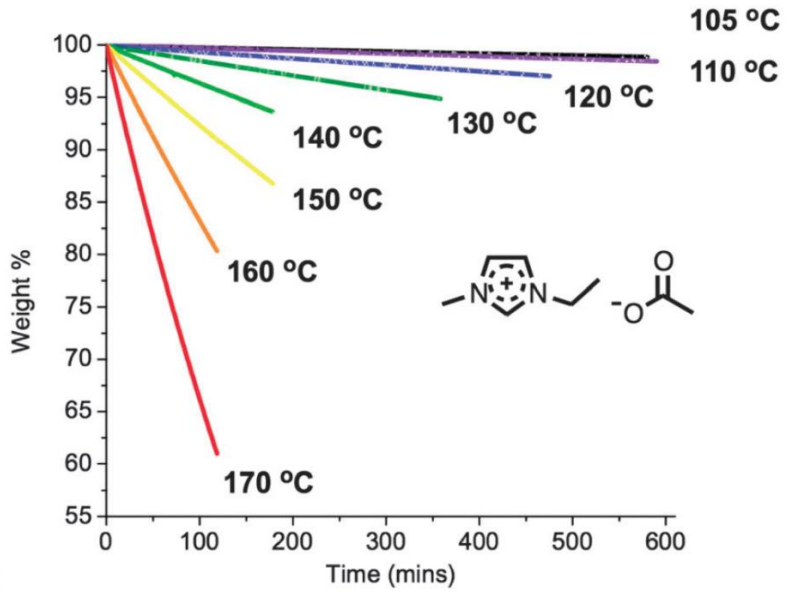

Figure 18 Decomposition of [emim][OAc] at elevated temperatures. Adopted from ref. 93, with permission from PCCP Owner Societies.

Imidazolium ILs composed of BF_4^-, PF_6^-, or NTf_2^- are reportedly more thermally stable compared to ILs composed of halides. The relative stability for anions seems to follow the order: $[PF_6]^-$ > $[BF_4]^-$ > $[AsF_6]^-$ >> I^-, Br^-, Cl^-. Inorganic anions can undergo endothermic thermal decomposition whereas with organic anions, such as $(C_2F_5SO_2)_2N^-$ and $(CF_3SO_2)_2N^-$ exothermic decomposition generally occurs, a phenomenon that is most likely a consequence of the sulfonyl groups.[94,97,98,99,100]

Furthermore, a comprehensive investigation has been published consisting of 66 different ILs; their stabilities were assessed with TGA methods. Carboxylate, dicyanamide-, and amino acid–containing ILs were the least thermally stable. Interestingly, the temperatures at which some decomposition had already occurred were significantly lower than the reported onset temperatures.[101] To support these data, Del Sesto *et al.* showed that common ILs such as [C_4mim][NTf_2] and [C_4mpyrrol][NTf_2] might already start degrading at 150 °C. Hence, the maximum operating temperature with ILs is considerably lower than their degradation temperature (e.g., the [emim][BF_4] degradation point is 455 °C but it decomposes at rate of 1.37 wt% per h at 200 °C). [102] It has become clear that degradation temperature overestimates the actual thermal stability.[103,104] Studies have collected information on the long-term IL thermal stabilities. For example, the stability of [bmim]Br has been investigated: In 10 hours more than 10 wt% can be lost at temperatures below its thermal decomposition temperature (**Figure 19**). [105]

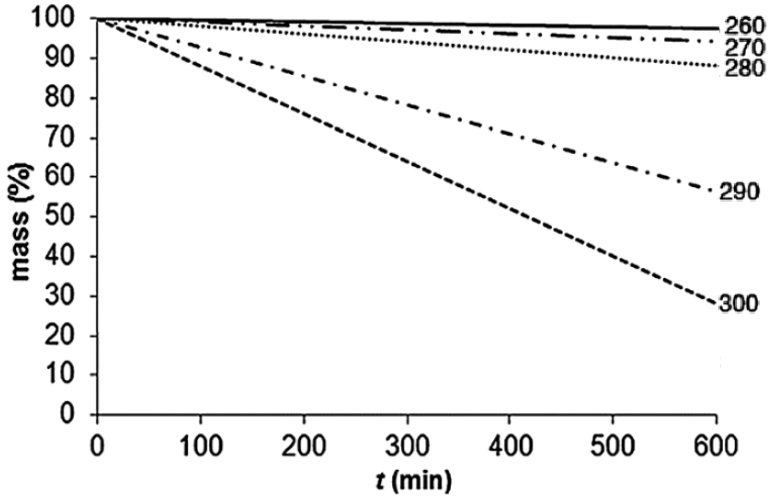

Figure 19 Isothermal thermogravimetric analysis (TGA) spectrum for [bmim]Br at different temperatures. Adopted from ref. 105, with permission from Springer Nature.

ILs have various decomposition pathways and their stabilities depend on their structures. In **Figure 20** some of the degradation pathways are illustrated. The decomposition pathways include rearrangements and various dealkylations. [106]

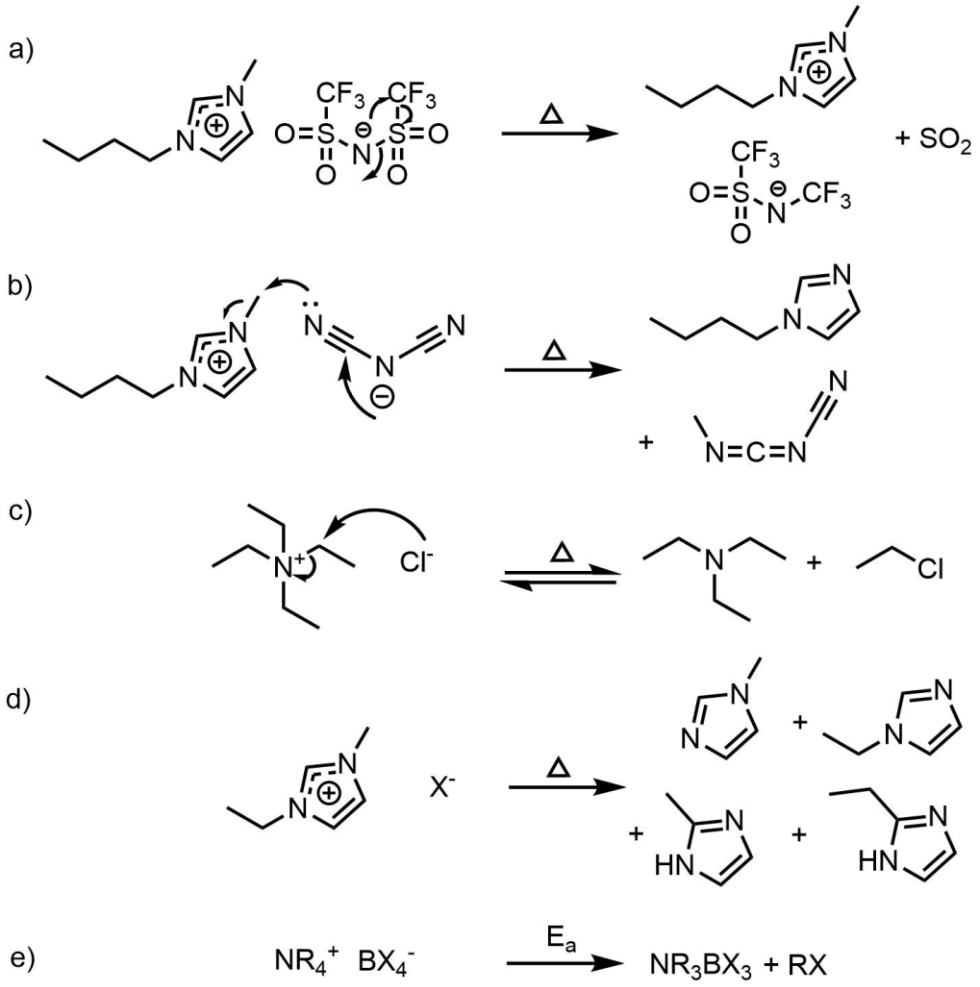

Figure 20 Some common decomposition pathways for ILs *via* dealkylation.[106]

The decomposition mechanism for phosphonium hydroxides was studied in the 1960s.[107] It seems that the hydroxides represent the most unstable species in the phosphonium family of ILs and organic electrolytes. ILs stability seems to be highly dependent on the anion.[108] Initial studies on the stability of $[P_{4444}][OH]$ mixtures were conducted with using proton nuclear magnetic resonance spectroscopy (^{1}H-NMR) and later extended with phosphorus nuclear magnetic resonance spectroscopy (^{31}P-NMR).[74,109] The instability of those solutions was subsequently confirmed at specific concentration and temperature ranges.[77] The decomposition products of phosphonium hydroxides are the corresponding phosphine oxides and hydrocarbons. For example, the decomposition products of $[P_{4444}][OH]$ are *n*-butane and corresponding phosphine oxide, tri-*n*-butylphosphine oxide (**Figure 21**).

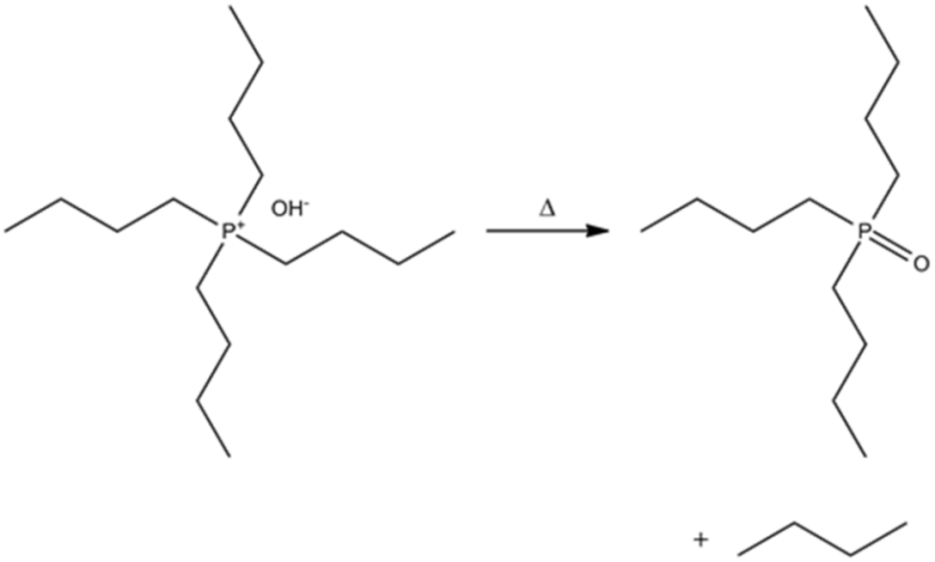

Figure 21 Thermal decomposition reaction of aqueous $[P_{4444}][OH]$.[109]

1.9 CHEMICAL STABILITY AND REACTIVITY OF IONIC LIQUIDS

ILs are usually studied in synthetic organic chemistry as solvents and/or catalysts. There are proof of the potentially reactive nature of some ILs that can alter reactivity of dissolved substrates, unexpected catalytic activities and in some cases unforeseen side product formations.[110]

One of the major issues for the imidazolium-based ILs is the acidity of the C_2 proton.[111] If the C_2 proton is released (**Figure 22**), a potentially reactive carbene is formed.[112,113] The carbene can lead to unexpected side reactions.[114,115]

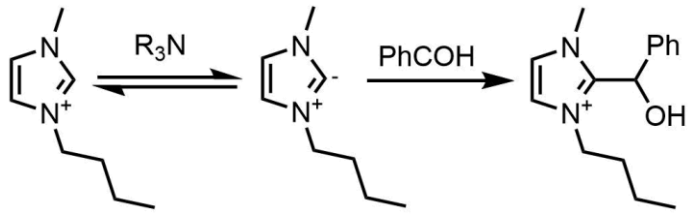

Figure 22 Proton release and nucleophilic attack by the imidazolium ring. Spontaneous carbene formation at the same position is also possible when heated.[115]

When a carbene is formed, ILs can react with cellulose during the dissolution by covalently binding to cellulose.[116] Heinze *et al.*[117] studied the

interactions with IL cations using simple model systems of cellulose (such as cello-oligomers [DP = 6–10]). One of the carbon signals of the glucose unit disappeared after dissolving the model compound to [emim][OAc]. This finding suggested the formation of a new covalent bond between glucose and the imidazolium ring. This phenomenon was later verified with ^{13}C-isotopic and fluorescence labeling by Ebner *et al.* They also stated that the bond formation is strongly catalyzed by bases.[116] In fact, the bond formation can be suppressed by the absence of bases.[118] This fact is probably an issue of the purity of the IL. Indeed, the reactivity of the C_2 position in dialkylimidazolium is well known and documented in the field of nitrogen heterocycle carbene chemistry.[118]

Faria *et al.*[119] studied the reactivity of [amim][$N(CN)_2$] under high pressure and found oligomerization of the cation (**Figure 23**). They noted that this reaction could provide novel insight in developing new synthetic routes for poly(ILs).

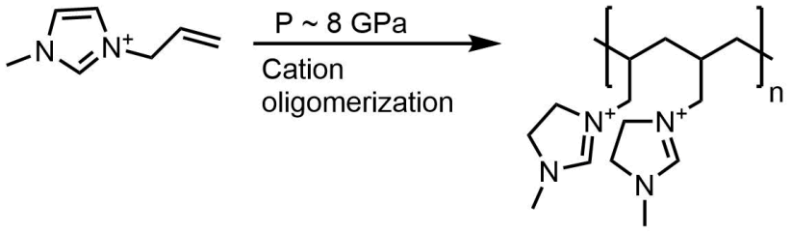

Figure 23 Cation oligomerization of [amim][$N(CN)_2$] under high pressure.[119]

Tseng *et al.*[120] reported an alkylation reaction using tetraalkylphosphonium chlorides with benzoate salts. In the reaction, tetraalkylphosphonium donates an alkyl group to the benzoate to yield aromatic ketones (**Figure 24**). The reaction might not be useful because it allows for low conversions and requires microwave assistance and a relatively high temperature. However, as a side reaction it should not be overlooked.

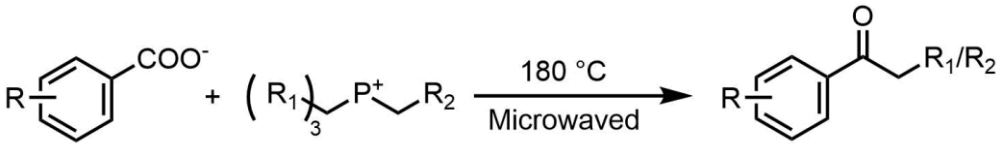

Figure 24 Tetraalkylphosphonium salt donates one of its alkyl groups to form aromatic ketones.[120]

The stability of the anion is important for the ILs in their applications and toxicity studies. In the presence of a halogen anion, there may be a serious concern if the hydrolytic stability of the anion is not sufficient. Indeed, additional efforts are required to avoid the liberation of toxic and corrosive compounds such as HF, HBr or HCl. Some of the homologues of alkyl sulfate anions, such as methyl and ethyl sulfate, are known for their sensitivity to hydrolysis.[121,122] At elevated temperatures–and in the presence of H_2O–these anions can form the corresponding alcohols and hydrogen sulfates. These side reactions are highly undesirable because the IL can have dramatically altered properties after the ion exchange. In addition, an acidic proton can be formed that may be reactive in many situations. For long-chain alkyl sulfates, the sensitivity towards hydrolysis is lower.[121,122] ILs with PF_6^- ions can be hydrolytically unstable. They have the potential to release compounds such as HPO_2F_2, H_2PO_3F, H_3PO_4, and highly toxic and corrosive HF as decomposition products. Some of the non-catalyzed reactions in PF_6^-–containing ILs are suggested to be catalyzed by unintentionally formed HF. [44,123]

Various alkyl halides were converted to alkyl thiocyanates with high yields by using [bmim][SCN] as a reagent and solvent (**Figure 25**). The IL can be conveniently regenerated using KSCN, a feature that renders it viable for use the expensive IL component as a reactant.[124]

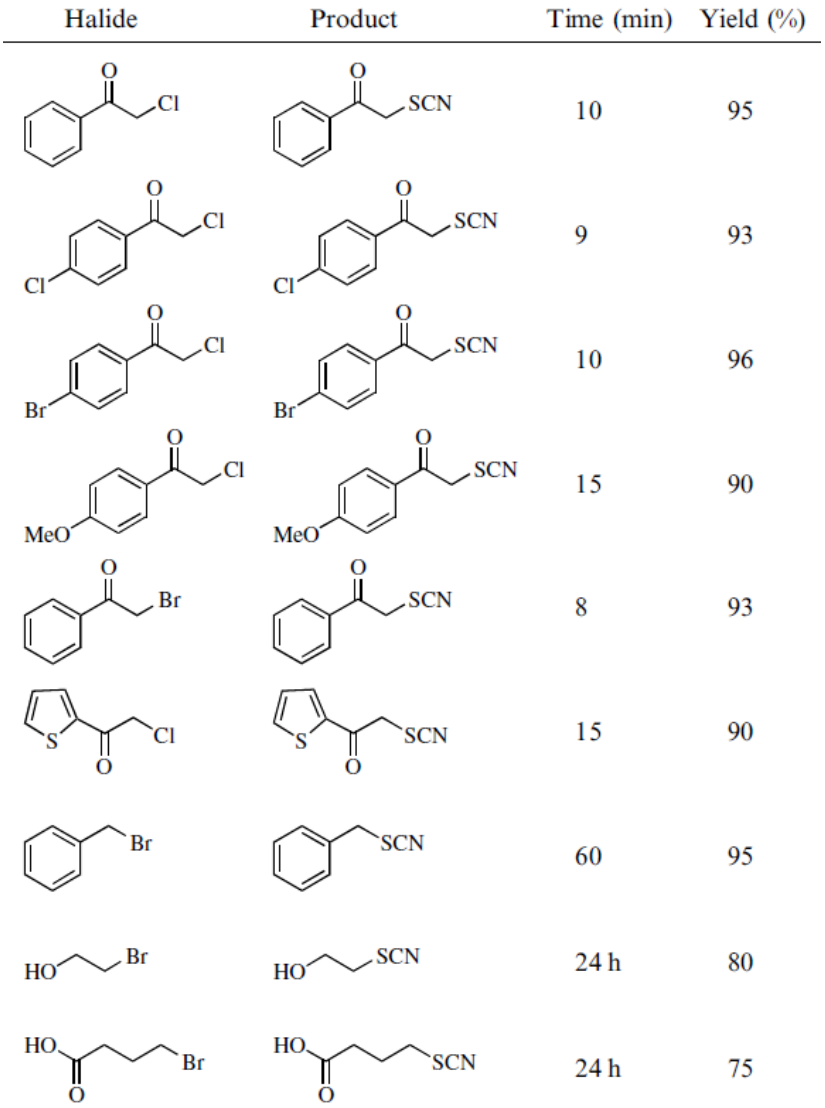

Figure 25 Reactions between alkyl halides and [bmim][SCN] to yield alkyl thiocyanates. Adopted from ref. 124, with permission from Elsevier.

1.10 SUMMARY

New materials and methods are needed to combat global warming and to eventually replace fossil-based materials and products. As the world population increases, challenges related to a sustainable future will become even more urgent. One of the big issues is the limited cotton production for textiles. Therefore, there is an increasing pressure to produce man-made fibers in order to produce clothing and other textiles for the growing population. An attractive choice for this application is cellulose that is isolated from sources other than cotton. Cellulose can also potentially replace other fossil-based

materials such as plastic in certain applications. Moreover, liquid fuels can be produced from cellulose *via* saccharification and fermentation, among other reactions.

There is currently worldwide research about producing renewable materials that have competitive properties compared to products we have today. The driving force for this goal is the depletion of fossil supplies and environmental issues such as global warming and the accumulation of plastic waste in the sea. Cellulose-based materials represent solutions for these issues. However, cellulose is not easy to convert into products due to its insolubility. ILs and electrolyte solutions can dissolve cellulosic fibers and cellulose can be potentially obtained and advantageously modified in this media.

ILs have numerous advantageous and disadvantageous traits. For example, ILs are typically non-volatile, which is an excellent trait because they do not emit any volatile organic compounds (VOCs). However, this feature makes them difficult to recycle because in most cases they cannot be distilled. Dissolved material can potentially accumulate in the IL and reduce the efficiency of the solution in the process, a phenomenon that can ultimately lead to IL waste.

ILs are typically relatively expensive. Currently, they are not mass produced in such a volume that their prices would be at the same level as industrial organic solvents; therefore, there is no fair direct cost comparison.

Like any compounds, ILs can be reactive. Although they are typically chemically stable, they do have inherent reactivity that derive from the nature of the cation or the anion. For example, the imidazolium reactivity is difficult to control unless the acidic proton is substituted with another moiety (e.g., alkyl group). This substitution naturally increases to the cost of the production of such ILs. In some rare cases, the reactivity can be harnessed for advantageous use, e.g., catalytic conversions, whereas an IL can act as a catalyst and a solvent.

Overall, ILs have many peculiar properties, and because the number of different ILs is countless, there is always a potential to find new ILs for a specific task.

2 AIMS OF THE STUDY

This thesis comprises of two main research topics: the fractionation of biomass utilizing ILs and the chemical stability of ILs.

The first research goal was to study whether hydrophobic ILs have beneficial attributes when used in processing biomass. This was aim studied by the fractionation of wheat straw and post-process technical lignin using hydrophobic phosphonium ILs.

The second goal was to utilize aqueous $[P_{4444}][OH]$ solution to fractionate wheat straw and produce carbohydrate-rich fractions while extracting most of the lignin and silicates (**I**). The third goal was to determine the thermal stability of the aqueous $[P_{4444}][OH]$ solution (**I**).

The next goal was to improve the fractionation of wheat straw and aspen using hot water extraction (HWE) before the actual cooking. The hypothesis was that the HWE would be a convenient way to extract most of the hemicelluloses while simultaneously increase the effectiveness of the actual fractionation process (**II**).

Another research hypothesis was that inorganic compounds in pulp may accumulate in the IL after it is reused several times (**III**).

The next research hypothesis was that because DBN is hydrolytically unstable, the acetate salt [DBNH][OAc] may also be hydrolytically unstable. The goal was to assess recyclability of [DBNH][OAc] by determining its hydrolytic stability with high-performance liquid chromatography (HPLC) analysis (**IV**, **V** and **VI**).

3 RESULTS AND DISCUSSION

This section covers the experimental work of this thesis. The experimental work was conducted from January 2012 to January 2018. The work presented in this section explores the fractionation of biomass and the chemical stability of ILs. This section starts with the synthesis of a hydrophobic phosphonium IL and fractionation of wheat straw with it and three other hydrophobic phosphonium ILs (Chapter 3.1) followed by fractionation of technical lignin with hydrophobic phosphonium ILs (Chapter 3.2). The synthesis of IL precursors (DBN-derivatives) is presented in Chapter 3.3, which is followed by determining the chemical stability of DBN-based ILs (Chapter 3.4). The chemical stability of aqueous $[P_{4444}]OH$ solution is presented in Chapter 3.5, followed by fractionation of wheat straw using $[P_{4444}]OH$ in Chapter 3.6. A comparison of a variety of solvent systems for the fractionation of aspen and wheat straw is presented in Chapter 3.7. All experimental details are in Chapter 4 in the same order as the work presented in this chapter.

3.1 SYNTHESIS AND APPLICATIONS OF PHOSPHONIUM IONIC LIQUIDS

Many ILs are synthesized by a simple alkylation (typically methylation or butylation) of an organic compound which leads to a positive charge on a hetero atom (typically nitrogen or phosphorus). Consequently, an organic salt is formed as a result. If this organic salt is in liquid form below 100 °C it can be called an IL. There are countless organic salts that can be synthesized this way; however, currently the most useful ILs for processing lignocellulosic biomass include phosphonium and ammonium salts, imidazolium salts, and the protic salts of nitrogen containing superbasic compounds such as TMG, DBN and DBU (see **Figure 5** for their structures).

Tetraalkyl phosphonium salts can have a hydrophobic character depending the alkyl chains and the anion. Trioctylmethylphosphonium triflate ($[P_{8881}][OTf]$) was synthesized from trioctylphosphine (P_{888}) and methyl triflate. The reaction can be performed without a solvent (**Figure 26**). Methyl

triflate is a strong methylating agent and will rapidly methylate a phosphine to form a phosphonium triflate salt.

P_{888} can oxidize in air to trioctylphosphonium oxide (OP_{888}) which seemed to be unreactive in methylation. The OP_{888} content in the synthesized $[P_{8881}][OTf]$ was determined to be about 8 mol% using ^{31}P NMR. The ability to extract the phosphonium oxide side product out of the IL with various solvents and solvent systems was studied without success.

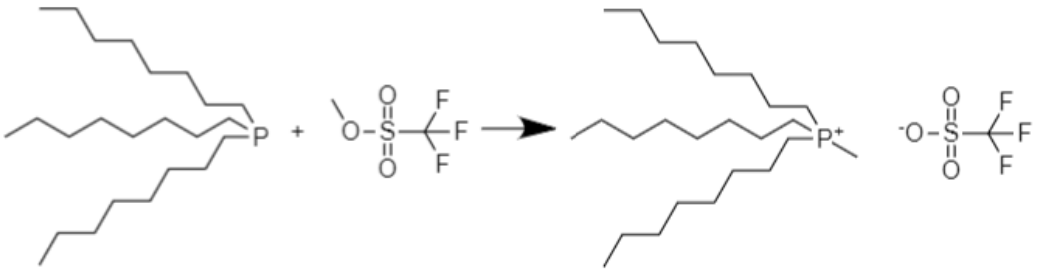

Figure 26 Reaction between trioctylphosphine and methyl triflate to form $[P_{8881}][OTf]$.

$[P_{8881}][OTf]$ accompanied with commercially available hydrophobic phosphonium salts such as trihexyl(tetradecyl)phosphonium chloride ($[P_{14666}]Cl$), triisobutylmethylphosphonium tosylate ($[P_{4441}][OTs]$) and trihexyl(tetradecyl)phosphonium dicyanamide ($[P_{14666}][DCM]$) was used to extract wheat straw. Only swelling was observed, likely because the collected wheat straw inhibited an increased weight even after washing. The ILs penetrated the straw but were very difficult to remove. Furthermore, they seemed to require excessive washing in boiling solvents.

In the research, $[P_{14666}]Cl$ had a synergistic effect with HCl: This mixture significantly extracted material from wheat straw, but this finding was previously reported in the literature.[125]

3.2 IMIDAZOLIUM SALTS WITH A HYDROPHOBIC ANION FOR FRACTIONATION OF TECHNICAL LIGNIN

Hydrophobic imidazolium-based ILs 1-ethyl-3-methylimidazolium dimethyl phosphate ([emim][DMP]), 1-ethyl-3-methylimidazolium tricyanomethanide

([emim][TCM]) and 1-ethyl-3-methylimidazolium triflate ([emim][OTf]) were used to fractionate technical lignin. These liquids were compared to common laboratory solvents. The objective of this study was to investigate whether there is any benefit to using ILs in order to improve the quality of the technical lignin. Lignin with low solubility is assumed to be more condensed and thus less reactive than the more soluble portions. Therefore, the less soluble portion is regarded as less useful. Traditional laboratory solvents do not dissolve lignin very efficiently without derivatization.

To study the effectiveness of the ILs in lignin fractionation, technical lignin was mixed with IL and the mixture was stirred at room temperature or 50 °C. Precipitation was induced in two steps with water. The weight percentages of the collected fractions are shown in **Table 4.**

Table 4. *Yields for fractionation of lignin (percentage of dry technical lignin) with hydrophobic [emim] salts.*

		RT			50 °C		
	Material description	[emim] [DMP]	[emim] [TCM]	[emim] [OTf]	[emim] [DMP]	[emim] [TCM]	[emim] [OTf]
1	Insoluble	64.7	11.2	73.7	17.9	0.0	11.2
2	1st precip.	22.3	8.9	3.3	50.2	21.2	49.1
3	2nd precip.	10.0	35.7	1.1	3.3	40.2	30.1
4	Remains in IL	3.0	44.2	21.9	28.6	38.6	9.6

At room temperature conditions, only [emim][TCM] effectively dissolved lignin. However, large portions of the dissolved lignin remained in the IL after both additions of water as the antisolvent. [emim][DMP] and [emim][OTf] poorly dissolved lignin at room temperature. [emim][DMP] responded well to the addition of anti-solvent; only 2.9 % of the lignin was not found in the solid fractions. The response to the anti-solvent with [emim][OTF] was very poor: The vast majority of the dissolved lignin stayed in solution. This phenomenon can be partially explained by the difficult centrifuging of the solution.

When the mixtures were heated to 50 °C, the ILs were much more effective at dissolving lignin. In the case of [emim][TCM] all lignin was dissolved and more than 60 % of it could be precipitated. [emim][DMP] and [emim][OTf]

dissolved lignin quite efficiently and most of the lignin could be precipitated. Furthermore, there were fewer difficulties experienced in centrifugation.

Technical lignin was only partially dissolved in traditional laboratory solvents (1-butanol, acetone, dimethyl carbonate, ethyl acetate and ethanol). Gel permeation chromatography (GPC) results of the collected fractions are shown in **Figure 27** (in comparison to the untreated technical lignin).

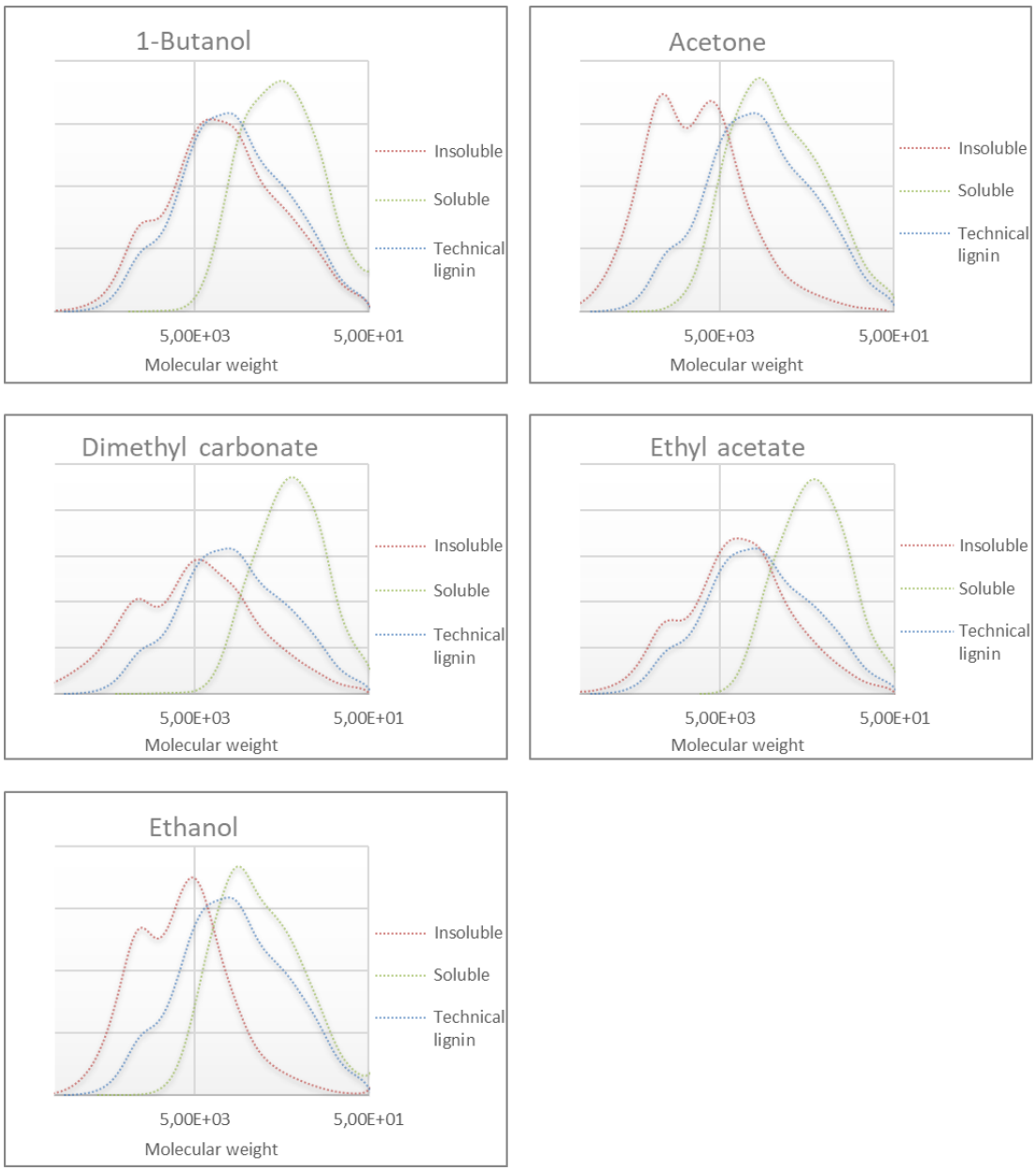

Figure 27 Gel permeation chromatography results of collected fractions using common laboratory solvents. The samples were acetylated and dissolved in THF prior to analysis and all chromatograms were normalized.

The advantage of using traditional solvents is their volatility; consequently, all the lignin can be collected by simply distilling off the solvent after centrifugation and finally drying in an oven. The data revealed that the solvents dissolved only the lower molecular weight fraction; most of the higher molecular weight fraction was not dissolved. There were significant differences in the abilities of the solvents to dissolve the technical lignin. Acetone dissolved almost all of the technical lignin, while other solvents only partially dissolved it. For fractionation purposes, acetone was probably the most promising solvent because it left only the highest molecular weight fraction undissolved.

In conclusion, it was difficult to find any advantages using ILs over traditional solvents for this application. The most problematic issue was that all of the lignin could not be precipitated from the IL. This deficit would likely make the recyclability of the IL in this process extremely difficult. Arguably, more anti-solvent would have been needed to increase the precipitate yields. However, the scope of this research was to use relatively small amounts of anti-solvent to reduce the energy requirement for solvent evaporation and to study the difference of response to the anti-solvent among the ILs.

3.3 SYNTHESIS OF PRECURSORS FOR IONIC LIQUIDS WITH INCREASED HYDROLYTIC STABILITY

Using computer simulations, the research group concluded that 9-methyl-1,5-diazabicyclo(4.3.0)non-5-ene (9-mDBN) might be more hydrolytically stable than the commercially available DBN. The group started a project for the synthesis of 9-mDBN by using natural products such as gamma-valerolactone (GVL) or levulinic acid (LA) as raw materials. The final goal was to synthesize [9-mDBNH][OAc] IL. It was assumed to have similar capabilities to dissolve large quantities of cellulose, along with increased hydrolytic stability in comparison to [DBNH][OAc].

The first attempt was to let GVL react with diamino propane (DAP) at high temperatures according to patents.[126,127,128] The desired reaction pathway is shown in **Figure 28**.

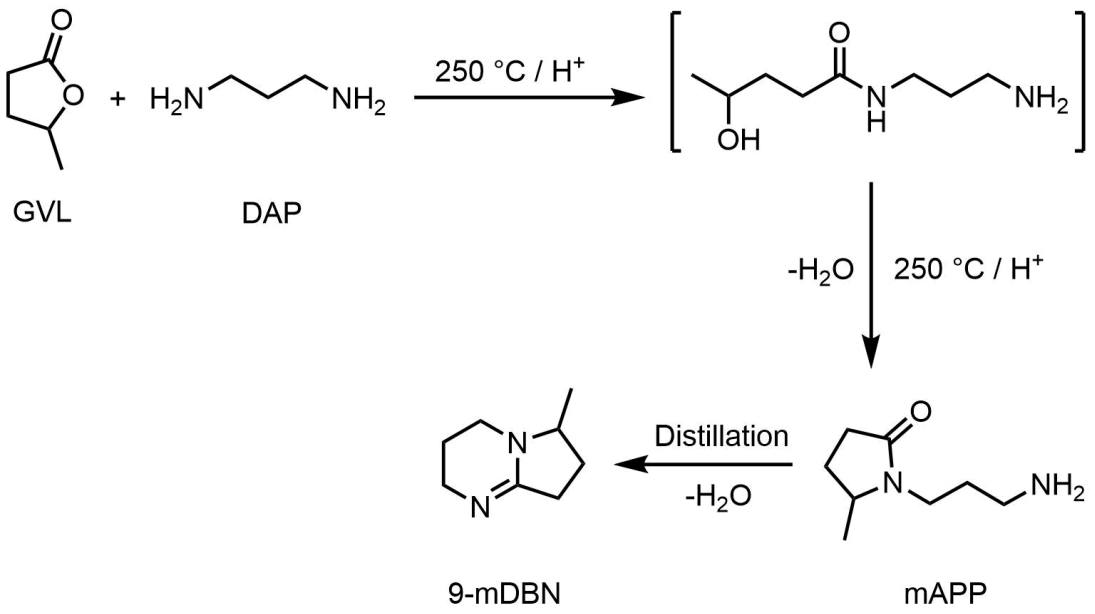

Figure 28 Synthesis route for 9-mDBN from GVL and DAP.

By changing the reaction conditions with this reaction pathway, typically very small fraction of the reaction mixture yielded 1-(3-aminopropyl)-5-methylpyrrolidin-2-one (mAPP). From one reaction mixture, the dehydrative distillative (last step) was performed, and 9-mDBN was isolated with a poor yield (below 10 %) and at technical purity. An acetate salt of this product was made, and 5 w/w% of microcrystalline cellulose was successfully dissolved in it. Obviously, the yield and purity from the synthesis was not satisfactory. Nevertheless, these data demonstrated that 9-mDBN could be synthesized from mAPP by distillation. Another reaction pathway was tested for the synthesis of mAPP; it utilized Raney nickel (RaNi) catalyzed reductive chemistry (**Figure 29**).

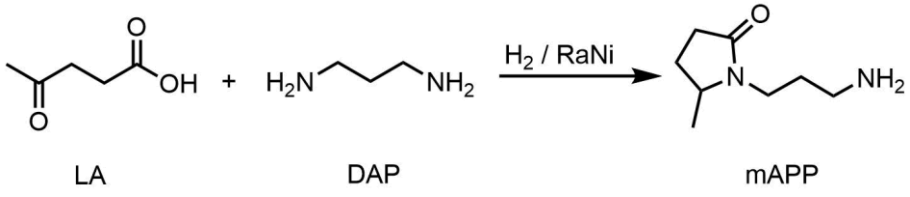

Figure 29 Synthesis of mAPP with reductive RaNi chemistry from LA and DAP.

The synthesis in **Figure 29** yielded the desired product (mAPP); however, many side reactions occurred (**Figure 30**). Analysis of the crude reaction

mixture was challenging because some of the products were non-volatile. Therefore, only rough estimations based on gas chromatography–mass spectrometry (GC-MS) analysis were possible(**Figures 44–52.)**. Furthermore, the complementary NMR-analyses were challenging given the complex reaction mixtures. In **Table 5** some of the conducted experiments are shown with a rough estimate of product distribution.

Table 5. *Some examples of the conducted experiments and rough relative product distribution based on gas chromatography–mass spectrometry (GC–MS) data in order to synthesize mAPP with reductive RaNi chemistry. The structures of the side-products **1**, **2** and **3** are shown in **Figure 30**.*

	LA (g)	DAP (g)	RaNi (g)	H_2O (g)	tBuOH (g)	T (°C)	t (h)	H_2 cons.	mAPP	**1**	**2**	**3**
1	2	9	0.4	21	0	100	24	n.r.	5	*	5	0
2	2	3.1	0.4	25	0	140	5	n.r.	2	*	7	0
3	2	3.1	0.4	22	0	80	16	n.r.	9	*	1	0
4	2	3.1	2	25	0	100	16	n.r.	10	*	<1	0
5	2	3.1	2	0	0	80	20	65 %	7	*	3	1
6	2	3.1	2	5	20	60	20	87 %	9	*	1	<1
7	2	3.1	2	5	20	40	20	44 %	**	*	**	**
8	2	1.5	2	5	20	60	20	156 %	10	*	<1	1
9	2	1.5	2	0	25	40	40	136 %	0	*	0	0

Product distribution is expressed in equivalents found in GC-MS chromatograms; their sum were normalized roughly to approximately 10. The results are not quantitative due to the lack of standards.

n.r. H_2 consumption not recorded.

* Product **1** did not appear in the GC chromatograph due to its low volatility

** Not analyzed because of low H_2 consumption.

In addition to the desired product (mAPP), the formation of a few side products was observed in most cases. The possible reaction route for these side products is shown in **Figure 30**.

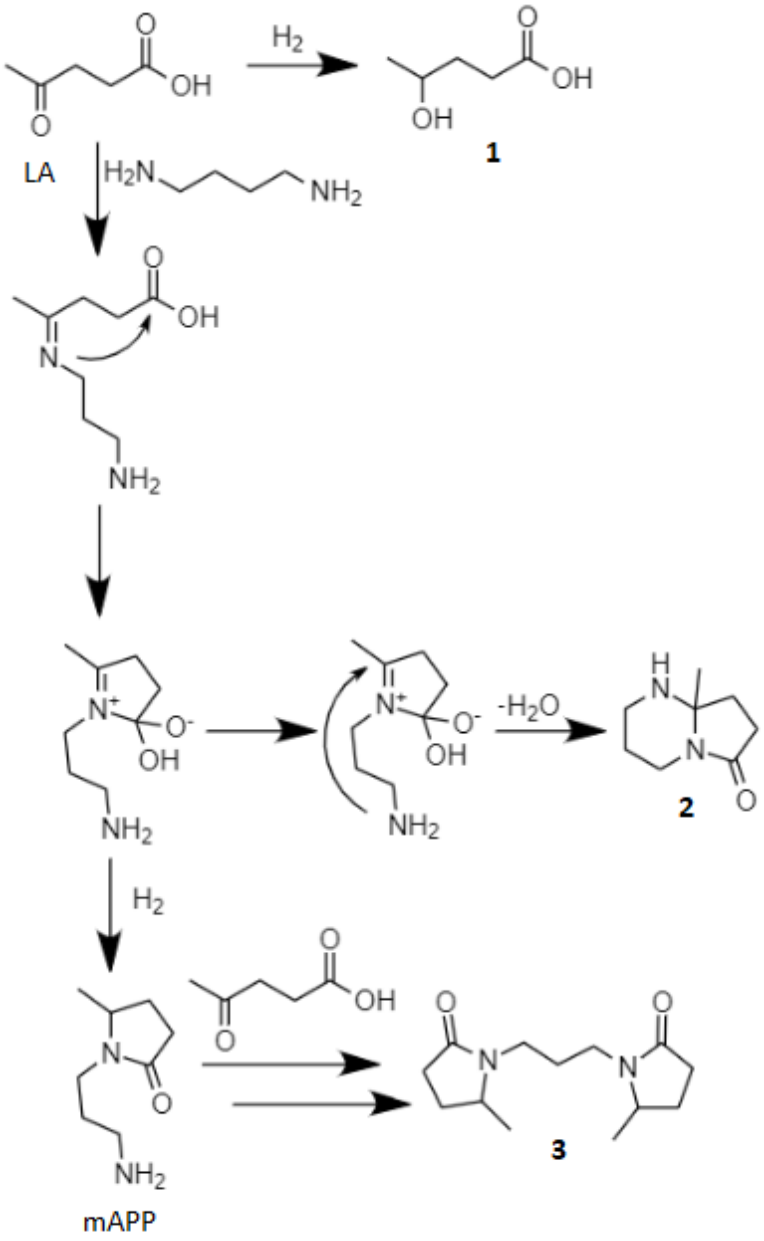

Figure 30 Formation of side products **1**, **2** and **3** in the synthesis of mAPP with reductive RaNi chemistry.

In the first side reaction, LA was reduced to 4-hydroxy valeric acid which no longer undergoes the desired reaction with DAP (**Figure 30**). In the second side reaction the cyclization step was desired and followed by a competitive step between the reduction to mAPP and the intramolecular addition to the double bond. The addition reaction formed a double ring compound that is not a superbase (compound **2**, **Figure 30)**. The third major

side reaction was the reaction between mAPP and LA (compound **3**, **Figure 30)**.

There were ostensibly a few successful reaction set-ups. However, most of them also contained a significant amount of side product **1** (based on NMR analysis, data not shown). The majority of the detected product was mAPP but at the time it was decided to test other synthesis routes to obtain purer product with fewer side reactions. Other synthesis routes, such as reduction over Pd/C and reduction with $NaBH_4$, were examined using LA and DAP as starting compounds. These reactions conditions did not yield the desired mAPP.

In conclusion, several pathways were tested in order to synthesize 9-mDBN *via* mAPP with only moderate success. The reduction at high H_2 pressure over RaNi seemed to give reasonable yield of mAPP according to H_2 consumption; however, the products in those experiments were never isolated. Overall, the amount of the side product **1** is significant and unavoidable at these conditions. The quantity of **1** was difficult to analyze because it was not volatile enough to appear in the GC analysis. In addition, the starting materials did not show in the GC chromatogram. Therefore, the H_2 consumption was the only indication of possible desired reactions. With NMR, it was possible to get rough estimates of the product distribution, but this method was unreliable due to overlapping signals. The analysis was also tested with liquid chromatography–mass spectrometry (LC-MS), but the quantification of products was not possible because all products did not separate in the chromatogram. Quantification would have also required pure calibration standards.

3.4 RECYCLABILITY IN THE IONCELL-F PROCESS

The protic distillable IL 1,5-diazabicyclo(4.3.0)non-5-eneium acetate ([DBNH][OAc]) has been shown to have excellent direct-dissolution capabilities for dissolving cellulose; in IONCELL-F lyocell processing it can produce high tenacity fibers.[89] These fibers can potentially be used in textile production. As a potential downside, DBN as a free base is highly susceptible to hydrolysis in aqueous solutions; however, the stability of its acetate salt was

unknown. This factor may potentially complicate the recycling [DBNH][OAc] in processes where it is in contact with water. Water has been typically used as an anti-solvent in recovering dissolved cellulose. After cellulose regeneration water must be removed from the IL *via* distillation. This process can cause hydrolysis of the IL. In this work, the hydrolysis kinetics of [DBNH][OAc] were measured using HPLC analysis. [129,130]

The most relevant temperature range to study the stability of [DBNH][OAc] was the common cellulose regeneration temperature applied in fiber spinning applications (60-90 °C).[131,132] This range is also the common water evaporation temperature under reduced pressures. The concentration range of 60–90 % [DBNH][OAc] in water was a wide enough to observe the concentration dependency of the hydrolysis reaction and the subsequent amide formation reaction (**Figure 31**).

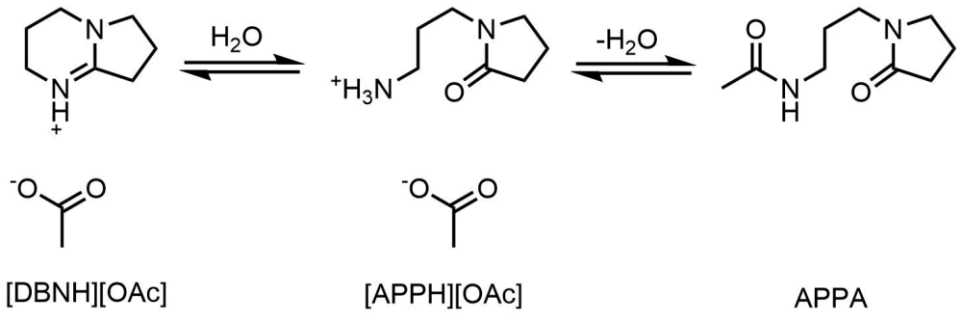

Figure 31 The hydrolysis pathway of [DBNH][OAc] to 1-(3-ammoniopropane)-pyrrolidin-2-one acetate ([APPH][OAc]) and further to a relatively stable product 1-(N-acetyl-3-aminopropane)-pyrrolidin-2-one (APPA). Reaction kinetics were measured with high performance liquid chromatography.

In the first reaction in **Figure 31** one can assume that a hydroxide ion attacks the ring to yield the corresponding ring-opening pyrrolidinone product [APPH][OAc]. This assumption is based on the fact that the hydrolysis reaction is very rapid for DBN, which as a superbase eagerly deprotonates water.[133] The acetate salt solution was found to be basic (confirmed with pH–paper) but it was predicted to have a significantly lower hydrolysis rate. In the second reaction, [APPH][OAc] further reacts to a relatively stable product, namely 1-(N-acetyl-3-aminopropane)-pyrrolidin-2-one (APPA; **Figure 31**).

The initial experiment was to heat a 90 % solution of [DBNH][OAc] in water to 90 °C, which is close to the boiling point of water and a realistic

processing temperature. The relative molar ratios of the analyzed compounds (DBNH, APPH and APPA) are shown in **Figure 32**.

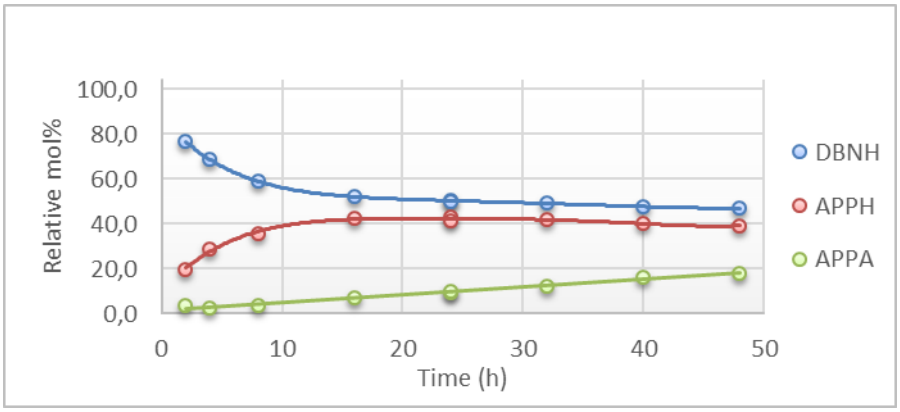

Figure 32 High performance liquid chromatography analysis results for the relative concentration of [DBNH][OAc], [APPH][OAc] and APPA after different reaction times (2–48 h) of 90 % [DBNH][OAc] in water.

[APPH][OAc] was initially formed fast; its concentration reached the maximum when the formation of APPA was as fast (or faster) than the formation of [APPH][OAc] (**Figure 32**). The following linear phase of [DBNH][OAc] hydrolysis seemed to have a steady phase that was roughly the same rate at which APPA was formed, while the concentration of [APPH][OAc] remained nearly constant (**Figure 32**).

Interestingly, the hydrolysis reaction for [DBNH][OAc] seemed to be faster when less water was present. Additionally, the reaction was extremely slow at very dilute concentrations, e.g., HPLC or NMR sample concentrations. In **Figure 33** the relative concentration of [DBNH][OAc] is shown over the course of 2–48 h at different temperatures with varying initial concentrations of [DBNH][OAc] in aqueous solution.

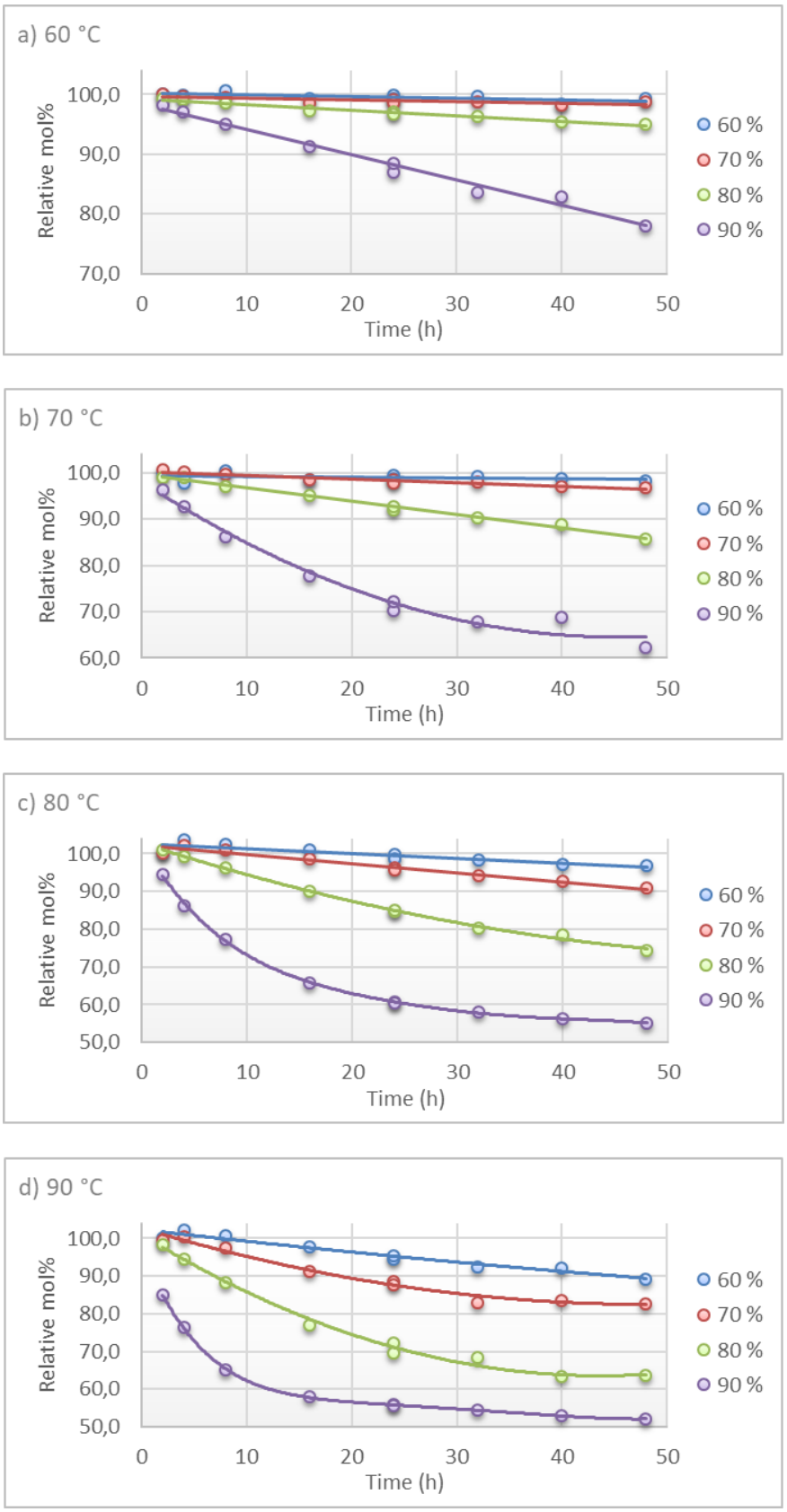

Figure 33 Relative concentration of [DBNH][OAc] over time at different temperatures and in different initial concentrations.

As seen in the **Figure 33**, the hydrolysis occurred faster when less water was present. Hydrolysis is typically faster when there is more water; however, for some reason the hydrolysis had inverse reaction kinetics. Arguably, the hydrolysis mechanism must be the reason for the inverse kinetics. Hydrolysis tests were conducted using a small excess of free DBN or acetic acid to investigate how they affected the kinetics and identify clues for the hydrolysis mechanism. The solutions in these tests contained 80 w/w% of [DBNH][OAc], 10 w/w% water and 10 w/w% DBN or acetic acid (**Figure 34**).

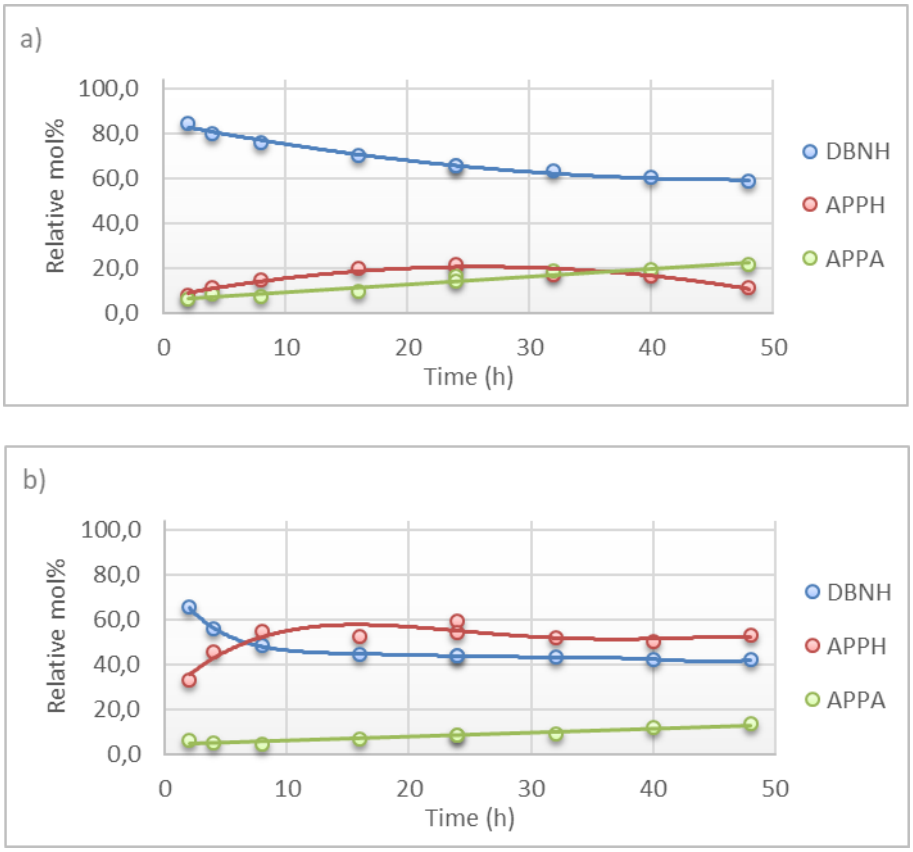

Figure 34 Hydrolysis kinetics of 80 w/w% [DBNH][OAc] in water (10 w/w%) with (a) 10 w/w% acetic acid or (b) 10 w/w% DBN.

Figure 34a shows that the excess acetic acid catalyzed the formation of APPA to a degree that the relative molar concentration of APPA exceeded the concentration of $[APPH]^+$ after approximately 35–40 hours. Acetic acid did not seem to affect the hydrolysis of $[DBNH]^+$ (**Figure 33** and **Figure 34**). This phenomenon was arguably because acetic acid is not a strong enough acid to decrease the probability of the formation of a hydroxide ion to the extent

that it would play a major role in affecting the hydrolysis kinetics. On the contrary, the free DBN in the solution catalyzed the hydrolysis. DBN was hydrolyzed rapidly, and the catalytic hydrolysis of DBN and $[DBNH]^+$ cation continued until all the free DBN was consumed. Subsequently, the reaction slowed down significantly–it seemed to proceed at roughly the same rate as APPA was forming (**Figure 34b**) consistent with the earlier experiment (**Figure 32**).

If the hydroxide anion attacked the ring to initiate the hydrolysis, then different anions should have drastically different rates of hydrolysis. It was hypothesized that it would be very unlikely for a chloride anion to accept the proton from water to form a hydroxide anion; therefore, the hydrolysis of [DBNH]Cl should not occur. In reaction set-up, the $[DBNH]^+$ cation was paired with less basic anions, such as Cl^-, $[CF_3COO]^-$, and $[CF_3SO_3]^-$, and compared to the rate of hydrolysis of [DBNH][OAc] (**Figure 35**). The hydrolysis slowed down significantly with the less basic anions. As hypothesized, [DBNH]Cl was not hydrolyzed under these conditions (**Figure 35**). This observation supported the hypothesis that the hydroxide anion attacked the ring. $[DBNH][CF_3SO_3]$ hydrolysis was below the reliable detection limit, and $[DBNH][CF_3COO]$ was slightly hydrolyzed but this reaction was significantly slower than [DBNH][OAc]. These data revealed that the anion dictates the hydrolysis kinetics at these conditions.

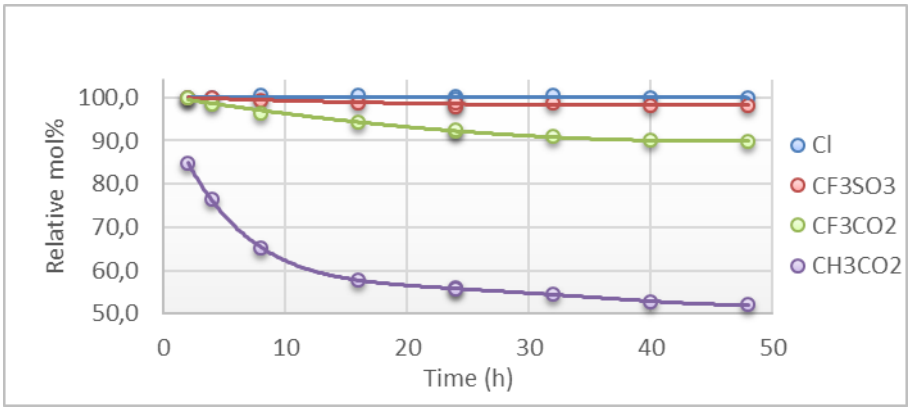

Figure 35 Kinetics of $[DBNH]^+$ cation paired with different anions.

As a conclusion for this work, the hydrolysis was markedly concentration and temperature dependent. The effect of anion in the hydrolysis reaction was

assessed by pairing $[DBNH]^+$ with anions including $[CF_3COO]^-$, $[CF_3SO_3]^-$, and Cl^-, in comparison with $[CH_3COO]^-$; however, the cellulose–dissolving capabilities of the different anions were not determined. The former anions had very different basicities compared to the acetate. Given this fact it was possible to show the significance of anion in the salt which ultimately determined the rate of hydrolysis of the $DBNH^+$ cation. A more thorough analysis of these results–complimented with computer simulations–will be published later.

In the publication by Parviainen *et al.,*[134] the sustainability of the IONCELL-F process was simulated in a batch process. In the study cellulosic pulp was successively dissolved and regenerated from [DBNH][OAc]. In addition to the potential issues with hydrolytic stability, it was necessary to investigate the build-up of ash (i.e., non-volatile inorganic compounds such as salts) from the cellulosic pulp into the recycled IL. Given the research that was performed in a batch process, it was convenient to analyze the ash content of the recovered IL after every batch. Quantities of the accumulated inorganics were relatively low because of their low contents in cellulosic pulp. However, it was important to thoroughly study the accumulation of ash because ideally the IL should be used countless times before it becomes waste. The accumulation of ash is shown in **Figure 36**. At the observed rate, after 100 cycles the ash build-up reaches approximately 5 w/w %. It is unknown whether this rate affects the process, at which point the IL becomes saturated with inorganics, and how it affects the cellulose dissolution properties. The chemical composition of the salts was not analyzed.

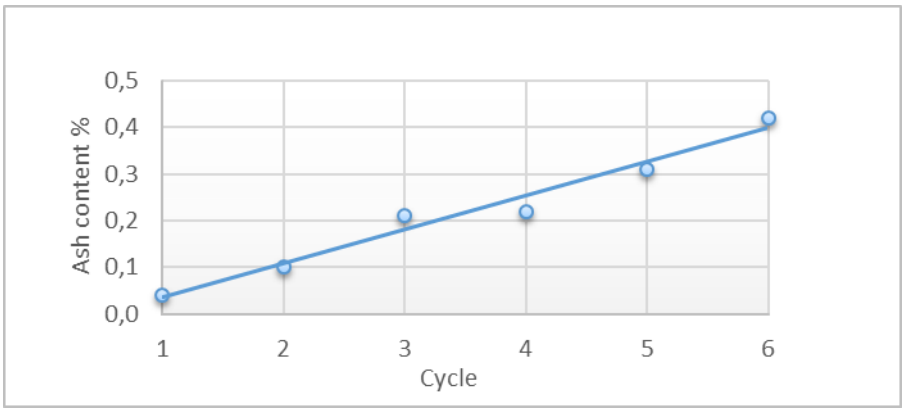

Figure 36 Accumulation of ash in [DBNH][OAc] in a simulation of IONCELL-F batch process.

One potential benefit in the sustainability of the IONCELL-F process is that the [DBNH][OAc] is a distillable IL and can therefore be separated from non-volatile impurities in order to extend the life cycle of the IL. Ahmad *et al.*[135] attempted to thermally separate [DBNH][OAc] from aqueous solutions to simulate the stability of the IL at distillation conditions. As seen from the results, a small quantity of the [DBNH][OAc] was also distilled in those conditions (**Table 6**). In order to assess the decomposition of [DBNH][OAc], HPLC analysis was used similarly to the previous work.[129,130]

Table 6. *Decomposition of [DBNH][OAc] under distillative conditions.*

	Water in residue	[DBNH][OAc] in residue	[APPH][OAc] in residue	Water in distillate	[DBNH][OAc] in distillate	[APPH][OAc] in distillate
1	11.68	84.91	3.39	99.66	0.06	0.27
2	10.65	85.40	3.94	99.69	0.06	0.24
3	10.79	85.37	3.83	99.83	0.04	0.12
4	9.16	86.96	3.86	99.49	0.06	0.44
5	6.78	88.24	4.96	99.28	0.06	0.65
6	5.31	89.54	5.14	98.35	0.17	1.47
7	6.55	88.64	4.81	99.23	0.11	0.65
8	5.01	89.27	5.72	98.89	0.09	1.01
9	5.01	88.90	5.99	98.77	0.11	1.11

Notably, it was difficult to remove all the water from the IL (**Table 6**). At relatively mild conditions, more than 11 w/w% of water was still found among the collected IL-rich residue. In order to decrease the water content, the

temperature and vacuum needed to be increased change that increased the portions of hydrolysis product [APPH][OAc].

3.5 CHEMICAL STABILITY OF [P_{4444}][OH]

As a continuation to the study of wheat straw fractionation with highly hydrophobic phosphonium ILs (Chapter 3.1), this work examined aqueous solutions of [P_{4444}][OH]. The initial tests clearly established that this electrolyte solution can extract lignin from wheat straw. Therefore it was necessary to thoroughly assess its properties.[109] The commercial solution was 40 w/w%, and it was assumed to be possible to tune the dissolving properties by manipulating the concentration. However, it was found quite early that a white solid appeared on the inner surface of the evaporation flask that contained highly concentrated solutions. By using ^{31}P NMR, it was confirmed that the phosphonium component underwent irreversible decomposition (**Figure 21**). The data from the first stability experiments are shown in **Table 7**.

Table 7. *Stability of [P_{4444}][OH] at different concentrations.[109]*

	[P_{4444}][OH]:H_2O (w/w%)	Temp. (°C)	Time (h)	Stability
1	40:60	90	24	Stable
2	50:50	90	24	Stable
3	60:40	40	24	Unstable
4	70:30	-	-	*

* 70:30 (w/w%) could not be reached due to the decomposition during concentration of the solution.

Cellulose is reportedly rapidly dissolved in 60 w/w% [P_{4444}][OH] solution.[74] However, contrary to the earlier report, the 70% (w/w%) [P_{4444}][OH] solution could not be reached because decomposition occurred during the vacuum concentration. The solution of 60 w/w% [P_{4444}][OH] solution also began to slowly decompose at 40 °C.

With these initial results, it was necessary to further investigate the stability of the [P_{4444}][OH] solution in order to assess its applicability at the 60 w/w% concentrations. Preliminary testing revealed that it was already unstable at 40 °C, but the decomposition was extremely slow. The stability was assessed at 60, 70 and 80 °C, all of which are typical processing temperatures that are clearly below the boiling point of water. The determined decomposition kinetics are shown in **Figure 37**.

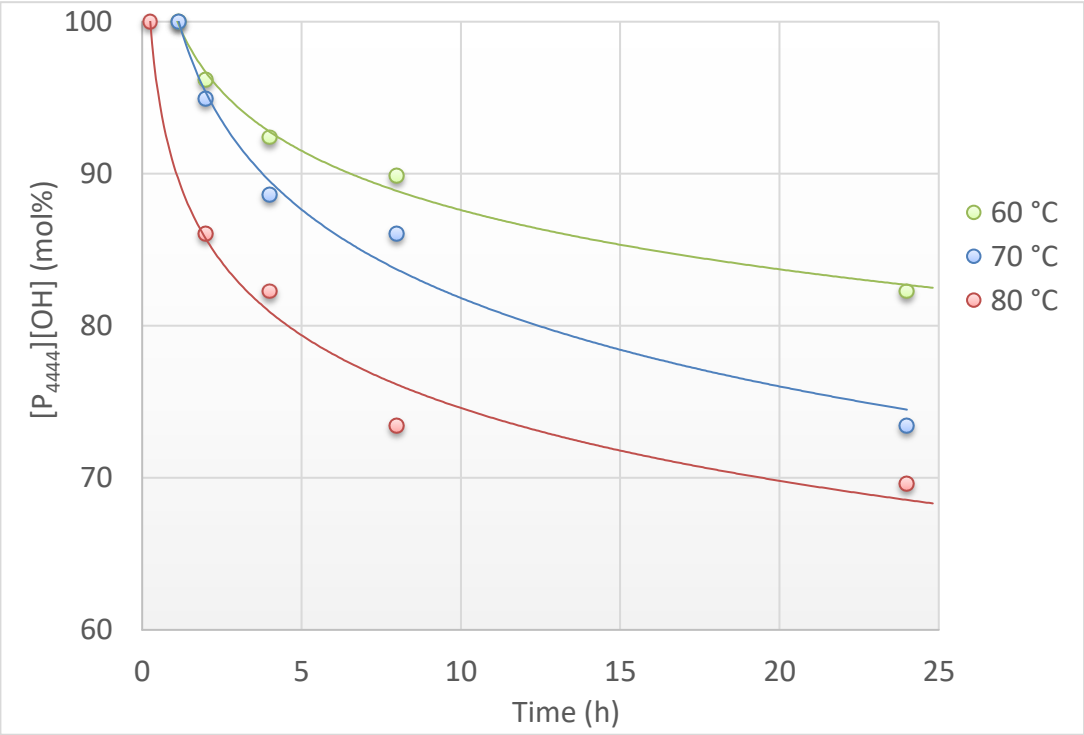

Figure 37 Decomposition kinetics of [P_{4444}][OH] as a 60 w/w% solution at different tempeatures.[109]

The trendline suggested that during the first minutes there was slight delay before decomposition began. This phenomenon made sense because in the reaction set-up the samples were placed in the oven from room temperature and naturally it took a few minutes before the sample reached temperatures where the decomposition commenced. As the temperature increased, decomposition of the 60 w/w% occurred faster. After 2 hours at 80 °C, there was significant decomposition (14 mol%). The decomposition continued relatively rapidly: after 24 h less than 70 % of the phosphonium component was left. At lower temperatures, the decomposition was slower. However, after

24 h, ^{31}P NMR analysis revealed that only 82 and 74 mol% of the original $[P_{4444}]^+$ was found at 60 and 70 °C, respectively.

This research highlighted that increasing the concentration of the $[P_{4444}][OH]$ solutions must be performed near room temperature. Increasing the concentration above 60 w/w% augments the risk of decomposition. In conclusion, any processing using the 60 w/w% $[P_{4444}][OH]$ solution should be near room temperature conditions to avoid solvent decomposition.

3.6 EXTRACTION OF WHEAT STRAW WITH $[P_{4444}][OH]$ SOLUTIONS

Wheat straw is an interesting biomass as a side stream from wheat harvesting; it is commonly treated as a waste. It has a high carbohydrate content– approximately 35–45 w/w% cellulose and 20–30 w/w% hemicellulose. It also has a relatively low lignin content, approximately 15–25 w/w%. Due to this herbaceous biomass, it contains extractives up to about 5 w/w%, starch about 3 w/w%, and minerals, such as silicates, up to about 10 w/w%. Silicates can cause issues in large-scale production because they are difficult to remove from the soluble portion of the spent liquor.

After the publication from Abe *et al.*[74] trials were performed to treat wheat straw using $[P_{4444}][OH]$.[109] Notably, 60 w/w% $[P_{4444}][OH]$–which dissolved cellulose–did not extract cellulose from wheat straw, instead it markedly extracted lignin. By optimization of the process, carbohydrate-rich fractions with a low lignin content could be collected.

It was assumed that the dissolving properties would be greatly altered by using an acid (i.e. HCl) to neutralize $[P_{4444}][OH]$ to form an aqueous IL solution that would precipitate the dissolved lignin in the spent phosphonium solution. The particle size of the wheat straw had to be reduced in order to remove most of the extractives from wheat straw before the treatment. In fact, it is necessary to remove the extractives because they greatly hinder the lignin content analysis using the acetyl bromide method[136,137]. The acetyl bromide method was extremely effective for this purpose because it required a small sample size (4–6 mg).

Before cooking the wheat straw, it was milled, and extractives were removed. After cooking, the undissolved portion (S1) was washed, and the liquid portion was acidified with HCl. HCl converted the $[P_{4444}][OH]$ solution into $[P_{4444}]Cl$ solution and induced precipitation of S2. S2 was washed and the $[P_{4444}]Cl$ discarded. Theoretically it could be converted back to $[P_{4444}][OH]$, however, that phenomenon was not demonstrated. The proposed process scheme is shown in **Figure 38**.

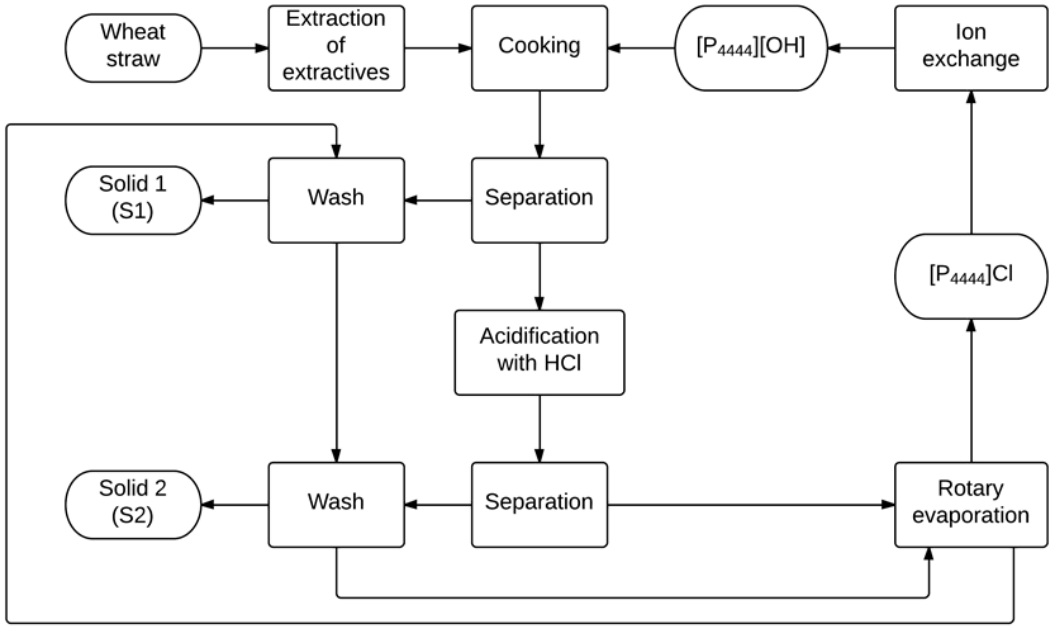

Figure 38 The proposed processing scheme that uses $[P_{4444}][OH]$ for treating wheat straw.[109]

The optimization step was conducted using a post-process wheat straw-bran mixture that was a side product in another project.[138] The processing conditions and lignin contents are shown in **Table 8**. The yields were approximately 40 % of the original post-process wheat straw. Accurate yields were difficult to measure because of the low amounts of material used in the optimization process which led to extremely low amounts of collected fractions. To avoid decomposition of the expensive phosphonium component, a 40 w/w% solution was used for the treatment–the cellulose dissolving 60 w/w% solution was found to be unstable (Chapter 3.4).

The lignin content of untreated extractive-free post-process wheat straw was measured to be 22.7 w/w%. By processing with $[P_{4444}][OH]$, this content was reduced to less than 10 w/w% (**Table 8**, entries 4, 6, 7, and 10). A 2 h extraction time was sufficient for the extraction; the most important parameter seemed to be the temperature.

Table 8. *Optimizing the process of the treatment of post-process wheat straw.*[109]

	$[P_{4444}][OH]$ concentration (w/w%)	Wheat straw loading (w/w%)	Temp. (°C)	Time (h)	Lignin content (w/w%)
1	Untreated	-	-	-	22.7
2	40	5	RT	2	15.5
3	40	5	50	2	12.3
4	40	5	70	2	9.3
5	40	5	RT	4	14.3
6	40	5	50	4	8.6
7	40	5	70	4	9.1
8	40	2.5	RT	4	12.3
9	40	2.5	50	4	11.0
10	40	2.5	70	4	8.4
11	60	5	RT	4	14.0

The next step was to compare the optimized process to the non-sulfated NaOH cook. At this point, the untreated extractive-free wheat straw was used instead of the post-process wheat straw–bran mix. The untreated extractive-free wheat straw had a lignin content of 22.4 w/w% according to the acetyl bromide method. Wheat straw was treated with aqueous 40 w/w% $[P_{4444}][OH]$ solution–and for comparison, with 1.5 M NaOH solution–at 90 °C for 2 h in a round bottom flask at a slightly larger scale in order to obtain measurable quantity of the S2. The results are shown using the optimized process in **Table 9**. The aqueous 40 w/w% $[P_{4444}][OH]$ provided slightly lower yields and lower lignin contents for S1 compared to the 1.5 M NaOH extraction. Extraction using $[P_{4444}][OH]$ yielded S2 with a moderate lignin content (13.2 w/w%). Acidification was not attempted for the recovered NaOH solution. The ash content was similar between the two methods.

Notably, more than half of the ash was soluble in boiling water. This finding indicated that most of the ash was in a relatively soluble form and was removed in the washing step if the alkaline extraction process did not already solubilize the inorganic ash components.

Table 9. *Composition of the obtained solids using the optimized wheat straw extraction.*[109]

	Treatment	Lignin (w/w%) S1 / S2	Ash (w/w%) S1 / S2	Yield* (w/w%) S1 / S2
1	Untreated	22.4	5.6	-
2	1.5 M NaOH	10.3	0.7	44
3	$[P_{4444}][OH]$	7.2 / 13.2	0.8 / 1.0	39 / 3

*Yields are expressed in w/w% of the original extractive-free wheat straw.

The collected solids were compared to reference materials (microcrystalline cellulose [Avicel], xylan from oat spelts, and corn stover enzymatic mild acidolysis lignin [EMAL]) using attenuated total reflectance–infrared spectroscopy (ATR-IR). This method demonstrated that the collected solid **S1** was a cellulose-rich fraction and solid **S2** was a hemicellulose-rich fraction (**Figure 39**).

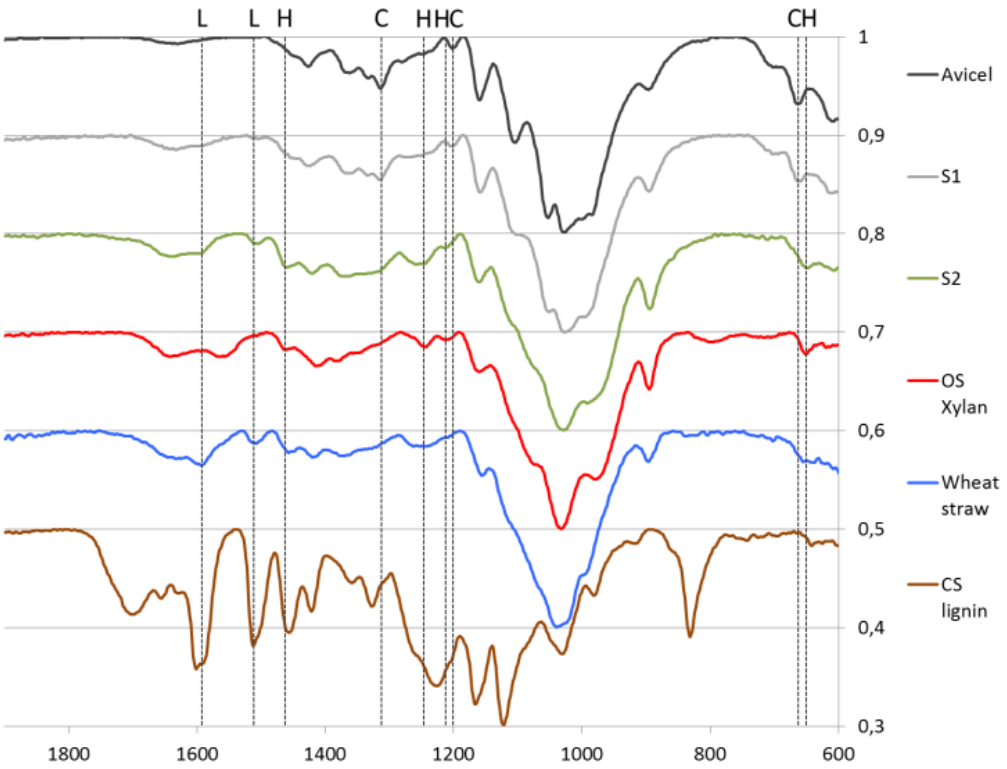

Figure 39 Attenuated total reflectance–infrared spectroscopy analysis of the solid fractions compared to reference materials: microcrystalline cellulose (Avicel), xylan from oat spelts, ball-milled wheat straw, and corn stover EMAL lignin. Assignments of the signals: L = Lignin, H = Hemicelluloses, C = Cellulose.[109]

Recycling in the proposed process (**Figure 38**) could have been performed with metathesis (e.g., ion exchange) from $[P_{4444}][Cl]$ to $[P_{4444}][OH]$. However, this method was not evaluated in this work. It is questionable whether this procedure would have been useful because there was residual biomass (mostly lignin and hemicelluloses) still dissolved in the solution.

3.7 FRACTIONATION OF LIGNOCELLULOSIC BIOMASS UTILIZING A MICROWAVE REACTOR

Wheat straw and aspen were fractionated using an aqueous IL solution in comparison to other sulfur-free processes.[139] The most common industrial fractionation methods are the sulfur-based Kraft and the sulfite processes. In the Kraft process, lignin is solubilized *via* chemical derivatization which also depolymerizes lignin and thus solubilizes lignin. In the sulfite process lignin is derivatized into a soluble lignin derivative. The objective of this work was to

compare the pulping efficiency of the non-derivatizing “sulfur-free” methods and study their effect on the lignin structure, mainly on the β-O-4 structure.

In a recent publication, triethylammonium hydrogen sulfate ([TEAH][HSO_4]), was found to be very promising in fractionation of biomass; it can be used as 80 % in aqueous solution. This solution reportedly has ‘self-cleaning properties’, and its price is close to common laboratory solvents such as acetone or toluene.[140] This low price makes the process potentially economically sound because there are often solvent losses when the spent liquor is collected and recycled.

In the study, [TEAH][HSO_4] was compared with formic acid, ethanolic NaOH, ethanolic Na_2CO_3 and aqueous HCl+NaOH processes.[140,141] Some of the processes were combined with HWE prior to the actual cooking process in order to determine whether it can be advantageous for actual pulping. The processing scheme is illustrated in **Figure 40**.

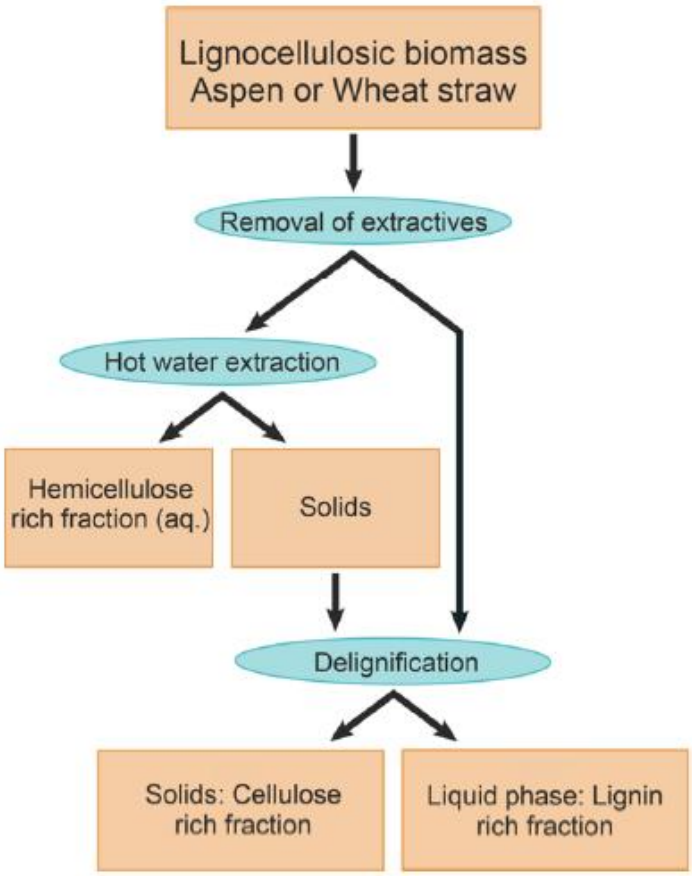

Figure 40 Processing scheme for delignifying aspen and wheat straw with and without hot water extraction. Adopted from ref. 139.

Table 10 presents the results for the insoluble portion (cellulose-rich fraction) in processing wheat straw. Given that extractives were removed before processing, the contents that were not hemicelluloses, lignin or ash were assumed to be cellulose.

Table 10. *The cellulose rich fraction yield and constituents using different solvent systems in wheat straw fractionation.*[139]

						Constituents in w/w%		
	"Cooking" liquors	T (°C)	Time (h)	Yield (w/w%)	Cellulose DP_w	Hemi-celluloses	Lignin	Ash
1	HCOOH	101	0.5	50	3500	9	4	14
2	HWE + HCOOH	101	0.5	44	3100	7	5	9
3	[TEAH][HSO_4]	120	4	41	1800	10	5	15
4	HWE + [TEAH][HSO_4]	120	4	39	800	8	7	12
5	EtOH / Na_2CO_3	130	2	66	5300	30	8	10
6	HWE + EtOH / Na_2CO_3	130	2	49	4200	15	8	9
7	EtOH / NaOH	130	2	66	5300	33	6	10
8	0.1 M HCl + 0.1 M NaOH	100	2+2	45	3300	14	16	0.5
9	1 M NaOH	130	2	39	4300	17	2	3

Most of the methods delignified wheat straw. Untreated extractive-free wheat straw contained 31 % (w/w) hemicelluloses, 23 % (w/w) lignin and 9 % (w/w) ash (i.e., inorganics such as silicates). Those figures can be used as a reference when comparing results in **Table 10**. Formic acid cooking seemed to be very efficient in delignification; however, it did not remove ash, a finding was indicated as increased ash content in the cellulose-rich fraction. HWE removed the hot water–soluble ash and decreased hemicellulose content but also slightly decreased the degree of cellulose polymerization (DPw). [TEAH][HSO_4] was very effective in delignification but poor at removing inorganics. The DPw of cellulose decreased drastically, a finding that indicated degradation of the cellulose polymer. The highest DPw of cellulose was obtained with the alkaline ethanolic cooks (**Table 10**, entries 5, 6, and 7). In

addition, the hemicellulose content of these experiments remained high. The sequential dilute HCl + NaOH system gave a very low ash content; however, the lignin content remained high and therefore it was not regarded as an effective fractionation method under these conditions. A reference method was a non-sulfated caustic soda NaOH cook, which yielded a relatively high cellulose DPw and hemicellulose content but low lignin and ash contents.

According to NMR results, the most abunant lignin β-O-4 structure remained mostly intact with all the methods except with [TEAH][HSO_4] (**Table 11**). This finding was expected because this treatment also degraded cellulose (**Table 10**, Entries 3 and 4). The [TEAH][HSO_4] seemed to decrease the Mw of lignin. The highest lignin Mw occurred with the formic acid cook (**Table 11**, entry 1). This result could be partially explained by the derivatization of the hydroxyl groups in lignin by formic acid. The alkaline organosolv cooks also extracted hemicelluloses into the lignin–rich fraction (**Table 11**, entries 5-9). Pre-extraction with HWE effectively reduced the quantity of hemicelluloses in the lignin fraction (**Table 11**, entry 6).

Table 11. *Precipitated lignin fraction from the spent liquor in fractionation of wheat straw.*[139]

	"Cooking" liquors	T (°C)	Time (h)	Yield (w/w%)	β-O-4 signals (HSQC)	M_w	Carbo-hydrate signal (HSQC)
1	HCOOH	101	0.5	13	Strong	4270	Weak
2	HWE + HCOOH	101	0.5	8	Strong	3640	Weak
3	[TEAH][HSO_4]	120	4	12	n.s.	2530	n.s.
4	HWE + [TEAH][HSO_4]	120	4	8	n.s.	2270	n.s.
5	EtOH / Na_2CO_3	130	2	8	Strong	3030	Strong
6	HWE + EtOH / Na_2CO_3	130	2	13	Strong	3120	Weak
7	EtOH / NaOH	130	2	14	Strong	3180	Strong
8	0.1 M HCl + 0.1 M NaOH	100	2+2	11	Strong	3700	Strong
9	1 M NaOH	130	2	24	Strong	2980	Strong

n.s. no signal

Similar experiments were performed using aspen. Aspen is a woody biomass, and contrary to wheat straw, it does not have significant amounts of extractives. Hence, the process should be less problematic. Although aspen is a wood species, it is relatively easy to pulp. Fractionation results for aspen are shown in **Table 12**.

Table 12. *The cellulose-rich fraction yields and constituents in fractionation of aspen using various solvent systems.*[139]

						Constituents in w/w%	
	"Cooking" liquors	T (°C)	Time (h)	Yield (w/w%)	Cellulose DP_w	Hemi-celluloses	Lignin
10	HCOOH	101	0.5	54	2100	10	4
11	HWE + HCOOH	101	0.5	47	1200	7	4
12	[TEAH][HSO_4]	120	4	34	900	7	5
13	HWE + [TEAH][HSO_4]	120	4	36	500	5	6
14	EtOH / Na_2CO_3	130	2	79	4100	22	17
15	HWE + EtOH / Na_2CO_3	130	2	42	1700	7	15
16	EtOH / NaOH	130	2	78	3900	22	17
17	0.1 M HCl + 0.1 M NaOH	100	2+2	60	1500	12	23
18	1 M NaOH	130	2	60	3600	11	20

Similar to the experiments with wheat straw, the formic acid cook was very effective in providing a cellulose-rich fraction with low lignin content. This phenomenon was especially true with aspen because it contained limited inorganics that were not found to be removed when extracting wheat straw (**Table 10**, entry 1). The cellulose DP_W was slightly decreased. [TEAH][HSO_4] was also an effective pulping solvent with aspen, denoted as a low yield. HWE did not seem to affect the cook other than further lowering the cellulose DP_W. A decreased DP_W may be unwanted for pulp and paper products; however, it may be beneficial, e.g., biofuel production *via* enzymatic hydrolysis. The remaining methods provided relatively high lignin contents in cellulose fraction, finding indicative of poor pulping. The cellulose DPw results for those methods may be unreliable because the high lignin content severely hindered

the dissolution of the fraction for the analysis. The NMR results showed that the β-O-4 structure of the extracted lignin-rich fractions remained mostly intact with all of the methods except with [TEAH][HSO_4] (**Table 13**, entries 12 and 13.). The yields were very low with the alkaline cooks. Interestingly, the alkaline cooks yielded very high Mw lignin (**Table 13**, entries 14–18.). This may be an indication of covalent linking between lignin and hemicelluloses. Formic acid provided lignin with higher Mw compared to [TEAH][HSO_4], but lower than most of the alkaline cooks. In the case of aspen, HWE pre-treatment seemed to be very effective in producing a lignin fraction with a low carbohydrate content.

Table 13. *Precipitated lignin fraction from the spent liquor in aspen fractionation.*[139]

	"Cooking" liquors	T (°C)	Time (h)	Yield (w/w%)	β-O-4 signals (HSQC)	M_w	Carbo-hydrate signal (HSQC)
10	HCOOH	101	0.5	12	Strong	5100	Weak
11	HWE + HCOOH	101	0.5	8	Strong	4080	n.s.
12	[TEAH][HSO_4]	120	4	11	n.s.	3080	n.s.
13	HWE + [TEAH][HSO_4]	120	4	5	n.s.	2230	n.s.
14	EtOH / Na_2CO_3	130	2	4	Strong	8910	Strong
15	HWE + EtOH / Na_2CO_3	130	2	6	Strong	4150	n.s.
16	EtOH / NaOH	130	2	4	Strong	9250	Strong
17	0.1 M HCl + 0.1 M NaOH	100	2+2	2	Strong	6450	Weak
18	1 M NaOH	130	2	4	Strong	3290	Strong

n.s. no signal

3.8 CONCLUSION

Wheat straw is a globally accessible agricultural side product that represents an abundant material for usage in biorefinery applications. It is an attractive choice for biomass because it has a high polysaccharide content and relatively

low lignin content. However, the fiber properties of cellulose in wheat straw are not as good as in wood cellulose. Therefore there are some limitations to its applicability in further processing.[39] On the other hand, paper-related products are not the only materials of interest when processing cellulosic materials. Aspen was more resistant to chemical processing than wheat straw. HWE seemed to significantly improve pulping with aspen, but there was simultaneously a slight cellulose degradation.

In this thesis, cellulose-rich materials were produced from wheat straw and aspen.[109,139] The set goals were achieved using organic electrolyte solutions such as $[P_{4444}][OH]$[109] and $[TEAH][HSO_4]$, in addition to the recently developed pulping methods and non-sulfated caustic soda (NaOH) cooking.[139] $[P_{4444}][OH]_{aq}$ is an interesting electrolyte solution that rapidly dissolved cellulose in high concentrations. After testing the solution, it became clear that it was not stable if concentrated to 60 wt% and heated. A 40 wt% $[P_{4444}][OH]_{aq}$ solution yielded slightly better results compared to cooking in a similar ionic strength NaOH solution. However, some major questions were raised concerning the recyclability, stability and economics of the system.[109] Several other pulping methods were compared, and the collected fractions were analyzed carefully.[139] Formic acid cooking seemed very promising; however, because it is acidic and has a reactive nature, the collected fractions were found to be modified and derivatized. Formic acid is also corrosive, a characteristic that must be considered in industrial scale production. $[TEAH][HSO_4]$ is an attractive electrolyte solution because it is inexpensive for an organic compound and it was claimed to have self-cleaning properties. The $[TEAH][HSO_4]$ solution seemed to be very efficient in delignification, but the fractions required additional washing steps to thoroughly remove electrolytes from the cellulosic material. The $[TEAH][HSO_4]$ method seemed to modify the lignin structure as identified with heteronuclear single quantum coherence (HSQC)-NMR. The organosolv methods (NaOH or Na_2CO_3 in aqueous ethanol) were interesting because they showed very low hemicellulose solubility, a phenomenon that resulted into higher yields of pulp. Organosolv with Na_2CO_3 in aqueous ethanol was promising for the pulping of wheat straw, but with aspen it showed only a low degree of delignification. Microwave

induced heating rapidly and effectively heated the samples. This work could be continued with other biomasses and studying the recyclability thoroughly.

The initial assumption was that the $[P_{4444}][OH]$ electrolyte solution would be stable based on the observation of previously published paper, but this prediction was not precisely the case. The stability was carefully assessed with ^{31}P NMR, which was a relatively quick, simple, and reliable method to determine the decomposition rate in different temperature and concentration series.[109]

The stability of [DBNH][OAc] was carefully assessed with experimental methods. [DBNH][OAc] was an interesting IL because it produced strong man-made cellulose fibers that might be used in textile fiber production with the IONCELL-F process. To investigate its stability, [DBNH][OAc] was mixed with water at varying concentrations and its hydrolytic stability was determined using HPLC. [DBNH][OAc] was much more stable than DBN. The mechanism of [DBNH][OAc] hydrolysis is particularly interesting because the hydrolysis was faster when less water was present. It was shown experimentally in that the anion plays a crucial role in the mechanism and with other anions than acetate the hydrolysis occurred at a different rate.[129,130]

4 EXPERIMENTAL PORTION

All chemicals and solvents were purchased from Sigma-Aldrich or ABCR and were used without further purification. Wheat straw and wheat straw–bran mix were procured from VALOWHEAT project partners (details are found in refs. 109 and 138. These raw materials were used in Chapter 3.6. The wheat straw–bran mix was used in the optimization step, and wheat straw was used in the final comparison at optimized conditions). Lignoboost post-process technical lignin was obtained from industrial partners. Wheat straw from southern Finland and naturally grown aspen from southern Finland were provided by the Natural Resources Institute Finland.

NMR samples were dissolved in $CDCl_3$, and data was acquired using a Varian Innova 600 MHz spectrometer at 27 °C. A 5 mm direct detection broadband probe-head was used, and data were processed with MestReNova (v.8.1.4-12489 or newer). The ^{31}P NMR spectra were acquired using inverse-gated decoupling on the proton channel and 1000 transients were collected with a spectral width 85000 Hz, an acquisition time of 1 s and a relaxation delay of 3 s. The ^{1}H NMR spectra were acquired by collecting 8 transients with a spectral width of 9600 Hz, an acquisition time of 2 s and a relaxation delay of 1 s. ^{13}C spectrum was acquired by collecting 400 transients with a spectral width of 36000 Hz, an acquisition time of 1.3 s and a relaxation delay of 1 s.

A Bruker Avance III 500 MHz FT-NMR-spectrometer was used with a BBFO broad-band probe. Lignin-rich samples were acetylated prior to analysis and dissolved in CDCl3. HSQC spectra of the lignin samples were collected using Bruker standard pulse sequence (hsqcetgp), with a 12.5 ppm spectral width in the F2 (1H) dimension (1024 data points and 215 ppm spectral width) and in the F1 (13C) dimension with 128 data points, using a 1.44347 s pulse delay and 16 scans. Spectra were processed using Bruker TopSpin 3.5pl7.

The GC-MS spectra were acquired with a Bruker Scion SQ 456-GC-MS-instrument using helium as carrier gas (flow rate of 1.3 ml/min). Separation of the volatile compounds was performed with a 30 m x 2.25 mm x 0.25 µm Agilent DB-5 MS UI (5 %-phenyl)-methylpolyoxysilane column. The split ratio

was 1:50 with a gradient method from 50 °C (hold 2 min), 30 °C/min to 180 °C, 40 °C/min to 280 °C (hold for 8 min) with acquisition delay 3.1 min. The mass spectra were collected within the 30–500 m/z range.

For hydrolysis experiments, HPLC-UV chromatograms were collected using an Agilent 1200 Series instrument with Agilent ZORBAX Eclipse XDB-CN, analytical 4.6 x 150 mm 5-µm column. The HPLC was equipped with a diode array detector for detection at 215 nm with a 4 nm band width. An isocratic mixture of acetate buffer (0.5 M NaCl/10 mM NaOAc, pH 4.0) and acetonitrile (95:5 Buffer:ACN) was used as a mobile phase in all analyses. The 5-µl injection volume of was injected to the isocratic mobile phase (0.8 ml/min) at 30 °C.

In GPC analysis, each sample was acetylated by acetic anhydride in pyridine before dissolving in THF, which was also used as the eluent. A refractive index (RI) and UV detector (at 254 nm) were used for detecting analytes, with a flow rate of 0.8 mL/min at 30 °C. A calibration curve was formed using eight polystyrene standards (Polymer Standards Service, Warwick, USA) with molecular weights between 474 and 76000 g/mol. The sample concentration was 1 mg/ml. Every sample was filtered through a 0.45 µm syringe filter (Acrodisc GHP Membrane, Waters) prior to injection.

In GPC analysis for the lignin-rich fractions, Waters Acquity APC equipment was used (Acquity APCTM XT 45 Å, 1.7 um, 4.6x150mm and XT 200 Å, 2.5um, 4.6x150mm columns from Waters Corporation, USA). GPC Empower® Software (Waters) was used for all data processing in order to obtain M_n (number-average molecular weight), M_w (weight-average molecular weight) and polydispersity index (PDI; M_w/M_n). All chromatograms were normalized.

For the carbohydrate-rich fractions, the GPC measurements were performed using an Agilent Infinity 1260 LC-system with RI detector. Separation was performed with pre-column (Agilent PLgel guard 50*7.5 mm) and three analytical columns (PLgel Mixed B, 10 µm, 300*7.5mm).

Ash contents in wheat straw samples were determined by thermally oxidizing the samples in a muffler oven at 600 °C and measuring material loss. Material loss was determined by utilizing pre-dried TGA vessels which were

weighed before and after muffler oven treatment using a Mettler Toledo TGA/SDTA851e TGA apparatus.

The lignin content in aspen, wheat straw, and wheat straw–bran mixture were analyzed acetyl bromide method. In the analysis, 5 ml of 25 % (w/w) AcBr in AcOH solution was added to 4–6 mg of biomass (which was accurately weighed in vials). Vials were capped with airtight caps equipped with Teflon liners. Vials were placed into a 50 °C oven or water bath for 2 h to digest; the samples were while gently shaken every 15 min. The mixtures were transferred into 100-mL volumetric flasks that contained 10 mL of 2 M NaOH and 25 mL of glacial AcOH. The volumetric flasks were filled to 100 ml with glacial AcOH. The absorbance was immediately read using a Varian Cary 50 Conc UV-VIS spectrometer. For the base line spectra, a blank sample was used. Acetyl bromide–soluble lignin was calculated according to the equation below:

$$\text{Lignin content (\%)} = 100\ \% * V * A / (\varepsilon * m * L)$$

where V is the volume of the sample (100 mL), A is the read absorbance value, ε is the plant specific absorbance (literature values for wheat straw and aspen are 17.54 and 17.898 g^{-1} L cm^{-1}, respectively) m is the weighed mass of sample (4 to 6 mg), and L is the pathlength (1 cm; i.e., the diameter of the cuvette).

4.1 SYNTHESIS AND APPLICATIONS OF PHOSPHONIUM IONIC LIQUIDS

$[P_{8881}][OTf]$ was synthesized at 60 °C by mixing equimolar amount of P_{888} and methyl triflate under an argon atmosphere. Methyl triflate was added dropwise. After the addition, the reaction mixture was incubated at 60 °C for 45 min and then allowed to cool in RT overnight prior to taking an NMR sample (sample dissolved in $CDCl_3$). The ^{31}P NMR spectrum showed the purity (92 mol%) of the collected product (**Figure 41**) based on the relative portions of phosphorus species. The ^{1}H NMR spectrum confirmed the structure of the main product (**Figure 42**) which was complimented by the ^{13}C NMR spectrum (**Figure 43**).

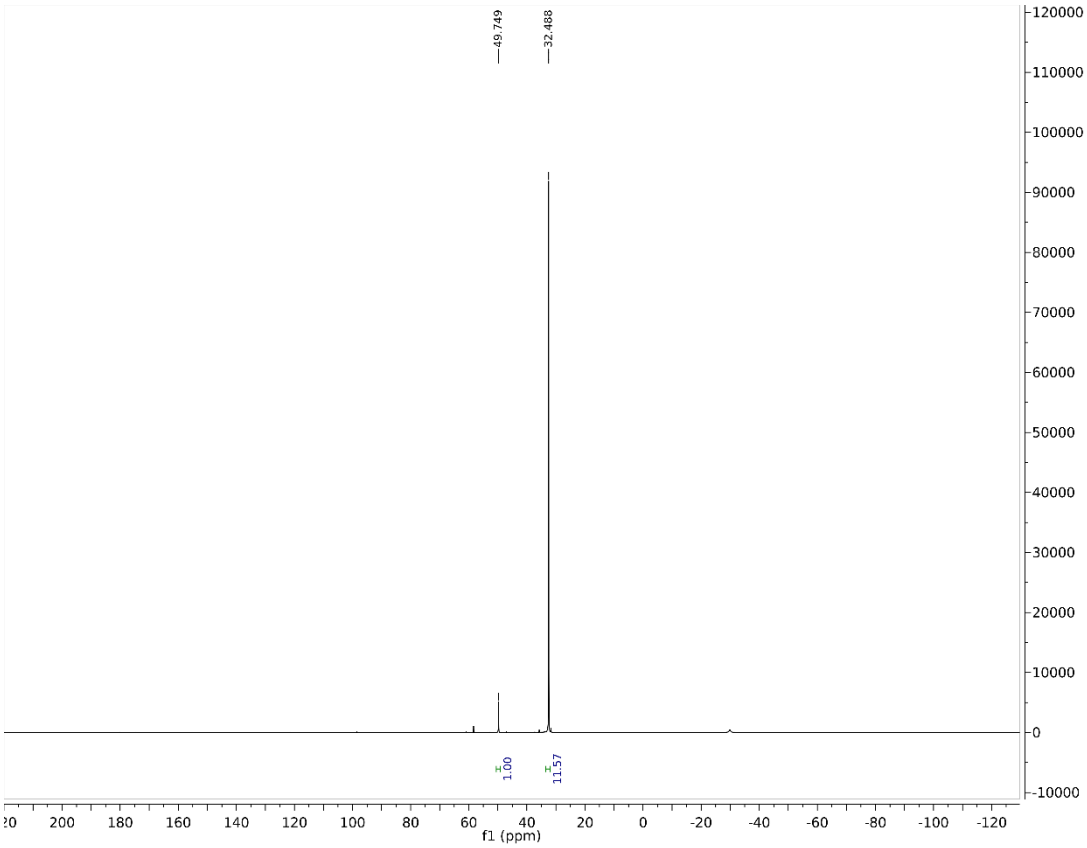

Figure 41 The ^{31}P spectrum of the crude reaction mixture of P_{888} and methyl triflate. The product was mainly $[P_{8881}][OTf]$. The side product was oxidized OP_{888}, which was found at a higher chemical shift. The product distribution was 11.6:1, which equals approximately 92 mol% purity of the $[P_{8881}][OTf]$.

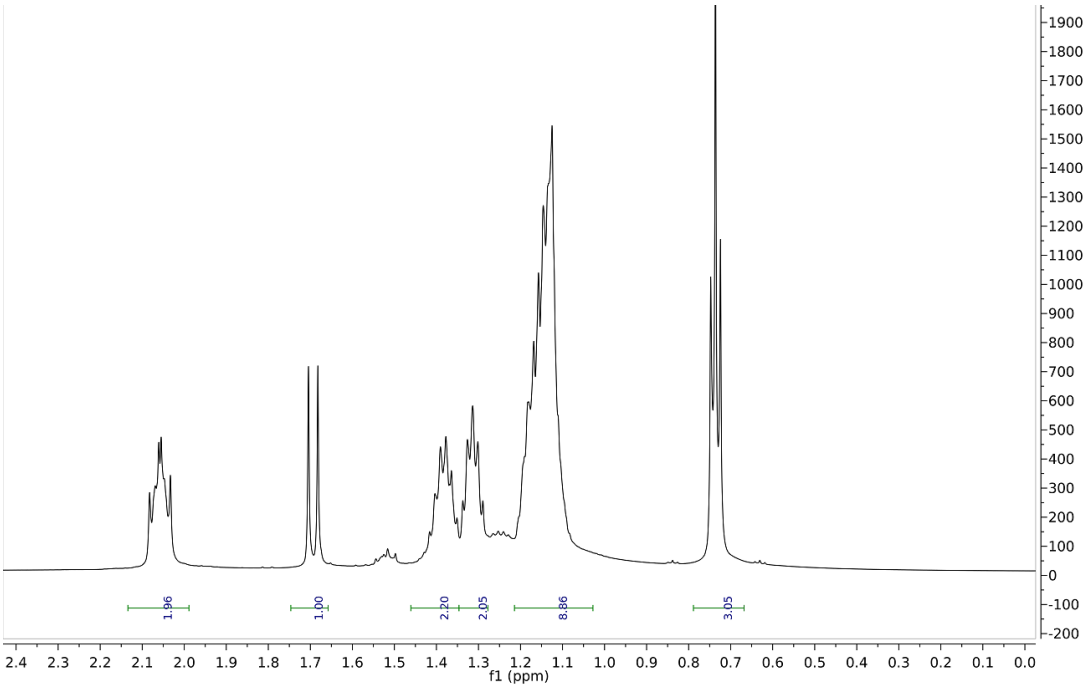

Figure 42 The ^{1}H spectrum of the crude mixture in which $[P_{8881}][OTf]$ was the main product.

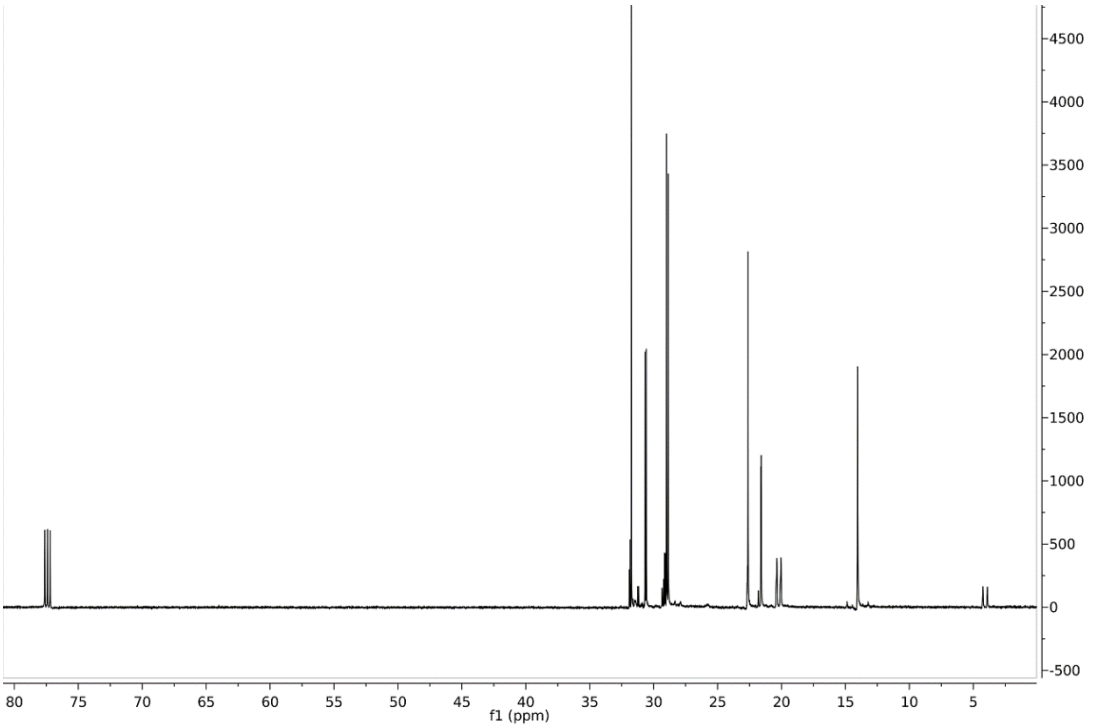

Figure 43 The ^{13}C spectrum of the crude mixture in which $[P_{8881}][OTf]$ was the main product.

4.2 IMIDAZOLIUM SALTS WITH A HYDROPHOBIC ANION FOR FRACTIONATION OF TECHNICAL LIGNIN

Moist technical lignin (0.1 g, which resembles 0.0894 g in dry weight) was mixed with 1.9 g of IL and the mixture was stirred for 1 h at room temperature or 50 °C. Subsequently, the mixture was centrifuged. The insoluble portion was washed twice with boiling water, centrifuged and dried in an oven at 70 °C overnight. Precipitation was induced for the soluble portion with 2 ml of water, which acted as an anti-solvent and greatly decreased the solubility of lignin in the IL. The mixture was centrifuged again. The precipitated lignin was washed twice with boiling water, centrifuged and dried in an oven at 70 °C overnight. For the aqueous IL mixture, another 2 ml of water was added to induce second precipitation. The second precipitate was also washed twice with boiling water, centrifuged and dried in an oven at 70 °C overnight.

4.3 SYNTHESIS OF PRECURSORS FOR IONIC LIQUIDS WITH INCREASED HYDROLYTIC STABILITY

GVL was mixed with 4 molar equivalents of DAP and 0.1 molar equivalents of NH_4Cl in a small bomb reactor under argon. The reactor was closed and heated at 200–250 °C in a fan oven. After 4.5–16 h the reactor was placed at room temperature to cool. After a few hours the reactor was carefully opened. A sample for GC-MS was prepared, and the sample was analyzed. Examples of GC-MS chromatograms are not included.

LA, DAP, RaNi, H_2O and/or t-BuOH were mixed in a bomb reactor. The reactor was pressurized with H_2 heated with an electric mantle to 40–140 °C for 5–40 hours. After cooling a GC-MS sample was prepared and analyzed. The results are collected in **Table 5**. Examples of the analyzed GC chromatograms are shown in **Figures 44–52** and the corresponding mass spectra in **Figures 53–55**.

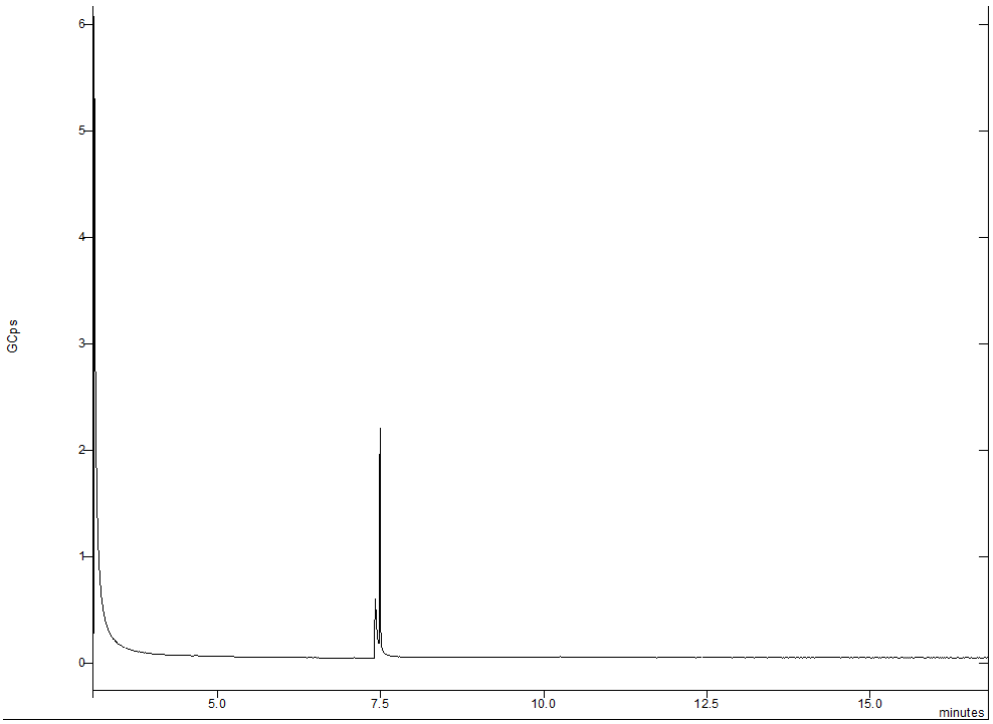

Figure 44 Gas chromatogram of **Table 5**, entry 1. The desired product mAPP (see **Figures 30** and **53**) was found at 7.42 min (m/z = 156), The side product (compound **2**, See **Figures 30** and **54**) was found at 7.49 min (m/z = 154).

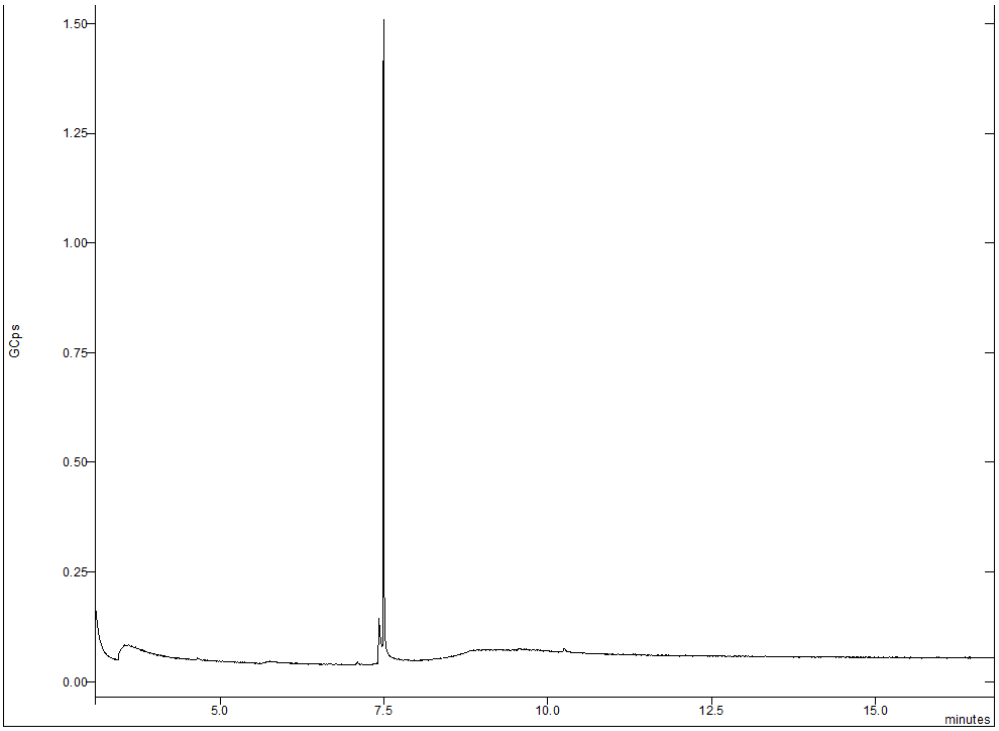

Figure 45 Gas chromatogram of Table 5, entry 2. mAPP (see **Figures 30** and **53**) was found at 7.42 min (m/z = 156), The side product (compound 2, see **Figures 30** and **54**) was found at 7.49 min (m/z = 154).

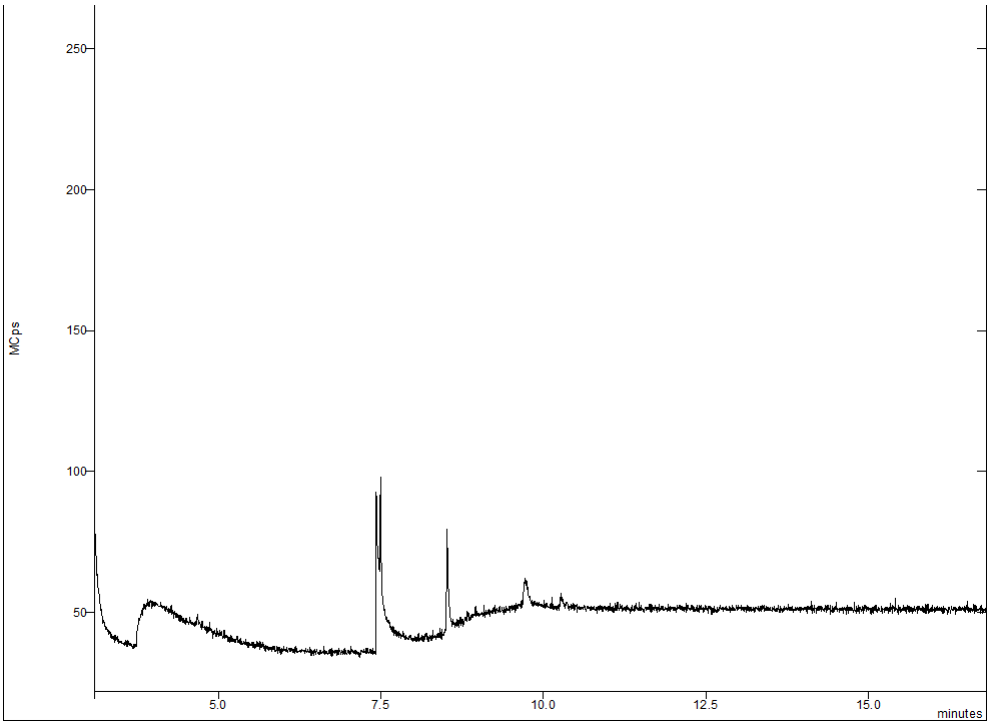

Figure 46 Gas chromatogram of Table 5, entry 3. mAPP (see **Figures 30** and **53**) was found at 7.42 min (m/z = 156), The side product (compound 2, see **Figures 30** and **54**) was found at 7.49 min (m/z = 154). Traces of a side product (compound 3, see **Figures 30** and **55**) were found at 9.54 min (m/z = 238). The signal at 8.5 min is impurity from the column.

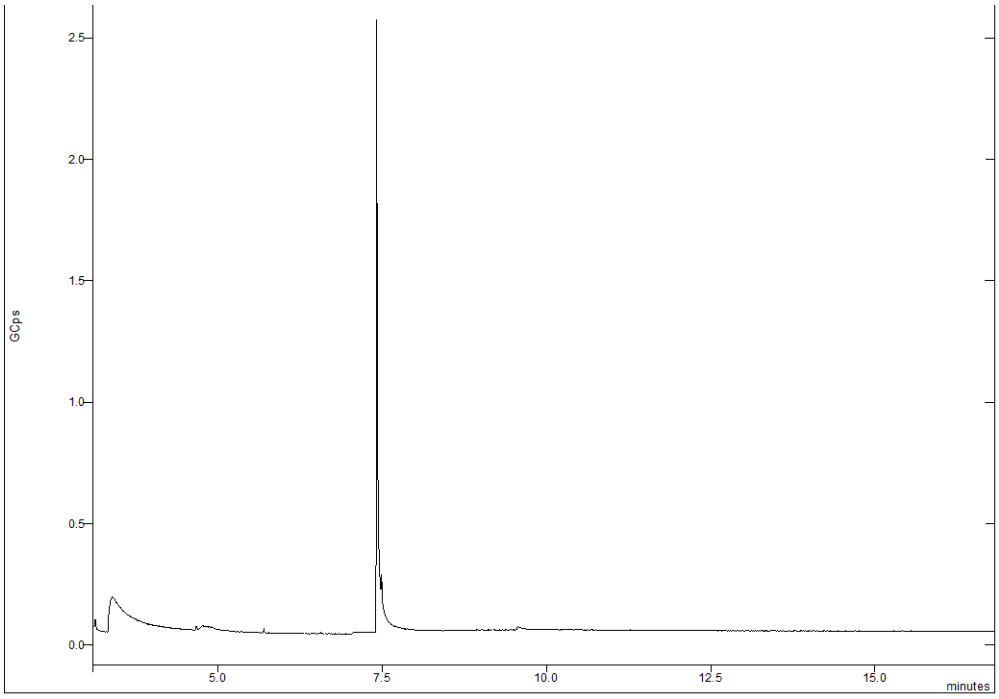

Figure 47 Gas chromatogram of Table 5, entry 4. mAPP (see **Figures 30** and **53**) was found at 7.42 min (m/z = 156), The side product (compound 2, see **Figures 30** and **54**) was found at 7.49 min (m/z = 154). Traces of a side product (compound 3, see **Figures 30** and **55**) were found at 9.54 min (m/z = 238).

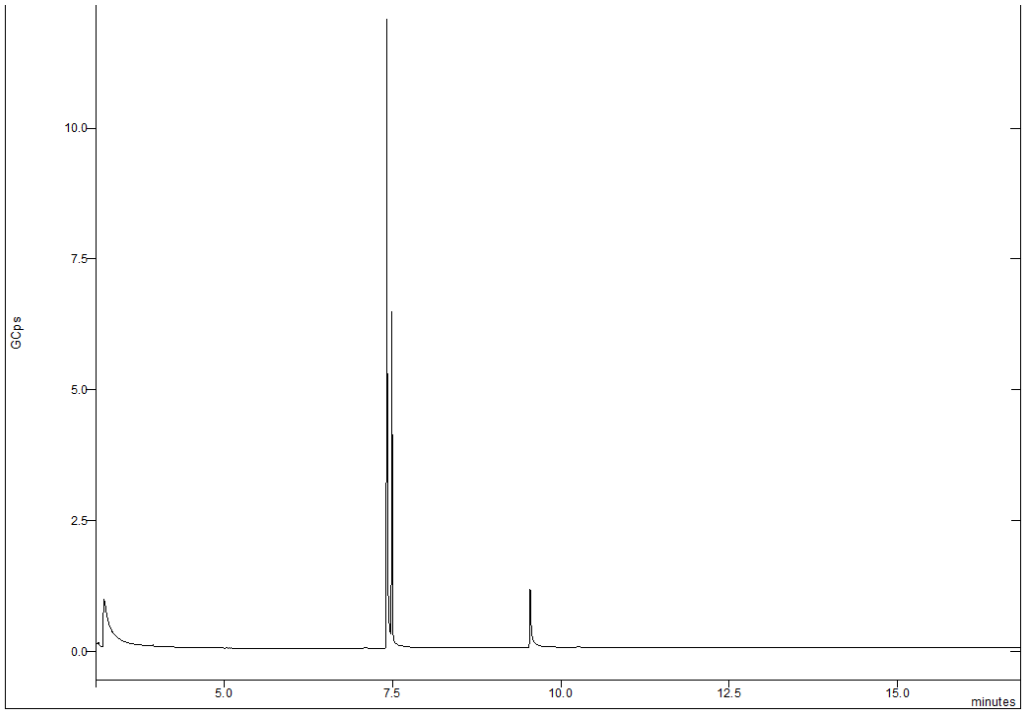

Figure 48 Gas chromatogram of Table 5, entry 5. mAPP (see **Figures 30** and **53**) was found at 7.42 min (m/z = 156), One side product (compound 2, see **Figures 30** and **54**) was found at 7.49 min (m/z = 154). Another side product (compound 3, see **Figures 30** and **55**) was found at 9.54 min (m/z = 238).

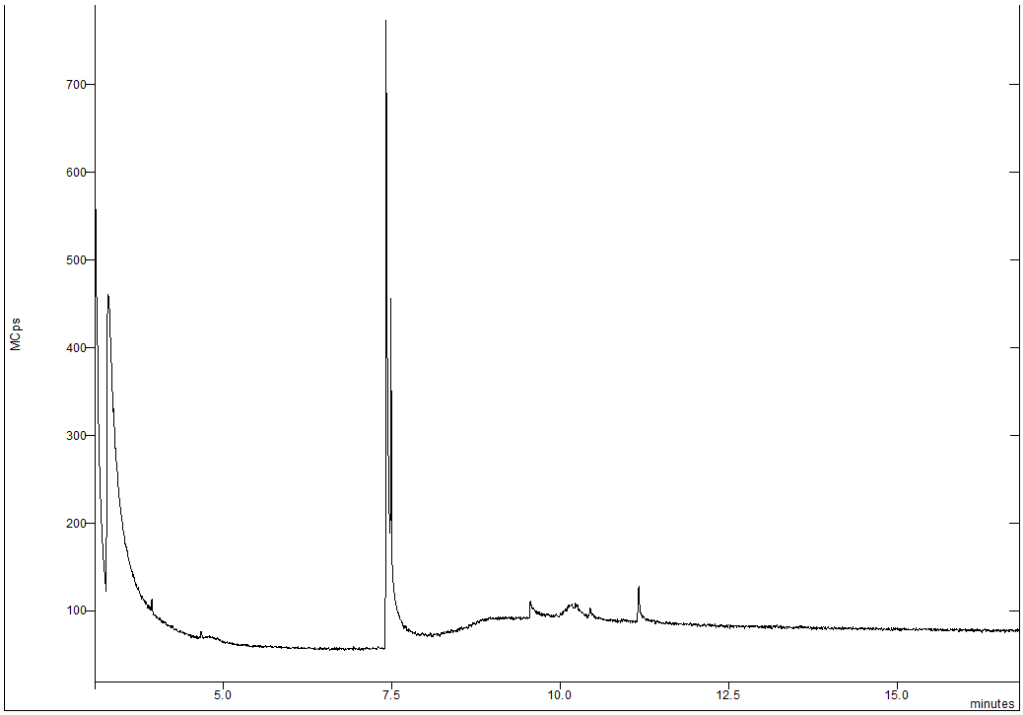

Figure 49 Gas chromatogram of Table 5, entry 6. mAPP (see **Figures 30** and **53**) was found at 7.42 min (m/z = 156), One side product (compound 2, see **Figures 30** and **54**) was found at 7.49 min (m/z = 154). Another side product (compound 3, see **Figures 30** and **55**) was found at a low quantity at 9.54 min (m/z = 238). Signals after 10 min are impurities from the column.

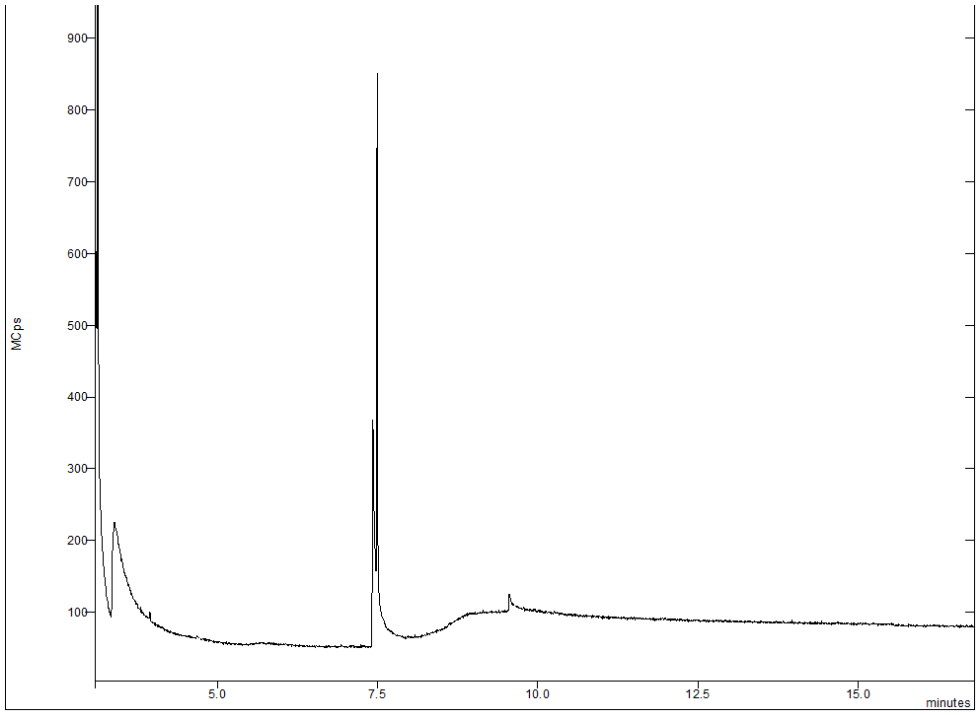

Figure 50 Gas chromatogram of Table 5, entry 7. mAPP (see **Figures 30** and **53**) was found at 7.42 min (m/z = 156), A side product (compound 2, see **Figures 30** and **54**) was found at 7.49 min (m/z = 154). A minimal amount of another side product (compound 3, see **Figures 30** and **55**) was found at 9.54 min (m/z = 238).

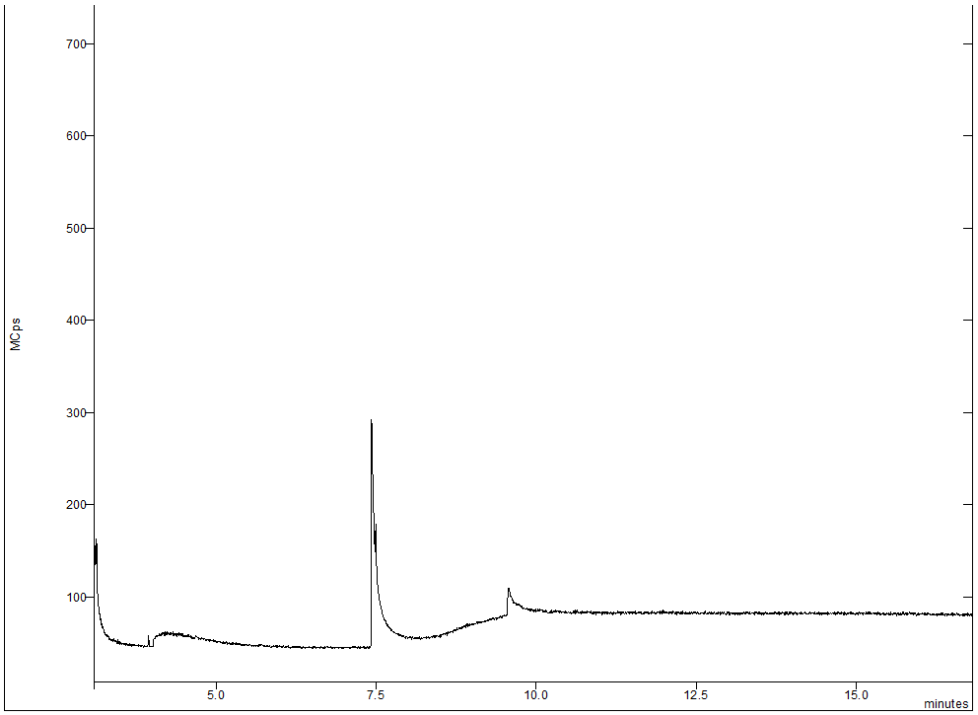

Figure 51 Gas chromatogram of Table 5, entry 8. mAPP (see **Figures 30** and **53**) was found at 7.42 min (m/z = 156), A side product (compound 2, see **Figures 30** and **54**) was found at 7.49 min (m/z = 154). Another side product (compound 3, see **Figures 30** and **55**) was found at 9.54 min (m/z = 238).

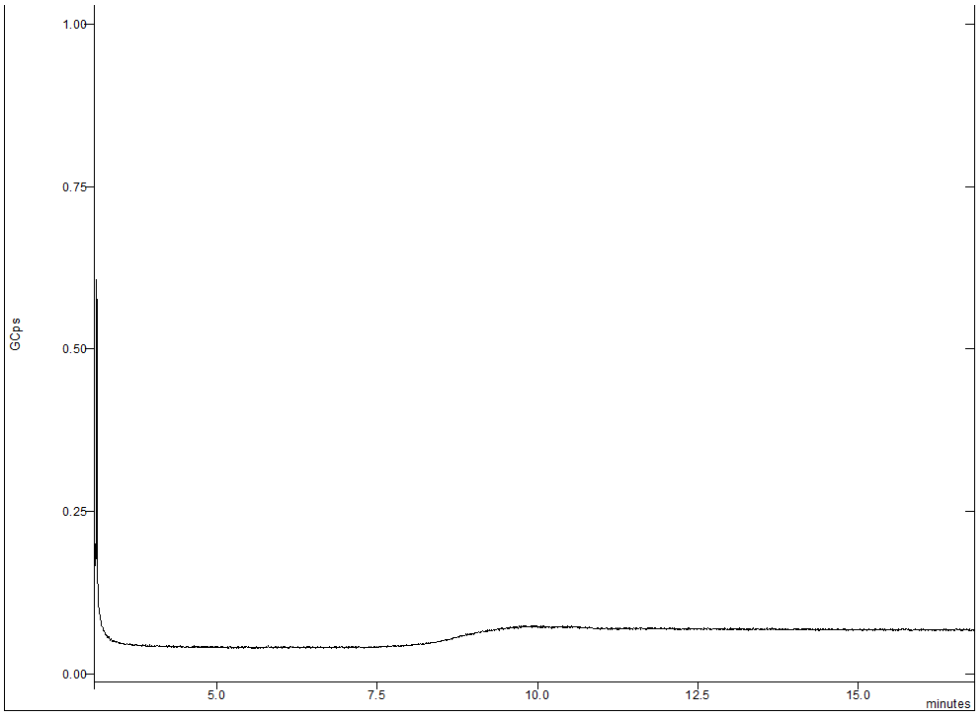

Figure 52 Gas chromatogram of Table 5, entry 9. No Signals were detected.

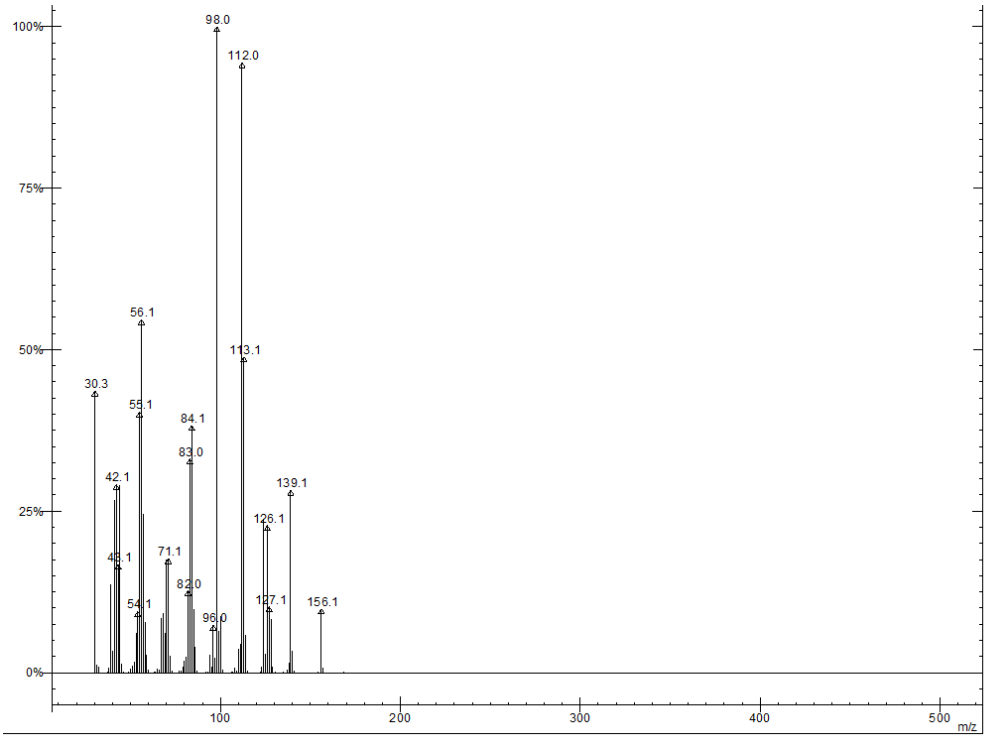

Figure 53 Mass spectrum of the desired product mAPP in **Figures 28–30**. The molecular ion peak was found at m/z = 156.

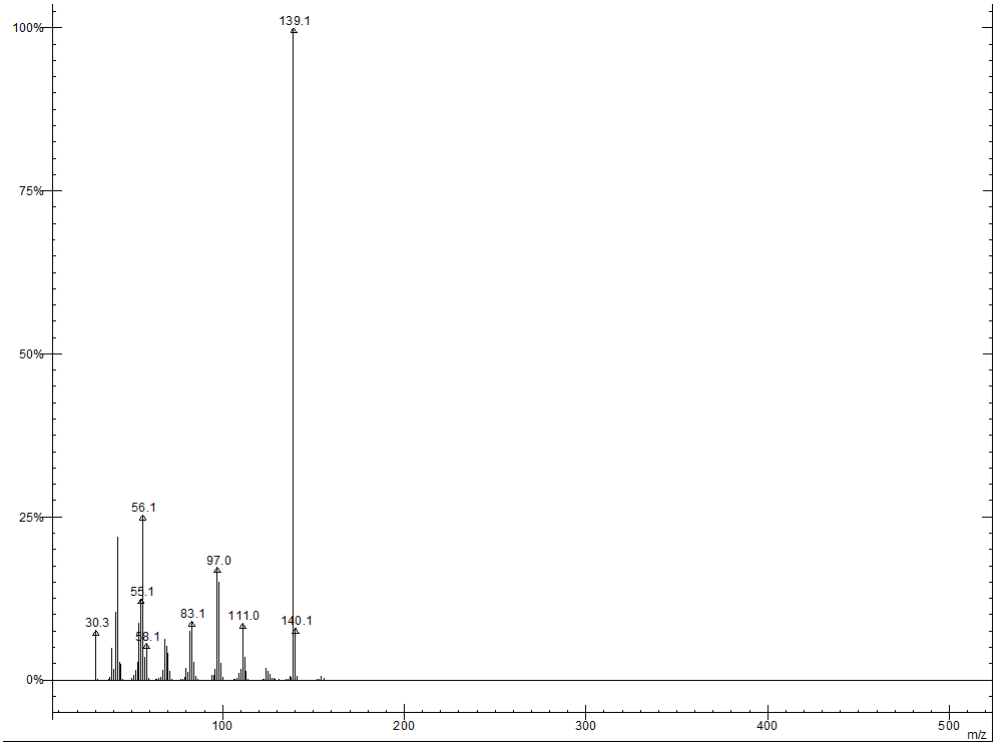

Figure 54 Mass spectrum of side product 2 in **Figure 30**. A weak molecular ion peak was found at m/z = 154.

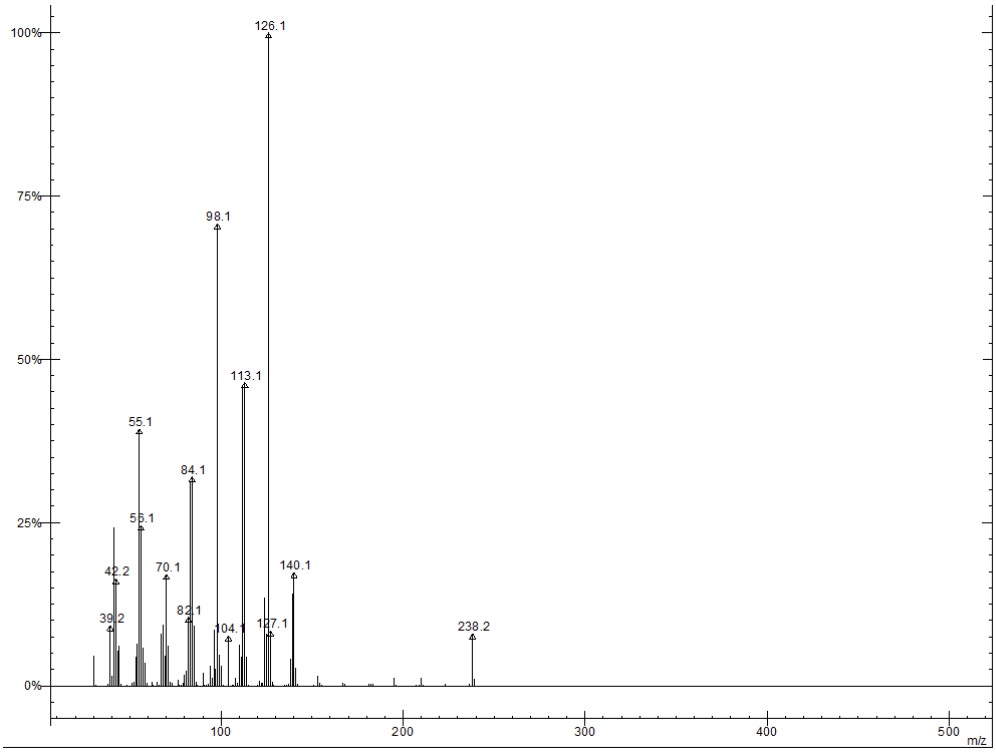

Figure 55 Mass spectrum of side product 3 in **Figure 30**. A molecular ion peak was found at m/z = 238.

4.4 RECYCLABILITY IN THE IONCELL-F PROCESS

[DBNH][OAc], [DBNH]Cl, [DBNH][CF_3COO] and [DBNH][CF_3SO_3] were synthesized by mixing equimolar quantities of DBN with acetic acid, HCl, CF_3COOH or CF_3SO_3H, respectively. Prior to analysis the products were dried at 80–100 °C under a vacuum.

Hydrolysis experiments were performed by mixing the IL with water in a 4-ml vial. Vials were placed in a heating block at 60–90 °C for 48 h. Samples were taken after 2, 4, 8, 16, 24 and 48 h and analyzed with HPLC. Analyses were performed using an isocratic elution with mixture of acetate buffer (0.5 M NaCl/10 mM NaOAc, pH 4.0), and acetonitrile (95:5 buffer:ACN) was used as a mobile phase. The injection volume was 5 µl and the flow rate was 0.8 ml/min at 30 °C.

4.5 CHEMICAL STABILITY OF $[P_{4444}][OH]$

The 50–60 % $[P_{4444}][OH]_{(aq)}$ solution was obtained by concentrating the commercial 40 % $[P_{4444}][OH]_{(aq)}$ solution using rotary evaporation at low pressured (15–25 mbar) at 25 °C.

A typical procedure for the $[P_{4444}][OH]_{(aq)}$ decomposition experiments was to fill a 1-ml glass vial with $[P_{4444}][OH]_{(aq)}$ solution and cap it with a plastic cap with an airtight liner. The vial was placed in a fan oven at the desired temperature. After 2, 4, 8 or 24 h, 50-µl sample was taken from the vial. An NMR sample was prepared by dissolving the sample in 700 µl of D_2O (containing H_3PO_4 as internal standard). The sample was thoroughly mixed by shaking and then transferred into a 5 mm NMR tube. In ^{31}P NMR spectra, $[H_3PO_4]^+$ was found at 0 ppm, tetra-*n*-butyl phosphonium cation ($[P_{4444}^+]$) was found at 33 ppm, and the decomposition product tri-*n*-butyl phosphine oxide was found at 61 ppm. Integration against the internal standard provided a correlation of the product distribution.

4.6 EXTRACTION OF WHEAT STRAW WITH $[P_{4444}][OH]$ SOLUTIONS

The utilized biomass (wheat straw and wheat straw:bran mixture) were provided by project partners at the Université de Toulouse, France.

After milling to pass through a 45-mesh sieve, the extractives were removed by washing the powdered wheat straw twice with 70 v/v% ethanol and once with 1:1 (v/v) chloroform:methanol. The powdered wheat straw was then dried in a fan oven at 60 °C for several days. After cooking with $[P_{4444}][OH]$, the mixture could be simply filtered and washed with distilled water followed by further washing in boiling distilled water to remove the residual electrolyte solution from the collected solid (S1). The collected liquid could be neutralized with an acid such as HCl, a process that significantly changed the dissolution properties of the solution. This induced a precipitation (S2) which was also washed thoroughly with distilled water. The collected liquid could be then

evaporated to dryness to yield [P_{4444}][Cl] as a spent liquor when HCl was used for acidification of the solution.

4.7 FRACTIONATION OF LIGNOCELLULOSIC BIOMASS UTILIZING A MICROWAVE REACTOR

Before feeding the wheat straw into a Wiley mini-mill (Thomas Scientific) to pass through a 60-mesh sieve, the remaining chaffs were removed by hand. Extractives were removed by using a mixture of EtOH and $CHCl_3$:MeOH.

Aspen was obtained as sawdust. It was first sterilized by brief immersion in 90 °C distilled water and further washed with acetone before finally drying in a fan oven at 50 °C. The dry, sterilized sawdust was fed to the Wiley mill to pass through a 60-mesh sieve. Extractives were removed by stirring the powderized aspen in acetone overnight. Biotage Initiator™ 2.0 and Anton Parr Monowave 450 microwave reactors were used for the microwave assisted extraction. A vessel made from silicon carbide was used for experiments that involved more alkaline solutions.

A mixture of 1.0 g wheat straw or aspen powder (extractive-free) was weighed in a microwave reactor vial, 20 ml solvent was added, and a magnetic stir bar placed in the vial. After extracting, the solids were isolated using vacuum filtration. The solid was washed with compatible solvent to yield a carbohydrate-rich fraction. A lignin-rich fraction was collected from the liquid fractions. Alkaline solutions were acidified, and lignin was left to coagulate overnight. From the formic acid solution, lignin was isolated by concentrating the mixture in a few milliliters and then adding it drop-wise to distilled water (40 ml). Solutions of [TEAH][HSO_4] volatiles were removed, and the mixture was diluted with distilled water (to approximately 80 ml total volume) and left to coagulate overnight.

In HWE, 1.0 g of extractive-free wheat straw or aspen powder was extracted with distilled water for 5 min at 185 °C. Solids were filtered and further washed with distilled water. The solid was then dried before a delignification procedure. The liquid portion was evaporated to yield a hemicellulose fraction.

5 REFERENCES

[1] United Nations, Department of Economic and Social Affairs, Population Division (2019), World Population Prospects 2019: Ten Key Findings. https://population.un.org/wpp/Publications/ (**12.7.2019**).

[2] F. M. Hämmerle. *Lenzinger Berichte* **2011**, *89*, 12–21.

[3] ICAC (International Cotton Advisory Committee), USDA (United States Department of Agriculture), "Cotton Production". **2011**.

[4] C. Okkerse and H. van Bekkum. *Green Chem.* **1998**, *1*, 107–114.

[5] A. J. Ragauskas, C. K. Williams, B. H. Davison, G. Britovsek, J. Cairney, C. A. Eckert, W. J. Frederick Jr., J. P. Hallett, D. J. Leak, C. L. Liotta, J. R. Mielenz, R. Murphy, R. Templer and T. Tschaplinski. *Science* **2006**, *311*, 484–489.

[6] M. Stöcker. *Angew. Chem. Int. Ed.* **2008**, *47*, 9200–9211.

[7] Borregaard annual report 2012 (http://www.borregaard.com/) (1**2.7.2019**).

[8] Brief description of the Inbicon technology on the biconsortium page https://biconsortium.eu/members/orsted (**12.7.2019**).

[9] A. A. Khan, W. de Jong, P. J. Jansens and H. Spliethoff. *Fuel Process. Technol.* **2009**, *90*, 21–50.

[10] J. E. G. van Dam, B. de Klerk-Engels, P. C. Struik and R. Rabbinge. *Ind. Crops Prod.* **2005**, *21*, 129–144.

[11] K. J. Edgar, C. M. Buchanan, J. S. Debenham, P. A. Rundquist, B. D. Seiler, M. C. Shelton and D. Tindall. *Prog. Polym. Sci.* **2001**, *26*, 1605–1688.

[12] T. Kulomaa, J. Matikainen, P. Karhunen, M. Heikkilä, J. Fiskari and I. Kilpeläinen. *RSC Adv.* **2015**, *5*, 80702–80708.

[13] J. Sirviö, A. Honka, H. Liimatainen, J. Niinimäki and O. Hormi. *Carbohydr. Polym.* **2011**, *86*, 266–270.

[14] S. Zhang, J. Sun, X. Zhang, J. Xin, Q. Miao and J. Wang. *Chem. Soc. Rev.* **2014**, *43*, 7838–7869.

[15] Y. Habibi, L. A. Lucia and O. J. Rojas. *Chem. Rev.* **2010**, *110*, 3479–3500.

[16] X. F. Sun, R. C. Sun, P. Fowler and M. S. Baird. *J. Agric. Food Chem.* **2005**, *53*, 860–870.

[17] A. Raghuraman, V. Tiwari, J. N. Thakkar, G. T. Gunnarsson, D. Shukla, M. Hindle and U. R. Desai. *Biomacromolecules* **2005**, *6*, 2822–2832.

[18] C. M. Welker, V. K. Balasubramanian, C. Petti, K. M. Rai, S. DeBolt and V. Mendu. *Energies* **2015**, *8*, 7654–7676.

[19] D. Stewart. *Ind. Crops Prod.* **2008**, *27*, 202–207.

[20] J. B. Binder, M. J. Gray, J. F. White, Z. C. Zhang and J. E. Holladay. *Biomass Bioenergy* **2009**, *33*, 1122–1130.

[21] J. E. Holladay, J. J. Bozell, J. F. White and D. Johnson. *Top Value-Added Chemicals from Biomass.* PNNL-16983. **2007**. (**12.7.2019**).

[22] E. A. Borges da Silva, M. Zabkova, J. Araújo, C. Cateto, M. Barreiro, M. Belgacem and A. E. Rodrigues. *Chem. Eng. Res. Des.* **2009**, *87*, 1276–1292.

[23] J. H. Clark, F. E. I. Deswarte and T. J. Farmer. *Biofuel Bioprod. Bior.* **2009**, *3*, 72–90.

[24] R. S. Fukushima and B. A. Dehority. *J. Anim. Sci.* **2000**, *78*, 3135–3143.

[25] O. Theander and E. A. Westerlund. *J. Agric. Food Chem.* **1986**, *34*, 330–336.
[26] P. J. Van Soest. *J. Assoc. Off. Agric. Chem.* **1963**, *46*, 829–835.
[27] P. J. Van Soest and R. H. Wine. *J. Assoc. Off. Anal. Chem.* **1968**, *51*, 780–785.
[28] M. Shimojo and I. Goto. *Jpn. J. Zootechnol. Sci.* **1984**, *55*, 838–842.
[29] T. Kondo, K. Mizuno and T. Kato. *J. Jpn. Grassl. Sci.* **1987**, *33*, 296–299.
[30] J. B. Lowry, A. C. Conlan, A. C. Schlink and C. S Mcsweeney. *J. Sci. Food Agric.* **1994**, *65*, 41–49.
[31] R. D. Hatfield, H. G. Jung, J. Ralph, D. R. Buxton and P. J. Weimer. *J. Sci. Food Agric.* **1994**, *65*, 51–58.
[32] P. J. Van Soest. *J. Anim. Sci.* **1967**, *26*, 119–128.
[33] R. S. Fukushima and R. D. Hatfield. *J. Sci. Food Agric.* **2001**, *49*, 3133–3139.
[34] J. C. del Río, J. Rencoret, P. Prinsen, Á. T. Martínez, J. Ralph and A. Gutiérrez. *J. Agric. Food Chem.* **2012**, *60*, 5922–5935.
[35] M. M. Kabir, M. J. Taherzadeh and I. Sárvári Horváth. *Biofuel Res. J.* **2015**, *8*, 309–316.
[36] C. Atik and S. Ates. *BioRes.* **2012**, *7*, 3274–3282.
[37] U. Ali, V. Bijalwan, S. Basu, A. K. Kesarwani and K. Mazumder. *Carbohydr. Polym.* **2017**, *161*, 90–98.
[38] R. M. Vera, R. Bura and R. Gustafson. *Biotechnol. Biofuels* **2015**, *8*, 226.
[39] X. Pan and Y. Sano. *Bioresour. Technol.* **2005**, *96*, 1256–1263.
[40] A. Kamel, H. Al jibouri, G. Turcotte, J. Wu and C.-H. Cheng. *Energy Sci. Eng.* **2015**, *3*, 541–548.
[41] F. E. I. Deswarte, J. H. Clark, A. J. Wilson, J. J. E Hardy, R. Marriott, S. P. Chahal, C. Jackson, G. Heslop, M. Birkett, T. J. Bruce and G. Whiteley. *Biofuels Bioprod. Bioref.* **2007**, *1*, 245–254.
[42] T. Schantz-Hansen. Logging methods and peeling of Aspen. Lake States Aspen report No. 3. **1948**. https://www.fs.fed.us/nrs/pubs/LSFES_aspen_reports/1948_lakestates_aspen_3.pdf (**17.7.2019**)
[43] J. Gorke, F. Srienc and R. Kazlauskas. *Biotechnol. Bioprocess Eng.* **2010**, *15*, 40–53.
[44] J. G. Huddleston, A. E. Visser, W. M. Reichert, H. D. Willauer, G. A. Broker and R. D. Rogers. *Green Chem.* **2001**, *3*, 156–164.
[45] P. Walden. *Bull. Acad. Imper. Sci. (St. Petersburg)* **1914**, 1800.
[46] A. W. T. King, J. Asikkala, I. Mutikainen, P. Järvi and Ilkka Kilpeläinen. *Angew. Chem. Int. Ed.* **2011**, *50*, 6301–6305.
[47] M. Armand, F. Endres, D. R. MacFarlane, H. Ohno and B. Scrosati. *Nat. Mater.* **2009**, *8*, 621–629.
[48] H. Zhao. *Chem. Eng. Commun.* **2006**, *193*, 1660–1677.
[49] A. Brandt, M. J. Ray, T. Q. To, D. J. Leak, R. J. Murphy and T. Welton. *Green Chem.* **2011**, *13*, 2489–2499.
[50] J. P. Hallett and T. Welton. *Chem. Rev.* **2011**, *111*, 3508–3576.
[51] M. Zavrel, D. Bross, M. Funke, J. Büchs and A.C. Spiess. *Bioresour. Technol.* **2009**, *100*, 2580–2587.
[52] Y. Wang, L. Wei, K. Li, Y. Ma, N. Ma, S. Ding, L. Wang, D. Zhao, B. Yan, W. Wan, Q. Zhang, X. Wang, J. Wang and H. Li. *Bioresour. Technol.* **2014**, *170*, 499–505.

[53] I. Kilpeläinen, H. Xie, A. W. T. King, M. Granström, S. Heikkinen and D. S. Argyropoulos. *J. Agric. Food Chem.* **2007**, *55*, 9142–9148.

[54] T. Li, Q. Fang, H. Chen, F. Qi, X. Ou, X. Zhao and D. Liu. *RSC Adv.* **2017**, *7*, 10609–10617.

[55] A. M. da Costa Lopes, K. G. João, A. R. C. Morais, E. Bogel-Łukasik and R. Bogel-Łukasik. *Sustain. Chem. Process* **2013**, *1*, 3.

[56] V. P. Natalia and K. R. Seddon. *Chem. Soc. Rev.* **2008**, *37*, 123–150.

[57] H. Wang, G. Gurau and R. D. Rogers. *Chem. Soc. Rev.* **2012**, *41*, 1519–1537.

[58] B. Lindman, G. Karlström and L. Stigsson. *J. Mol. Liq.* **2010**, *156*, 76–81.

[59] B. Medronho and B. Lindman. *Curr. Opin. Colloid Interface Sci.* **2014**, *19*, 32–40.

[60] C. Graenacher, US Patent, 1943176, **1934**.

[61] R. P. Swatloski, S. K. Spear, J. D. Holbrey and R. D. Rogers. *J. Am. Chem. Soc.* **2002**, *124*, 4974–4975.

[62] T. Erdmenger, C. Haensch, R. Hoogenboom and U. S. Schubert. *Macromol. Biosci.* **2007**, *7*, 440–445.

[63] A. Parviainen, A. W. King, I. Mutikainen, M. Hummel, C. Selg, L. K. Hauru, H. Sixta and I. Kilpeläinen. *ChemSusChem* **2013**, *6*, 2161–2169.

[64] M. Ungurean, Z. Csanádi, L. Gubicza and F. Péter. *BioRes.* **2014**, *9*, 6100–6116.

[65] L. Kyllönen, A. Parviainen, S. Deb, M. Lawoko, M. Gorlov, I. Kilpeläinen and A. W. T. King. *Green Chem.* **2013**, *15*, 2374–2378.

[66] M. Iguchi, T. M. Aida, M. Watanabe and R. L. Smith Jr. *Carbohydr. Polym.* **2013**, *92*, 651–658.

[67] R. Rinaldi. *Chem. Comm.* **2011**, *47*, 511–513.

[68] H. Zhang, J. Wu, J. Zhang and J. He. *Macromolecules* **2005**, *38*, 8272–8277.

[69] T. Heinze, K. Schwikal and S. Barthel. *Macromol. Biosci.* **2005**, *5*, 520–525.

[70] N. Sun, M. Rahman, Y. Qin, M. L. Maxim, H. Rodríguez and R. D. Rogers. *Green Chem.* **2009**, *11*, 646–655.

[71] W. Lan, C.-F. Liu and R.-C. Sun. *J. Agric. Food Chem.* **2011**, *59*, 8691–8701.

[72] A. M. da Costa Lopes, K. G. João, D. F. Rubik, E. Bogel-Łukasik, L. C. Duarte, J. Andreaus and R. Bogel-Łukasik. *Bioresour. Technol.* **2013**, *142*, 198–208.

[73] D. Fu, G. Mazza and Y. Tamaki. *J. Agric. Food Chem.* **2010**, *58*, 2915–2922.

[74] M. Abe, Y. Fukaya and H. Ohno. *Chem. Commun.* **2012**, *48*, 1808–1810.

[75] M. Abe, T. Yamada and H. Ohno. *RSC Adv.* **2014**, *4*, 17136–17140.

[76] M. Abe, S. Yamanaka, H. Yamada, T. Yamada and H. Ohno. *Green Chem.* **2015**, *17*, 4432–4438.

[77] B. B. Y. Lau, E. T. Luis, M. M. Hossain, W. E. S. Hart, B. Cencia-Lay, J. J. Black, T. Q. To and L. Aldous. *Bioresour. Technol.* **2015**, *197*, 252–259.

[78] P. G. Jessop, D. J. Heldebrant, X. Li, C. A. Eckert and C. L. Liotta. *Nature* **2005**, *436*, 1102.

[79] P. G. Jessop, S. M. Mercer and D. J. Heldebrant. *Energy Environ. Sci.* **2012**, *5*, 7240–7253.

[80] P. Domínguez de María. *J. Chem. Technol. Biotechnol.* **2014**, *89*, 11–18.

[81] Q. Zhang, N. S. Oztekin, J. Barrault, K. De Oliveira Vigier and F. Jerome. *ChemSusChem* **2013**, *6*, 593–596.

[82] I. Anugwom, P. Mäki-Arvela, P. Virtanen, P. Damlin, R. Sjöholm and J.-P. Mikkola. *RSC Adv.* **2011**, *1*, 452–457.

[83] I. Anugwom, P. Mäki-Arvela, P. Virtanen, S. Willför, R. Sjöholm and J-P Mikkola. *Carbohyd. Polym.* **2012**, *87*, 2005–2011.

[84] I. Anugwom, P. Mäki-Arvela, P. Virtanen, S. Willför, P. Damlin, M. Hedenström and J.-P. Mikkola. *Holzforschung* **2012**, *66*, 809–815.

[85] I. Anugwom, V. Eta, P. Virtanen, P. Mäki-Arvela, M. Hedenström, M. Yibo, M. Hummel, H. Sixta and J.-P. Mikkola. *Biomass Bioenergy* **2014**, *70*, 373–381.

[86] I. Anugwom, V. Eta, P. Virtanen, P. Mäki-Arvela, M. Hedenström, M. Hummel, H. Sixta and J.-P. Mikkola. *ChemSusChem* **2014**, *7*, 1170–1176.

[87] Q.-P. Liu, X.-D. Hou, N. Li and M.-H. Zong. *Green Chem.* **2012**, *14*, 304–307.

[88] A. J. Holding, M. Heikkilä, I. Kilpeläinen and A. W. T. King. *ChemSusChem* **2014**, *7*, 1422–1434.

[89] A. Michud, M. Tanttu, S. Asaadi, Y. Ma, E. Netti, P. Kääriainen, A. Persson, A. Berntsson, M. Hummel and H. Sixta. *Text. Res. J.* **2016**, *86*, 543–552.

[90] L. Chen, M. Sharifzadeh, N. Mac Dowell, T. Welton, N. Shah and J. P. Hallett. *Green Chem.* **2014**, *16*, 3098–3106.

[91] A. George, A. Brandt, K. Tran, S. M. S. Nizan S. Zahari, D. Klein-Marcuschamer, N. Sun, N. Sathitsuksanoh, J. Shi, V. Stavila, R. Parthasarathi, S. Singh, B. M. Holmes, T. Welton, B. A. Simmons and J. P. Hallett. *Green Chem.* **2015**, *17*, 1728–1734.

[92] P. J. Scammells, J. L. Scott and R. D. Singer. *Aust. J. Chem.* **2005**, *58*, 155–169.

[93] M. T. Clough, K. Geyer, P. A. Hunt, J. Mertes and T. Welton. *Phys. Chem. Chem. Phys.* **2013**, *15*, 20480–20495.

[94] T. J. Wooster, K. M. Johanson, K. J. Fraser, D. R. MacFarlane and J. L. Scott. *Green Chem.* **2006**, *8*, 691–696.

[95] W. Li, N. Sun, B. Stoner, X. Jiang, X. Lu and R. D. Rogers. *Green Chem.* **2011**, *13*, 2038–2047.

[96] D. Fu and G. Mazza. *Bioresour. Technol.* **2011**, *102*, 8003–8010.

[97] S. Busi, M. Lahtinen, M. Kärnä, J. Valkonen, E. Kolehmainen and K. J. Rissanen. *Mol. Struct.* **2006**, *787*, 18–30.

[98] C. P. Fredlake, J. M. Crosthwaite, D. G. Hert, S. N. V. K. Aki and J. F. Brennecke. *J. Chem. Eng. Data* **2004**, *49*, 954–964.

[99] Y. J. Kim and R. S. Varma. *J. Org. Chem.* **2005**, *70*, 7882–7891.

[100] M. R. R. Prasad, K. Krishnan, K. N. Ninan and V. N. Krishnamurthy. *Thermochim. Acta* **1997**, *297*, 207–210.

[101] Y. Cao and T. Mu. *Ind. Eng. Chem. Res.* **2014**, *53*, 8651–8664.

[102] R. E. Del Sesto, T. M. McCleskey, C. Macomber, K. C. Ott, A. T. Koppisch, G. A. Baker and A. K. Burrell, *Thermochim. Acta* **2009**, *491*, 118–120.

[103] M. E. Van Valkenburg, R. L. Vaughn, M. Williams and J. S. Wilkes *Thermochim. Acta* **2005**, *425*, 181–188.

[104] A. Seeberger, A.-K. Andresen and A. Jess. *Phys. Chem. Chem. Phys.* **2009**, *11*, 9375–9381.

[105] I. H. J. Arellano, J. G. Guarino, F. U. Paredes and S. D. Arco. *J. Therm. Anal. Calorim.* **2011**, *103*, 725–730.

[106] C. Maton, N. De Vos and C. V. Stevens. *Chem. Soc. Rev.* **2013**, *42*, 5963–5977.

[107] W. E. McEwen, G. Axelrad, M. Zanger and C. A. Van der Werf. *J. Am. Chem. Soc.* **1965**, 87, 3948–3952.
[108] T. Linder and J. Sundermeyer. *Chem. Commun.* **2009**, 2914–2916.
[109] U. Hyväkkö, A. W. T. King and I. Kilpeläinen. *BioRes.* **2014**, *9*, 1565–1577.
[110] S. Chowdhury, R. S. Mohan and J. L. Scott. *Tetrahedron* **2007**, *63*, 2363–2389.
[111] R. A. Olofson, W. R. Thompson and J. S. Michelman. *J. Am. Chem. Soc.* **1964**, *86*, 1865–1866.
[112] A. J. Arduengo III, R. L. Harlow and M.Kline. *J. Am. Chem. Soc.* **1991**, *113*, 361–363.
[113] A. J. Arduengo III. *Acc. Chem. Res.* **1999**, *32*, 913–921.
[114] J. N. Rosa, C. A. M. Afonso and A. G. Santos. *Tetrahedron* **2001**, *57*, 4189–4193.
[115] V. K. Aggarwal, I. Emme and A. Mereu. *Chem. Commun.* **2002**, *0*, 1612–1613.
[116] G. Ebner, S. Schiehser, A. Potthast and T. Rosenau. *Tetrahedron Lett.* **2008**, *49*, 7322–7324.
[117] T. Heinze, S. Dorn, M. Schoebitz, T. Liebert, S. Koehler and F. Meister. *Macromol. Symp.* **2008**, *262*, 8–22.
[118] S. Sowmiah, V. Srinivasadesikan, M. C. Tseng and Y. H. Chu. *Molecules* **2009**, *14*, 3780–3813.
[119] L. F. O. Faria, M. M. Nobrega, M. L. A. Temperini, R. Bini and M. C. C. Ribeiro. *J. Phys. Chem. B* **2016**, *120*, 9097–9102.
[120] M.-C. Tseng, H.-C. Kan and Y.-H. Chu. *Tetrahedron Lett.* **2007**, *48*, 9085–9089.
[121] J. D. Holbrey, W. M. Reichert, R. P. Swatloski, G. A. Broker, W. R. Pitner, K. R. Seddon and R. D. Rogers. *Green Chem.* **2002**, *4*, 407–413.
[122] P. Wasserscheid, V. R. Hal and A. Bösmann. *Green Chem.* **2002**, *4*, 400–404.
[123] R. P. Swatloski, J. D. Holbrey and R. D. Rogers. *Green Chem.* **2003**, *5*, 361–363.
[124] A. Kamal and G. Chouhan. *Tetrahedron Lett.* **2005**, *46*, 1489–1491.
[125] S. S. Keskar, L. A. Edye, W. O. S. Doherty and J. P. Bartley. *J. Wood Chem. Technol.* **2012**, *32*, 71–81.
[126] C. Chuster, A. Seib and G. v.Bank. German patent, 730182, **1943**.
[127] F. Müller. German patent, 1,121,924, **1968**.
[128] O. Werbitzky, U. Daum and R. Bregy. US Patent, 5,723,605, **1998**.
[129] U. Hyväkkö, J. Helminen, A. Parviainen A. W. T. King and I. Kilpeläinen. "Hydrolytic stability of novel distillable ionic liquids: A kinetic and computational study". Poster presented at the FIBIC annual seminar, Helsinki, **2013**.
[130] J. Helminen, U. Hyväkkö, V. Mäkelä, A. Parviainen, K. Vyavaharkar, A. W. T. King and I. Kilpeläinen. "Stability of recyclable ionic liquids". Poster presented at the ACel Symposium, Helsinki, **2015**.
[131] L. J. Hauru, M. Hummel, A. Michud and H. Sixta. *Cellulose* **2014**, *21*, 4471–4481.
[132] H. Sixta, A. Michud, L. Hauru, S. Asaadi, Y. Ma, A. W. King, I. Kilpelainen and M. Hummel. *Nord. Pulp Pap. Res. J.* **2015**, *30*, 43–57.
[133] A. M. Hyde, R. Calabria, R. Arvary, X. Wang and A. Klapars. *Org. Process Res. Dev.* **2019**, *published online.* (**21.8.2019**)

[134] A. Parviainen, R. Wahlström, U. Liimatainen, T. Liitiä, S. Rovio, J. K. J. Helminen, U. Hyväkkö, A. W. T. King, A. Suurnäkki and I. Kilpeläinen. *RSC Adv*. **2015**, *5*, 69728–69737.

[135] W. Ahmad, A. Ostonen, K. Jakobsson, P. Uusi-Kyyny, V. Alopaeus, U. Hyväkkö and A. W. T. King. *Chem. Eng. Res. Des.* **2016**, *114*, 287–298.

[136] K. Iiyama and A. F. A. Wallis. *Wood Sci. Technol.* **1988**, *22*, 271–280.

[137] K. Iiyama and A. F. A. Wallis. *J. Sci. Food Agric.* **1990**, *51*, 145–161.

[138] L. Jacquemin, R. Zeitoun, C. Sablayrolles, P. Y. Pontalier and L. Rigal. *Process Biochem.* **2012**, *47*, 373–380.

[139] U. Hyväkkö, R. Maltari, T. Kakko, J. Kontro, J. Mikkilä, P. Kilpeläinen, E. Enqvist, P. Tikka, K. Hildén, P. Nousiainen and J. Sipilä. *Published online in ACS Omega* **2019**. https://doi.org/10.1021/acsomega.9b02619

[140] A. Brandt-Talbot, F. J. V. Gschwend, P. S. Fennell, T. M. Lammens, B. Tan, J. Weale and J. P. Hallett. *Green Chem.* **2017**, *19*, 3078–3102.

[141] a) S. Zhou, L. Liu, B. Wang, F. Xu and R. Sun. *Process Biochem.* **2012**, *47*, 1799–1806.

b) D. Barana, A. Salanti, M. Orlandi, D. S. Ali, and L. Zoia. *Ind. Crops Prod.* **2016**, *86*, 31–39.

c) C. Tang, Y. Chen, J. Liu, T. Shen, Z. Cao, J. Shan, C. Zhu and H. Ying. *Ind. Crops Prod.* **2017**, *95*, 383–392.

d) G. T. Mihiretu, M. Brodin, A. F. Chimphango, K. Øyaas, B. H. Hoff and J. F. Görgens. *Biores. Technol.* **2017**, *241*, 669–680.